ASPECTS OF AMIDIZATION OF CHITOSAN

by

Ackah Toffey

Dissertation submitted to the faculty of the
Virginia Polytechnic Institute and State University
in partial fulfillment of the requirements for the degree of

DOCTOR OF PHILOSOPHY

in

Wood Science and Forest Products

APPROVED:

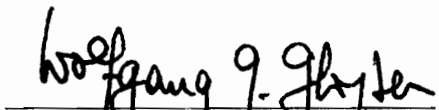

Wolfgang G. Glasser, Chairman

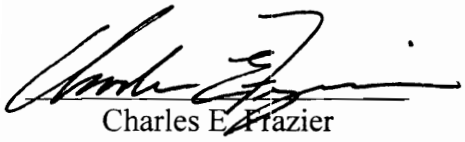

Charles E. Frazier

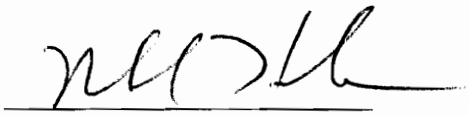

Richard F. Helm

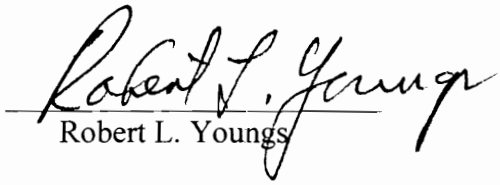

Robert L. Youngs

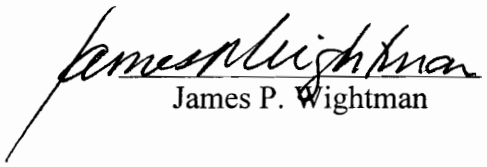

James P. Wightman

September, 1996
Blacksburg, Virginia

Keywords: Amidization, Imidization, Vitrification, Glass transition, Chitin, Chitosan

ASPECTS OF AMIDIZATION OF CHITOSAN

By

Ackah Toffey

Committee Chairman: Wolfgang G. Glasser
Wood Science and Forest Products

(ABSTRACT)

The intent of this research was to develop an understanding of an amidized chitosan-from-chitosan regeneration process discovered in our laboratory. In this study several characterization methods including DMTA, TMA, TGA, X-ray diffraction, FTIR, solid state CP-MAS ^{13}C NMR, and HPLC were used to study the transformation of various ionic complexes of chitosan (N-acylate) to their respective N-acyl homologs of chitosan; and several properties of these materials were examined. DMTA and TMA provided information on changes in T_g as well as modulus-changes and glass formation underlying the transformation of the N-acylate to the N-acyl derivative. X-ray diffraction and FTIR shed some insights on the morphology of the N-acetyl homolog of chitosan in relation to native chitin. Solid state CP-MAS ^{13}C NMR provided evidence of the conversion of N-acylate to N-acetyl. Enzymatic hydrolysis of native chitin and amidized chitosan homologs and subsequent identification of fractions by HPLC allowed a comparison of various amidized chitosan homologs in terms of their recognition and degradation by chitinolytic enzymes.

Solid state CP-MAS ^{13}C showed that the heat treatment of the ionic complex of chitosan results in thermal dehydration leading to the formation of the N-acetyl

group at the C-2 of chitin. The DS of amidized chitosan varied between 0.1 and 0.6. T_g-changes with time and heating temperature were used as a variable to monitor amidization. Kinetics analysis indicated that the amidization of various ionic complexes of chitosan is a first order, two-phase process with activation energies of 14±1 kcal/mol and 21±2 kcal/mol for the first and second phase, respectively. These values did not vary with the type of acid used in the formation of the chitosan complex. This two-phase behavior is explained with the influence of vitrification on chain mobility.

In situ DMTA was found to be a suitable technique for monitoring the phase transformation of chitosonium acetate and chitosonium propionate from a rubbery to a glassy phase (vitrification). Consequently, the concept of TTT-cure diagram analysis was used to describe such phase changes and map out vitrification and full cure curves. As in thermosets, the vitrification curve describing glass formation in these materials is S-shaped. The time to full cure decreased with increasing heating temperature. The activation energy for vitrification is the same irrespective of the type of acid used in the preparation of chitosan complex.

Thermal analysis revealed that the T_g of N-acyl homologs of chitin displays a stepwise relationship with length of N-acyl substituent. These materials are characterized by two transitions designated as β- and α-relaxation. Additionally, enzymatic hydrolysis of N-acyl homologs of chitosan using an enzyme mixture of chitinase, chitosanase, and β-N-acetylglucosaminidase and subsequent identification

of fractions revealed that these enzymes recognize and degrade chitin irrespective of the N-acyl substituent at the C-2 position of chitin at any DS.

ACKNOWLEDGEMENTS

The author of this dissertation, Ackah Toffey, would like to express his sincere gratitude to his major professor, Dr. Wolfgang G. Glasser for the opportunity to work with him as a graduate student. During my study at Virginia Tech, Dr. Glasser was my voice when I could not speak; he was my wings when I could not fly; he was my strength when I was weak; he lifted me up when I could not reach; he was always there for me; and he saw me through all bad times. To Dr. Glasser, I sincerely say that I am very thankful for all the times that you stood for me; for all the joy that you brought into my life; for all the wrong that you made right; and for every academic dream that you made come true. Finally, I wish you well in all your endeavors.

I also extend my appreciation to Dr. Charles E. Frazier, Dr. Richard F. Helm, Dr. Robert L. Youngs, and Dr. James P. Wightman for their invaluable input into this dissertation. I am delighted for the chance to work with them.

The support of members of Dr. Glasser's group, including Ulli Becker, Dr. Rajesh Jain, Jason Todd, Mazlan Ibrahim and Jody Jervis, is also acknowledged with gratitude. And not to forget Dr. Gamini Samaranayake for his immense contribution in developing my research study.

Many thanks also go to Dr. Geza Ifju, for the opportunity to study at Virginia Tech. Kaichang Li, also deserves my appreciation; he has been a good friend and provided a sense of companionship at all times. I will certainly miss him as I leave

Blacksburg. I also wish to acknowledge the assistance of Jim Ni with some of the experiments reported in this dissertation.

" For every successful task, the woman in the life of a man is behind it". Certainly, my wife, Sophia A. Toffey, deserves my commendation. She was sustaining, enduring, loving, and supportive through it all. She provided a peaceful atmosphere at home; thank you, Sophia. And to my dear little daughter, Lucinda, thanks for the nice moments that you shared with me in the course of writing this dissertation.

Finally, I express my thanks to God for the strength and health all these years.

TABLE OF CONTENTS

LIST OF TABLES

LIST OF FIGURES

GLOSSARY OF SYMBOLS

A	pre-Arrhenius frequency factor	m^{-1}
DS	degree of substitution	
E'	storage modulus	Pa
E''	loss modulus	Pa
E_A	activation energy	kcal/mol
$E_{A,\ vit}$	activation energy for vitrification	kcal/mol
$E_{A,\ full\ cure}$	activation energy for full cure	kcal/mol
F	extent of reaction	%
f	frequency	hz
G'	storage shear modulus	Pa
G''	loss shear modulus	Pa
G_o	modulus of uncured polymer	Pa
G_∞	ultimate modulus	Pa
k	reaction rate constant	m^{-1}
M_w	weight average molecular weight	g/mol
M_n	number average molecular weight	g/mol
n	order of reaction	
p_{vit}	conversion at vitrification	
R	absolute gas constant	$8.314 Jmol^{-1}K^{-1}$
R^2	correlation coefficient	
T	temperature	°C
T_c	cure temperature	°C
T_g	glass transition temperature	°C
$T_{g,o}$	glass transition temperature of uncured polymer	°C
$T_{g,\infty}$	ultimate glass transition temperature	°C
t_c	cure time	min
t_{vit}	vitrification time	min

ε	strain	%
ϕ	heating rate	$^{o}C\ min^{-1}$
σ	stress	Pa

CHAPTER 1

INTRODUCTION

1.0 INTRODUCTION

Significant interest exists in polysaccharides because of their biodegradability and environmental friendliness. Cellulose , the most known polysaccharide, and its derivatives have found applications in textiles, coatings and paints, membranes etc[1]. In recent years tremendous advances have been made in the utilization of other polysaccharides, particularly chitin and its derivative, chitosan. For example, in Japan, Hosogawa et al.[2,3], Isogai[4], Kobayashi et al.[5]Kurita et al.[6-8], Hirano et al.[9], Chandy et al.[10], Yabe et al.[11], and Mizushima[12] have been active in the development of chitin-derived materials. These scientists have independently demonstrated that many commercially viable products could arise from chitin-chitosan systems. These include applications in (a) agriculture, where chitin/chitosan can perform as fungicides; (b) in nutrition and water treatment, as flocculant; (c) in cosmetics, as moisturizer; (d) in biomedical applications, such as in artificial skin and anti-tumor agents, wound dressing, medical gauzes, etc.

Similarly, in North America, scientists are (have been) pursuing research on chitin and chitosan. For example, Wightman and coworkers have demonstrated the efficacy of chitosan as a chelating agent[13]. Glasser and coworkers are utilizing chitosan to produce beads of controlled pore sizes that may be useful for protein separations and water purification[14]. Allan et al. have reported on a novel method of utilizing chitosan in

paper making[15] where chitosan is precipated onto wood for the production of paper with improved wet strength. In a related study, scientists at McGill University have demonstrated that chitosan can improve significantly the wet strength of paper[16]. Hudson and associates have utilized crosslinked chitosan for the preparation of biodegradable fibers[17].

Chitosan and chitin research is also being carried out in Europe, where Muzarrelli and coworkers have been pioneers in developing biomedical devices from chitosan[18,19]. More recently scientists at the University of Leeds, England, have developed a unique approach to producing chitosan-based fibers[20]. The uniqueness of their method lies in taking advantage of the solubility of chitosan and ease of fiber spinning from the solubilized chitosan, and subsequent homogeneous N-acylation to produce chitin-like fibers with improved properties. The foregoing discussions underscore the significant strides that have been made and/or are being made in the utilization of chitin and chitosan.

A central theme to the utilization of chitin is its conversion to chitosan by alkaline hydrolysis. This is due to the limited solubility of chitin in most solvents, except dimethyl acetamide/lithium chloride. The utilization of chitosan commonly involves dissolution in dilute organic acid, preferably acetic acid, thereby forming the salt of chitosan, chitosonium acetate. The solution can be cast into films[21-23]; sprayed as a coating or cast as a membrane of controlled pore size[24]; spun into fibers[20]; or regenerated as beads. This is accompanied by neutralization with cold alkali to

regenerate chitosan. A major limitation of chitosan-based materials prepared by the above method (dissolution in acid followed by neutralization), particularly in coatings and composites applications, is limited moisture resistance[20,21]. On the other hand chitin is known to be moisture resistant. Yet it has received less attention in coatings and composites applications. Perhaps, its limited solubility accounts for the disinterest. In an attempt to get chitosan to be very moisture resistant several scientists have devised chemical means of crosslinking. Hudson and coworkers have successfully crosslinked chitosan with epichlorohydrin[17]. Their method involved reacting chitosan suspensions with a basic solution of epichlorohydrin and heating the resulting mixture to elevated temperatures. They have been successful in producing fibers from such products, where improved moisture resistance is achieved. In a related method, Dixon and Gomes have employed epoxy and glutaraldhyde resins to crosslink chitosan[25]. These materials were used successfully to protect marine structures from marine borers. These approaches represent efficient means of enhancing the moisture resistance of chitosan plus improving strength properties. However, they usually interfere with biodegradability and recycling requirements of composites, fibers etc. We have found that chitosonium acetate reverts to chitin on heating in a reaction resembling network formation. This process of chitin regeneration is a thermal dehydration phenomenon (**Figure 1-1**). The novelty of this discovery lies in (a) taking advantage of the solubility of chitosan as well as the superior properties of chitin, and (b) recreating characteristics typical of network polymers without impairing biodegradability and recycling requirements.

Of pertinent long-term interest to the study reported in this dissertation are the film forming qualities of chitosonium acetate and their potential application as a paper/wood coating. For instance, when used as a paper coating agent it would permit application of a water-soluble material (chitosonium acetate), compatible with the aqueous environment of the paper making process, to paper early in the process and subsequent drying downstream to produce chitin. Further, it can be expected that chitin films will exhibit excellent adherence to wood surfaces on account of their ionic attraction to acidic (wood) surfaces, and because of chitin's chemical structure, which is similar to that of cellulose. Currently most wood/paper finishes are based on curable (network-forming) resins or on solvent-soluble film-forming polymers that transform to chemically-inert and/or moisture-resistant finishes. The transition to a chemically-inert film or coating involves a process that is described as cure. This could be effected at room temperature or at elevated temperatures depending on the polymer system. Most studies dealing with wood and paper coatings assume that the use of elevated temperatures will produce a fully-cured or highly-crosslinked (high extent of cure) material with superior hardness, chemical and moisture resistance as well as strength properties. Despite positive effects of high extent of cure on hardness, chemical and moisture resistance, it is also identified with brittleness and loss of flexibility. To obtain an optimum balance between chemical/moisture resistance and flexibility requires a threshold extent of cure. Beyond this threshold the film may be overcured resulting in cracks, film pull-out from the substrate, pinholes and excessive shrinkage. Therefore,

the need to systematically investigate the process of cure and/or film formation as a first step in the development of a wood or paper coating cannot be overemphasized. Herein lies the "missing link" in most studies dealing with the development of a practical coatings technology for wood or paper, that is failure to gain a fundamental understanding of the process of cure and/or film formation. On the other hand, recent developments in the field of polymer and adhesion science unrelated to chitosan/chitin or wood/paper coatings research have contributed to advancements in the understanding of the process of cure and network formation using a combination of thermomechanical and spectrophotometric techniques. These advancements are credited to the extensive work of Gillham of Princeton University[26], who described the cure behavior of epoxy resins in relation to a time-temperature-transformation (TTT) diagram and cure kinetics using a torsional braid analysis (TBA). This technique for quantitatively evaluating the cure behavior of thermosets has been adopted by some investigators to describe linear systems as well. For instance, Palmese and Gillham have described the conversion of polyamic acid to polyimide on the basis of the TTT cure diagram using a TBA[27]. This process is similar to chitin regeneration, i.e., both are thermal dehydration processes. Therefore, it is safe to say that related techniques, such as TBA and dynamic mechanical thermal analysis (DMTA) both should be viable options for revealing the transitional events associated with the transformation of chitosonium acetate to chitin. Additionally, the process could be described on the basis of TTT diagrams. An understanding of the cure behavior of the chitosonium acetate on the basis of TTT cure diagrams is likely to

significantly advance the ability of the paper/wood industry to employ biodegradable and recyclable chitin products as paper or wood coating agents. Kinetics analysis of the transformation of chitosonium acetate to chitin will provide quantitative information on the overall utility of chitin products in paper coating, and would help determine appropriate coatings and processing conditions in relation to desired end product characteristics.

1.1 OBJECTIVES AND OUTLINE OF STUDY

The overall intent of this study is to develop an understanding of the chitin-from-chitosan regeneration process. The specific objectives of this study are

(1). To evaluate the cure behavior of the ionic complex of chitosan on the basis of TTT cure diagrams.

(2). To determine and compare the kinetic parameters associated with the heat-induced transformation of various homologous ionic complexes of chitosan to chitin.

(3). To characterize various homologous of chitin in terms of their thermal transitions, and their recognition by enzymes and suspectibility to enzymatic degradation.

The study entails the description of novel techniques that provide both molecular and macromolecular-level information about chitin derivatives. These techniques are based on monitoring the behavior of chitin derivatives in situ or under post-exposure

conditions. This study is described in three sections, in addition to an introduction , literature review, and summary and recommended future studies, which deals with

(1). the kinetics of the heat induced conversion of chitosan to chitin, and the correlation between this heat-induced transformation and network formation of thermosetting resins;

(2). the cure behavior of N-acyl homologs of chitosan-based materials on the basis of time-temperature-transformation cure diagrams as well as a description of their morphology; and

(3). the kinetics of formation of N-acyl homologs of chitosan with formic, acetic, propionic and butyric acid, including thermal transitions, DS and enzymatic hydrolysis.

1.2 REFERENCES

1. Krassig, H.A., Cellulose:Structure, Accessibility and Reactivity, Polymer Monographs, Vol. 11, Gordon and Breach Sci. Pub., Yverdon, Switzerland, (1993).

2. Hosokawa, J., Nishiyama, M., Yoshihara, K., and Kubo, T., Ind. Eng. Chem. Res., 29, 800-805, (1990).

3. Hosokawa, J., Nishiyama, M., Yoshihara, K., and Kubo, T and Terabe A., Ind. Eng. Chem. Res., 30, 788-792, (1991).

4. Isogai, A., and Atalla, R. H., Carbohydr. Polym., 19, 25-28, (1992).

5. Kobayashi et al., In Proceedings of the 2nd Int. Conf. on chitin and chitosan, pp239-43 (1982).

6. Kurita, k., Sannan T., and Iwakura, Y., J. Applied Polym. Sci. 23, 511-515, (1979).

7. Kurita, k., Koyama, Y., and Taniguchi, A., J. Applied Polym. Sci. 31, 1169-1176, (1986).

8. Kurita, k., Chikaoka, S., and Koyama, Y., Chem. Letters, 9-12, (1988).

9. Hirano, S, Seino, S.H., Akiyama, Y., and Nonaka, I., Polym. Mater. Sci. Eng., 59, 897-901, (1989).

10. Chandy, T. and Sharrma, C.P., Polym. Sci. Technol., 38, 297-311, (1988), J. Colloid Interface. Sci., 130(2), 331-340, (1989).

11. Yabe, H., Y. Kawamura, Y. and Kurahashi, I., Jpn. Kokai Tokkyo Koho JP 63, 161,001, (1989).

12. Mizushima, M. Jpn. Kokai Tokkyo Koho JP 63, 165,307, (1988).

13. Maruca, R., Suder, B., J., and Wightman, J.P., J. Applied Polym. Sci. 27, 4827-4837, (1982).

14. Glasser, W.G., Todd, J. and Rajesh J., Personal Communications, (1995).

15. Allan, G. G., Carroll, J. P., Hirabayashi, Y., Murundamina, M., and Winterowd, J. G., Mat. Res. Soc. Symp. Proc., Vol. 197, 239-243 (1990).

16. Making Paper better with Shrimps, Nordic Pulp and Paper, 27 (2) 33-35, (1985).

17. Wei, Y.C., Hudson, S.M., Mayer, J.M., and Kaplan, D.L., J. Polym. Sci., Part A, 30, 2187-2193, (1992).

18. Muzzarelli, R.A.A , In Polymeric Materials for biomedical Applications, Dumitriu, S. and Szycher, M. eds, Marcel Dekker, NY pp430-40, (1992).

19. Biagini, G., Muzzarelli, R.A.A, Giardino, R., and Castaldini, C., In Proc. 5th Int. Conf. on chitin/chitosan" Princeton, NJ, USA, 199-207, (1991).

20 East, G.E., and Qin, Y., J. Appl. Poly. Sci., Vol. 50.1773-1779, (1993).

21. Averbach, B. L., "Film-forming capability of chitosan , in Proc.1st Int. Conf. on Chitin and Chitosan" Cambridge, USA, 199-207, (1978).

22. Hepturn, H.R., and Chandler, H.D., in: Proceedings of the 1st Int. Conf. on Chitin and Chitosan, Muzzarelli, R.A.A. and Pariser, Eds., MIT, (1978).

23. Mima, S., Miya, M., Iwamoto, R., and Yoshikawa, S., J. Appl. Polym. Sci., Vol. 28, 1909-1917, (1983).

24. Nakatsuka, S., and Andrary, A.L., J. Appl. Polym. Sci., 44, 17-28, (1992).

25. Dixon, B.G and Gomes, W.M., In 20th Proc. Water-borne, Higher-Solids, Powder, Coatings Symp. pp132-145, (1993).

26. Gillham, J.K., ASCHE J., 20, 6-12, 1974., and In: Structural Adhesives, Kinloch, A.J., Ed.,Elsevier Applied Sci. Pub., (1986).

27. Palmese, G.R., and Gillham, J.K., J. Appl. Polym. Sci., 34, 1925-1939, (1987).

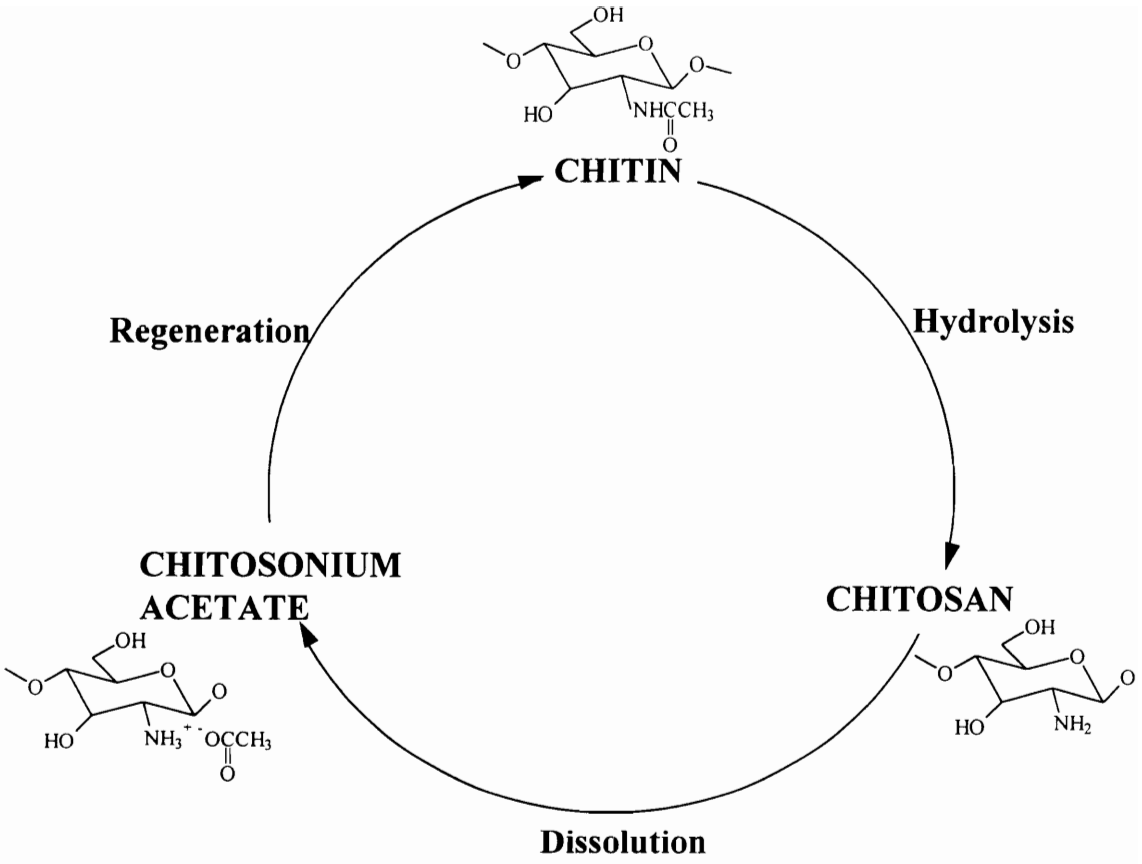

Figure 1-1. The regeneration of chitin from chitosan. This regeneration process involves thermal dehydration of the ionic complex of chitosan, chitosonium acetate.

CHAPTER 2

LITERATURE REVIEW

2.1 SCOPE

Chitin and chitosan represent a class of polysaccharides which are gaining interest among materials scientists. While chitosan is soluble in dilute organic acids, chitin is extremely difficult to dissolve. Therefore, the industrial utilization of chitin almost always involves its deacetylation to produce chitosan. However, it is difficult to completely deacetylate chitin without causing degradation of chitosan. Thus, chitosan contains N-acetylglucosamine and glucosamine units in varying proportions. The degree of N-acetylation (degree of deacetylation) and the sequence of acetyl groups dictate the properties of chitosan. Research on the utilization of chitosan in composites or plastics has drawn on thermal analysis methods. These methods are useful in so far as they provide information on degree of cure, viscoelastic response, molecular mobility etc. Dynamic mechanical thermal analysis is a useful technique for studying viscoelastic and cure properties of polymers, and has been applied in chitosan/chitin research.

Section 2.2 of this chapter provides a discussion of the structure, occurrence and morphology of chitin and chitosan and their potential applications. It also discusses the methods of isolation of chitin and preparation of chitosan, whilst providing illustrations of the various analytical methods which can be used to characterize the extent of deacetylation.

Section 2.3 presents a general discussion of the parameters that influence the thermomechanical behavior of polymers, and how this is revealed using the DMTA. It provides theoretical considerations of viscoelasticity of polymeric materials, whilst providing pertinent illustrations of the utilitzation of DMTA and related thermal methods in chitin / chitosan research.

In section 2.4 the phase transformation behavior of network forming polymers is outlined, and the concept of gelation and vitrification as depicted in a time-temperature-transformation (TTT) cure diagram is introduced. Finally, this section describes aspects of imidization, a parallel phenomenon to the regeneration of chitin from chitosonium acetate.

2.2 CHARACTERIZATION AND APPLICATIONS OF CHITIN/CHITOSAN

2.2.1 Occurrence, Chemical Structure and Morphology

2.2.1.1 Occurrence

Chitin is the second most abundant polysaccharide behind cellulose composing the largest portion of total biomass. It is present in close association with proteins and calcium carbonates in the shells of arthropods[1,2]. It is also present in fungal cell walls[3,4], marine lower plants and animals, and terrestial lower plants[5]. Chitin constitutes 1.4% of the fresh weight of insects. Crustaceans have 15-20% chitin in their shells[2]. The occurrence and potential sources of chitin is presented in the following **(Table 2-1)**[1]. Chitosan is usually derived by the chemical deacetylation of chitin. Nonetheless, it is present in fungi and specialized tissues of certain animals[6,7,8].

2.2.1.2 Chemical Structure

Chitin is a linear polysaccharide composed of β-(1→4)2-acetamido-2-deoxy-D-glucopyranose units. It is structurally similar to cellulose except for a substutition of an acetamide group in the C-2 position, instead of a hydroxyl group as in cellulose **(Figure 2-1).** As in cellulose each sugar unit present in chitin is rotated 180° with respect to each other. Consequently, chitin has a chitobiose repeat unit. Unlike cellulose, which is a homopolymer, chitin is considered as a heteropolymer because it is composed of both glucosamine and N-acetylglucosamine in various proportions. However, the subject of chitin as a heteropolymer has been debated. Zechmeister and Toth[9] have indicated that chitin is a homopolymer of acetylated glucosamine. Their conclusion was based on enzymatic hydrolysis of chitin that produced N-acetylglucosamine. However, it has been demonstrated by other scientists that there are some free amino groups in chitin as well[10,11].

Chitosan is the deacetylated form of chitin. As such it has an amino functionality in the C-2 position (**Figure 2-1**). However deacetylation of chitin is rarely complete, such that commercial chitosan has 10-25% of N-acetyl groups. Unlike chitin, where its heteropolymer character has been debated, chitosan is recognized by all scientists as a heteropolymer consisting of N-acetylglucosamine and glucosamine units. Scientists differ, however, on the sequence or the distribution of acetyl groups in chitosan. For example, Kurita et al.[12] have reported that when chitin is deacetylated under heterogeneous conditions the product has a blockwise distribution of acetyl groups. This

assertion was based on proton and carbon NMR experiments that produced frequencies of diads and triads consistent with a blockwise distribution of N-acetyl groups. Muzarelli and Rochetti [13] have reported to have observed a random distribution of acetyl groups in chitosan produced by homogeneous N-acetylation of chitosan. On the contrary, Varum and coworkers[14] have indicated that chitosan is characterized by a random distribution of acetyl groups irrespective of the conditions of preparation.

2.2.1.3 Morphology

Chitin exists in three crystalline forms, α, β and γ[15-19]. Most studies that have dealt with the morphology of chitin have been on α, and β chitin. The morphology of γ-chitin is poorly understood.

Blackwell and coworkers[17-19] have established, by X-ray difraction, that α-chitin has an orthorombic unit cell with dimensions a = 4.74A, b = 18.86A , and c = 10.32A, and antiparallel chain or sheet arrangement. They reported that the chains are linked by N-H...O=C hydrogen bonds between amide groups, and that all hydroxyl groups are involved in hydrogen bonding. These were described as O-3'-H...O-5 intramolecular, O-6-H...O-6' intermolecular and O-6'-H...O-7=C intramolecular hydrogen bonds. On the other hand, β-chitin has a monoclinic unit cell with dimensions of a = 4.85A, b = 9.26A, and c = 10.38A and a parallel chain structure. It is also characterized by the presence of N-H...O=C hydrogen bonds between amide groups.

α-chitin is the most stable form, and it also occurs more abundantly in nature than β-chitin. Major distinctions between these two forms of chitin are their swelling

and deacetylation behavior. β-chitin can readily be swollen by water, whilst α-chitin is relatively stable in water. This difference has been attributed to the existence of extensive intersheet bonding in chitin due to CH_2OH interactions with the carbonyl groups of adjacent sheets[19].

In a comparative deacetylation study of the two chitin forms, Kurita et al.[20] have demonstrated that β-chitin is more amenable to complete deacetylation without degradation. The sources and characteristic properties of chitin are presented in the following **Table 2-2**[21-30].

Using ^{13}C CP/MAS NMR, Vincendon and Roux[31] have established major differences in the spectrum of α-chitin and β-chitin. Both forms of chitin displayed a spectrum consisting of eight signals identified with the eight carbons of N-acetylglucosamine units. The chemical shifts are given in **Figure 2-2.** However, the signals identified as the C-3 and C-5 carbon atoms showed a marked distinction. Whilsts α-chitin showed well resolved double shifts, β-chitin displayed the two shifts as a single, relatively broad shift **(Figure 2-2).** Takai et al.[32] and Focher et al.[33] have independently made similar observations. Takai et al. have proposed that this difference may be due to changes in the configurations of C-3 and C-5 substituents on account of hydrogen bonding. It has been demonstrated by Vincendon and Roux[31] that β-chitin can be converted to α-chitin by dissolution followed by reprecipitation. These authors utilized lithium thiocyanate as a swelling agent at 100°C for 8 hours or 6N HCl at 25 °C for 1 hour. They were able to observe individual carbon signals for C-3 and C-5 following such treatments of β-chitin.

However, the signals were characterized by broad bases. This produced the interpretation that the transformation of β- to α-chitin is accompanied by the significant formation of amorphous regions.

2.2.2 Isolation and Deacetylation of Chitin

2.2.2.1 Isolation of Chitin

The commercial production of chitin involves isolation from the outer shells of crustaceans, mostly shrimps and crabs[1,2,4,5]. The isolation of chitin from these sources includes demineralization and deproteination. The process of demineralization involves treatment of ground shrimp or crab shells with 0.5-0.8 N HCl. This treatment ensures removal of predominantly $CaCO_3$ and also $Ca_3(PO_4)_2$. The demineralized material, comprising about 60-85% chitin, is treated with 1% w/w NaOH at room temperature for few minutes and washed several times to obtain chitin devoid of proteins. A scheme of the isolation method is presented **(Figure 2-3).**

2.2.2.2 Deacetylation of Chitin

2.2.2.2.1 Chemical Methods

The preparation of chitosan on a commercial scale involves deacetylation of chitin. This is accomplished by treatment of chitin with 47-50% w/w NaOH at 80-100°C for 2-6 hrs, under a blanket of nitrogen. The residue is washed thoroughly with water to obtain alkali-free chitosan. Commercial chitosan generally has degrees of deacetylation of 60-90%. A scheme of the deactylation method is presented **(Figure 2-3).**

The deacetylation of chitin by the above method was first described by Rigby[34] who reported about 82% deacetylation. Since then there have been several modifications of the process with each of the scientists involved claiming a superior form of deacetylation. For example, Horowitz et al[35] described a process of deacetylation which involved fusion of chitin with solid NaOH at 180°C under nitrogen, and precipitation of the chitin-NaOH melt into ethanol. They claimed 95% level of deacetylation. Additionally, Peniston and Johnson[36] produced chitosan directly from crab waste. Their procedure involved treatment of crab shells with 30-35% alkali solution at 120°C whereby simultaneous deacetylation and removal of proteins and minerals is accomplished.

However, all these methods are limited by extensive degradation of chitin. Other scientists have published on novel approaches which produce high extents of deacetylation without degradation. For example, Pelletier et al.[37] and Focher et al. [33] have independently described deacetylation techniques based on "thermo-mechano-chemical" and "flash" treatments, respectively. The method of Pelletier et al. involved mercerization of chitin in 50% NaOH solution at 4°C for 24 hrs. The alkali-swollen chitin is suspended in 10% NaOH solution and fed into a reactor at 210-230°C and steam-treated for 90 sec. This treatment is followed by a sudden decompression of the material in a similar fashion as steam explosion of biomass. These authors have claimed complete deacetylation of the material without degradation. Focher et al. have previously described a related method to Pelletier et al. Their approach involved

treatment of chitin with 40% alkali solution for 30-270 minutes at 140-190°C under saturated steam conditions, with subsequent explosion of the material. They did not only claim complete deacetylation without degradation but that the chitosan produced by their method is more crystalline than conventionally-derived chitosan.

In a previous development, Domard and Rinaudo[38] have employed thiophenol and NaOH for deacetylation of chitin. Thiophenol is reported to prevent degradation of chitin and to act as a catalyst for speedy deacetylation. Focher et al. have pointed out that this procedure produces chitosan with non-uniform blocks of N-acetylglucosamine and glucosamine units and having different properties in comparison to commercial chitosan.

Although not of commercial value at the present, a method of directly isolating chitosan from fungal cells (recall chitosan is present in fungal cells) has been described by Arcidiacono and Kaplan [7]. This isolation method is shown schematically **(Figure 2-4).**

2.2.2.2.2 Bioconversion of Chitin to Chitosan

Chitin deacetylase enzyme catalyzes the conversion of chitin to chitosan by deacetylation of N-acetylglucosamine units [39]. Kafetzoupoulou and coworkers have started a study which is aimed at evaluating the use of chitin deacetylase for the conversion of chitin to chitosan and/or the biosynthesis of chitosan from fungi[40]. The advocacy for the enzymatic deacetylation of chitin is on the basis that the various chemical methods of commercial value produce chitosan with a broad range of

molecular weights and properties. They are of the opinion that these property variations are not useful for biomedical applications which require specific properties. However, to date no report is found in the literature that describes enzymatic deacetylation of chitin.

2.2.2.2.3 Microcrystalline Chitin and Chitosan

The term microcrystalline describes chitin or chitosan that has been subjected to physical and/or chemical methods to remove non ordered regions[41]. The preparation of microcrystalline chitin was first described by Dunn et al[42]. They utilized hydrochloric acid and elevated temperature for the removal of the disordered regions. Austin and Brine[43] have described a modification of the above method whereby a mixture of phosphoric acid and a lower aliphatic alcohol, e.g propanol was used. This method was reported to be superior to that of Dunn et al. because it ensures complete removal of non-ordered regions. The process of manufacturing microcrystalline chitosan was first described by Struszczyk[48]. This author reported that this form of chitosan is more suitable for biomedical applications on account of high bioactivity, high reactivity and chelating properties, and less variability. His process of microcrystalline chitosan formation involved dissolution of chitosan in aqueous acetic acid, followed by thermal treatment of the solution at 70°C , reprecipitation in NaOH solution and elaborate washing. At present microcrystalline chitosan is produced on a pilot scale by Firexta Oy, a Finnish company, and the Institute of Chemical Fibers in Poland. The schemes for microcrystalline chitin and chitosan preparation are shown in **Figure 2-5**[42,48].

2.2.3 Determination of Degree of Deacetylation (DD) of Chitosan

The degree of deacetylation (DD) expresses the relative ratios of N-acetylglucosamine and glucosamine units in chitosan. It influences profoundly the solubility of chitosan as well as its solution properties[45,46]. Various analytical methods have been utilized to determine this critical parameter. These methods include infrared spectroscopy[47-51], pyrolysis-gas chromatography[52], ultraviolet spectroscopy[53], circular dichroism[54], solid state ^{13}C NMR[33,37], thermal analysis[55], various titration schemes[56-60], acid[61] and enzymatic hydrolysis[62] and subsequent separation by HPLC, and more recently by near infrared spectroscopy[63]. The following discussion is devoted to the various methods which have received significant attention.

2.2.3.1 Titration Schemes

The DD-determination of chitosan by titration was first described by Broussignac[56] who formed the amine hydrochloride of chitosan and carried out a potentiometric titration of the excess acid. Other examples of titration schemes are presented below.

Rutherford and Austin have employed a titration procedure which involved hydrolysis of the acetyl groups of chitosan with strong alkali to produce acetic acid[57]. They were successful in distilling the acetic acid as an azeotrope with water and carrying out the titration. In another procedure directly related to Broussignac's method, Hayes and Davies[58] formed the hydrochloride salt of chitosan by dissolution in dilute HCl which was dissolved in water and titrated potentiometrically using NaOH.

Alternatively, Moore and Roberts[59] have employed a method involving treatment of chitosan with a solution of sodium periodate. The method involves the cleavage of α-amine alcohol units by sodium periodate followed by titration of the unconsumed periodate using sodium arsenite. More recently Raymond et al. have employed conductometric titration with some degree of success[60]. This method was based on monitoring the change in conductance of H^+ and OH^- with volume of titrant added. They reported that at a high acetyl content, DD from conductometric titration differed significantly from that found by solid state NMR. The reverse was true at low acetyl content. This implies the procedure is only useful at low acetyl contents. They proposed that at high acetyl content, the material is more crystalline such that only the amino groups in the amorphous regions and the surfaces of the crystallites are subjected to titration. Consequently, they indicated that it is necessary to supplement conductometric titration with other methods when dealing with chitosan with a wide range of DD.

2.2.3.2 FTIR

A quantitative measure of the extent of N-acetylation of chitosan employing FTIR spectroscopy has been devised by Domszy and Roberts[47]. In a typical FTIR spectrum, three absorption bands of importance are recognized at 1655, 1550 and 1310 cm^{-1}. They are designated as amide I, II and III, respectively.The method of DD-determination is based on utilizing the amide I band as a measure of the N-acetyl group content and the hydroxyl band at 3450 cm^{-1} as an internal standard to account for variation in film thickness or chitosan concentration. Other absorption band ratios have

been utilized by Sannan et al.[48]; [1550 cm^{-1} (amide II) as a measure of N-acetyl group content and C-H band and 2878 cm^{-1} as internal standard], Miya et al.[49]; [amide I vs. C-H (2878cm^{-1})]. Domszy and Roberts rejected Sannan et al.'s method on the following proposition; (1) the amide II band varied between 1595 and 1550 cm^{-1} depending on extent of N-acetylation, and that such variation will affect the authenticity of DD by such measurements; (2) the absorbance at 2878cm^{-1} depended on the length of N-acyl group, such that a different calibration is needed for various N-acyl groups where one is dealing with chitosan produced by homogeneous N-acylation. This proposition is supported by Muzarrelli et al.[64]. They have also demonstrated that calibration lines are affected by the method of deacetylation such that, unless the right calibration is used, DD-values from FTIR are prone to errors; and (3) the DD of Sannan et al. varied from those of other methods.

Previously, Sannan et al. have claimed without proof that the absorption of moisture by chitosan will affect the hydroxyl band at 3450cm^{-1} and DD determined using this band as a reference would be erroneous. However, Domszy and Roberts have demonstrated that adsorbed moisture does not significantly influence this band. It is worth noting that the values of Domszy and Roberts' work compare favorably with other methods.

Other studies have suggested that FTIR-data, which depend on deconvoluting the amide I band, have inherent resolution difficulties, particularly at low acetyl contents [51].

2.2.3.4 CP-MAS ^{13}C-NMR

Several reports have indicated that CP-MAS ^{13}C-NMR is the method of choice for the determination of N-acetyl content (Pelletier et al.[37] ; Focher et al.[33]; Raymond et al.[60]). The quantitative principle underlying the determination of degree of deacetylation involves the comparison (ratio) of the integral of the acetamido-methyl resonance (this is proportional to the acetyl content) to the resonance of the glucose carbons.

2.3.3.4 Other Methods

Acid[61] and enzymatic hydrolysis[62] have also been employed for DD determinations. These methods are based on the degradation of chitosan by appropriate enzymes/acid and subsequent separation of N-acetyglucosamine and glucosamine/acetic acid. The equations permitting quantitative determination of DD are as follows;

$$DD\ (\%) = \left\langle \frac{161X}{43 - 42X} \right\rangle 100 \qquad \text{(acid hydrolysis)}^{61}$$

where X = m_x/M ; m_x is the amount of acetic acid, and M is the mass of the starting material, 43 is the molecular weight of the acetyl group, and 161 is the molecular weight of N-acetylglucosamine;

$$DD\ (\%) = \left\langle \frac{GlcN}{GlcN + GlcNAc} \right\rangle 100 \qquad \text{(enzymatic hydrolysis)}^{62}$$

where GlcN and GlcNAc are the concentrations of glucosamine and N-acetylglucosamine, respectively. The accuracy of these methods depends on whether or not complete hydrolysis of chitosan is achieved.

2.2.4 Determination of Molecular Weight of Chitin/Chitosan

The molecular weight of chitosan can be determined by HPLC[65], viscosimetric measurements[66], and light scattering[67].

Using acetic acid as eluent in the solvent delivery system and dextran as molecular weight standards, Wu has employed HPLC to determine the molecular weights of a series of chitosans prepared by varying the time of deacetylation[65]. They concluded that the molecular weight decreases considerably with time of deactylation **(Figure 2-6).** Muzarrelli et al. have studied the molecular weight of chitin and chitosan using light scattering[66]. They reported that chitosan has a weight average molecular weight of 4×10^5–7×10^5. Additionally, viscosimetric methods, which make use of the Mark-Houwink equation ($[\eta] = K\times M_w^a$), have been utilized in molecular weight measurements of chitin and chitosan[67]. However, Muzarrelli et al.[66] and Domard et al.[68] have indicated that the two critical parameters, K and a, of the Mark-Houwink equation vary with type or source of chitosan and conditions under which viscosities are measured. For example, different values of K and a have been reported as follows 8.93×10^{-2} and 0.71[69], 1.28×10^{-4} and 0.85[70], and 1.81×10^{-3} and 0.93-1.26, respectively[71]. As such, molecular weights from viscosimetric measurements are unreliable. Nonetheless, recent work by Wang et al. has established a relationship between DD and the parameters K and a as follows[67];

$$K = 1.64\times10^{-30} \times DD^{14}$$

$$a = -1.02\times10^{-2} \times DD+1.82$$

Therefore, knowledge of DD permits the determination of molecular weights using the above equations for K and a, and the Mark-Houwink equation. Consequently, they have derived a graphical dependence of K and a on the degree of deacetylation (**Figure 2-7**)[67]. Values of molecular weights of chitin have been presented previously **(Table 2-2).**

2.2.5 Enzymatic Hydrolysis of Chitin and Chitosan

2.2.5.1 Introduction

The combined action of different enzymes working on specific components of organic materials results in the degradation of such material mixtures. Enzymes that degrade organic susbstrates, such as polysaccharides, occur in water and in soil, usually as a result of secretion of microorganisms during their life and/or feeding cycle(s). Such enzymes also occur in the digestive tracts of animals. Major enzyme groups that degrade or hydrolyze chitin and chitosan are described below with specific literature reports.

2.2.5.2 Chitin Deacetylase

Chitin deacetylase catalyzes the conversion of chitin to chitosan by causing deacetylation of the N-acetylglucosamine units. This enzyme was first identified and extracted from the fungus Mucor rouxii [39]. Various studies have been conducted on this enzyme since it was first described. These include the work of Aruchami et al.[72] , Trudel and Asselain [73] and, Kafetzoupoulous et al.[40]. The latter workers have obtained pure chitin deacetylase from Mucor rouxii. They reported that this enzyme needs at least four N-acetylglucosamine units in sequence before catalysis is initiated, and that its action is inhibited by carboxylic acids.

It is generally believed by various scientists that the presence of chitosan in fungi is related to the cooperative action of chitin synthetase and deacetylase[74,75]. That is, synthetase produces chitin by polymerization of N-acetylglucosaminyl units, then deacetylase hydrolyzes N-acetylglucosamine units to glucosamine units. That the cooperative action of chitin synthetase and deacetylase is required for the biosynthesis of chitosan has been proved independently by Bartnicki-Garcia[75], and Davis and Bartnicki-Garcia[74]. These scientists have demonstrated that chitin deacetylase acts more rapidly on nascent chitin compared to preformed chitin. They proposed that the difference in deacetylases' action on the two forms of chitin is related to differences in morphology. Preformed chitin was identified as a crystalline material with characteristically extensive hydrogen bonding between chitin chains. Consequently, N-acetylglucosamine units were less accessible to the hydrolytic action of the enzyme.

2.2.5.3 Chitinases

The combined action of two classes of chitinase results in the complete hydrolysis of chitin to N-acetylglucosamine (GlcNAc) units. Chitin is first hydrolysed by endochitinase to oligosaccharides and N,N-diacetylchitobiose[76]. Further hydrolysis to N-acetylglucosamine residues depends on the action of β-N-acetyl-hexosaminidase, which catalyzes the conversion of these products to GlcNAc. Though β-N-acetyl-hexosaminidase degrades all oligomers from the action of chitinase, it does so at a decreasing rate as the degree of polymerization increases[77]. These chitin-degrading enzymes occur in mixture in bacteria, fungi, plants and animals[78,79,80], and they can

degrade chitin of different sources. This is exemplified by the fungus *Aspergillus nidulans*. It bears enzymes (β-N-acetylglucosaminidase) that degrade chitin oligomers, enzymes (endochitinase) that cleave chitin chains, and enzymes (chitin deacetylase) that deacetylate chitin. These enzymes can as well act on chitin from other sources, including prawn and crab-derived chitin. Another example is the case of bacterial enzymes from *Streptomyces olivaceoviridis*. These contain various forms of chitinolytic enzymes that can act on fungal chitin and other forms of chitin. Microbial enzymes have been found to act on chitin having degrees of deacetylation of 53-76%. Using fungal chitinase, and chitinases from other microbial sources, Ohtakara et al.[80] found that the enzymes were most active on chitosan with N-acetylation of 20-45%. This produced the conclusion that chitinase activity may be studied using chitosan, provided the enzyme is devoid of chitosanase (chitosan-degrading enzymes).

Aiba[81] studied the action of bacterial enzymes on homogeneously produced N-acetylated chitosan. He reported that this type of chitin-degrading enzyme does not recognize differences in the sequence of N-acetyl groups along the chitosan chain; random vs. block-type distribution. This conclusion was reached on the basis that heterogeneously deacetylated chitin and homogeneously N-acetylated chitosan with the same extent of N-acetylation were hydrolysed at similar rates.

2.2.5.4 Chitosanase

Chitosanase, a chitosan-degrading enzyme is common in the bacterium *Bacillus circulans* and plant tissues, and the lysis of fungal cell walls. Yakubi[82] successfully

isolated this bacterium from soil and purified it to produce enzymes that hydrolyzed chitosan with degrees of deacetylation of 50-100%. However, the hydrolysis was such that only glucosamine dimers and trimers were produced. That the chitosanolytic hydrolysis produces only di- and trimers of glucosamine is further supported by the work of Pelletier et al.[37] involving the action of *Bacillus megaterium*-derived chitosanase. On the other hand, Osswald et al.[83], using chitosanase derived from plant tissues and bacteria (*Streptomycetes griseus*), detected glucosamine as well as oligomers of glucosamine. These authors demonstrated that chitosanolytic activity is influenced by the source of chitosan. They concluded that chitosanase substrate preference is as follows; shrimp>krill>crab.

2.2.5.5 Lysozymes

Chitin and chitosan are degraded to varying extent by lysozymes. These enzymes usually occur in the lymphoid system of vertebrates. Tokura examined the bioactivity of chitin and its derivatives on animal tissues using lysozymes[84]. He concluded that chitin derivatives were more susceptible to lysozyme action. Similar conclusions have been reached independently by Tokura et al.[85], Sashima et al.[86], and Kurita et al.[87].

Tokura et al. dealt with lysozymatic hydrolysis of chitin, carboxymethyl, butyrl, glycol, and dihyroxypropyl chitin. They reported that carboxymethyl chitin showed about 80% weight loss after one hour assay. On the contrary, the other materials exhibited not more than 4% weight loss in the same period. Chitin was the least susceptible to lysozyme hydrolysis. Using 31% deacetylated chitin fibers, 31%

deacetylated chitin films, and mercapto derivatives of chitin, Sashima et al. made similar observations. That is the order of susceptibility to lysozyme hydrolysis was as follows; 31% deacetylated chitin fibers<31% deacetylated chitin films< mercapto derivatives of chitin.

Aiba has studied the hydrolysis of chitosan with comparable extent of deacetylation, but produced by two different methods[88]. He concluded that chitosan produced by alkali hydrolysis under heterogeneous condition, and having 30% N-acetyl content is a block copolymer. On the other hand one produced by homogeneous N-acetylation of highly deacetylated chitin is a random copolymer. The latter chitosan only became susceptible to lysozyme hydrolysis at more than 50% N-acetylation compared to 30 % for the former.

2.2.6 Applications of Chitin and Chitosan

2.2.6.1 Introduction

One of the most desired properties of chitosan is its chelating ability. It can selectively bind materials such as cholesterol, fats, metal ions, and proteins. Its chelating ability has been utilized in areas of applications such as food processing and water purification[89]. Other useful properties of chitosan are antifungal action[90], wound healing acceleration[91,92], stimulation of immune response[93]. Studies have shown that chitosan is a good membrane forming polymer, and such membranes have found applications in water clarification and filtration[94], fruit coatings[95], and controlled release of

agrochemicals[96]. Other areas of application include papermaking[97-100], fibers[101,102], and biodegradable composites[103-105].

This section is centered on the following application areas; chelation, membranes, coatings and paper-making, fibers, and biodegradable composites. It suffices to say that chitosan and also chitin have major uses in biomedical applications, but a discussion in that direction is beyond the scope of this dissertation.

2.2.6.2 Chelation with Chitosan

The preponderance of amino groups in chitosan provides qualification for coagulation and flocculation, where chitosan can interact with negatively charged materials including proteins[106], solid dyes[107] and metal ions[107-110]. In the selective take-up of metal ions, it is believed that the nitrogen of the amino groups acts as an electron donor, thereby forming a complex. Complex formation was first described by Tzsezos[109] and later by Ogawa et al.[111]. These scientists proposed that metal ions could coordinate with 4 amino groups in D-glucosamine dimer units of chitosan. Muzarrelli compared the chelating ability of chitin, chitosan and other polymers and concluded that chitosan exhibited the best performance[108]. He related this conclusion to the high density of amino groups in chitosan. In a related study, Wightman and coworkers evaluated the efficacy of chitosan for the removal of chromium ions from water[112]. They reported that the free amino groups in chitosan removed ions more efficiently than acetyl groups in chitin. Contrary to these reports, Kurita et al.[113] have indicated that

chelation is not only controlled by the preponderance of amino groups, but also by factors such as morphology (crystalline vs amorphous) and hydrophilicity.

They reported that chitosan with 55% extent of deacetylation prepared under homogeneous conditions were essentially amorphous and water-loving. This exhibited better chelation over one prepared under heterogeneous conditions that is crystalline.

The capacity for binding with metal ions has been enhanced by various chemical modifications. Kurita et al.[113] and Koyama and Taniguchi[110] have independently demonstrated that crosslinking with glycine and/or glutaraldehyde produced a more than 22-fold increase of the adsorption capacity of chitosan. Furthermore, chitosan complexion with other polymers, such as glucan can be used to enhance the metal adsorption of chitosan[109,114].

2.2.6.3 Chitosan Membranes

Chitosan membranes can be produced by one of several methods, including evaporation of solvent from chitosan solution[115], crosslinking with reactive functionalities[116,117], chelation with anionic counterions, and complexion with other polymers[109].

The most often used method is the evaporation of solvent from chitosan solution. Such membranes are usually produced by dissolution of chitosan in dilute acetic acid and casting onto a suitable surface such as glass.

The preparation of crosslinked chitosan membranes involves the use of such reactive reagents as aldehydes, carboxylic anhydrides, and glutaraldehyde. For example,

Harino et al.[116] have reported on a method of formation of N-arylidene and N-acyl chitosan membrane. This involved formation of thin chitosan films from acetic acid solution, and immersion of such films in either aldehyde or carboxylic anhydride accompanied by heating to effect crosslinking. Chitosan membranes have also been formed with various counterions or polymers including octylsulfate and alginate[118,109].

Chitosan membranes have good permeability and have found applications in selective separation of water-ethanol mixtures. In an extensive study, Harino et al. examined a series of chitosan membranes with different N-acyl groups[116]. They concluded that depending on the casting solvent these membranes displayed different permeability rates. N-acetyl chitosan membranes however , were the best. In a related study, PVA-chitosan membranes have been described as efficient materials for the active transport of organic ions [119] such as benzoate, and halogen ions.

2.2.6.4 Coatings, Composites, Fiber-making and Paper-making with Chitosan

A novel method of utilizing chitosan in paper-making has been reported by Allan et al.[99]. Their approach involves precipitation of chitosan onto wood, glass, and polypropylene fibers, and forming paper sheets from the chitosan-coated fibers. It was observed that chitosan forms the most uniform coating with wood fibers, and strongly adheres to wood surfaces. It was possible to form paper-like sheets from chitosan-coated wood and glass fibers, but not from coated polypropylene fibers. Allan et al. observed better tensile strengths with the wood fibers than with glass fibers (0.65kN/m vs. 0.15

kN/m). A comparison of chitosan-coated and non-coated wood fibers indicated improved tensile strength in the former (0.65 kN/m vs. 0.41 kN/m).

Additionally, it has been reported that the treatment of the surface of paper with 1% and 0.5% chitosan solution increased the burst strength and folding endurance[120], and color fastness[121], respectively. In another paper-making technology with chitosan, Aizawa and Noda treated photographic paper with a layer of chitosan , where the surface resistance to electrostatic charging increased considerably over non-treated paper[122]. Chitosan solutions have been utilized as a paper-making additive with significant improvement of wet strength[97,100].

Isogai and Atalla from the US Forest Products Lab used an innovative approach to co-dissolving chitosan and cellulose[105]. They discovered that anhydrous trifluoroacetic acid (TFA) produces a homogeneous solution of chitosan and cellulose without causing degradation. On further dilution with acetic acid they could obtain a solution of low viscosity for easier casting of films. Neat films were obtained following solvent evaporation and neutralization with alkali. X-ray diffraction and scanning electron microscopy both suggested extensive mixing of the components at the molecular level. Using aqueous solutions of chitosan (pH 5) and finely suspended cellulose powder, Hosokawa et al. discovered that strong, filled composites can be formed by heating without prior neutralization[103, 104]. These authors have concluded that biodegradable composites with useful mechanical properties could be produced by these methods.

Several attempts have been made to spin chitosan and chitin into fibers [123-125]. Whilst significant success has been achieved with spinning of chitosan fibers, chitin fibers have been extremely difficult to produce. This is related to differences in solubility. Chitosan is readily soluble in dilute organic acids. The preferred method of producing chitosan fibers has therefore always involved wet-spinning chitosan solutions in dilute organic acids into an alkaline bath . A method of producing chitin fibers without having to deal with solubility problems have been devised by East and Qin[101]. Their approach involved formation of chitosan fibers by the usual method and subsequent acetylation. They reported that chitin fibers produced by this method exhibited improved thermal stability and tensile strength over chitosan fibers.

2.2.7 Crosslinking Reactions with Chitosan

Various crosslinking schemes have been devised to improve the performance of chitosan. These crosslinking agents include epichlorohydrin[102] , glutaraldehyde[117,126,127], and molybdate polyanions[128]. Kaplan and coworkers have crosslinked chitosan films by immersion of films in epichlorohydrin under basic conditions, and at elevated temperatures[102]. They observed that the the dry and wet tensile strengths of chitosan increased from 51MPa and 1MPa to 136MPa and 13MPa, respectively following crosslinking (network formation). The improved dry and wet tensile strengths can be attributed to better stress transfer and limited absorption of water by the network structure, respectively.

In another crosslinking method, Draget et al. have employed in situ mechanisms to crosslink chitosan[128]. The method involved dispersion of solid molybdate in a buffered chitosan solution whereby the polymer is crosslinked by formation of heavily negatively charged molybdate polyoxy anions.

Various scientists have reported on the use of glutaraldehyde as a crosslinking agent for chitosan. For example, Koyama and Taniguchi have indicated that crosslinking of chitosan with glutaraldehyde produced an amorphous material[126]. In another report, Roberts and Taylor examined the effects of several parameters, including temperature and acetic acid concentration, on the gelation of chitosan dissolved in acetic acid/glutaraldehyde systems[117]. They observed that the time to gelation decreased with increased temperature and with decreased acetic acid concentration, but increased with increased chitosan or glutaraldehyde concentration. The decreased rate of gelation with decreased acid concentration produced the conclusion that the gelling mechanism involves unprotonated amine groups. These authors proposed that the mechanism of crosslinking of chitosan with glutaraldehyde is one of Schiff base formation as shown in **Figure 2-8.** This proposal contradicted that of Richards and Knowles[127], and later that of Muzarrelli et al.[129]. The latter scientists have previously proposed that the mechanism involved formation of Michael-type adducts between α, β-unsaturated aldehyde groups in glutaraldehyde and amino groups in chitosan as shown in **Figure 2-9**. Roberts and Taylor have refuted this proposal on account that UV/visible light and NMR spectroscopy did not give any evidence of Michael-type adducts.

In another development Hosokawa et al. have claimed a crosslinking reaction between chitosan and cellulose[103]. Using chitosan dissolved in acetic acid and finely suspended cellulose powder, these scientists formed strong composites by heating. Carbonyl enrichment of the cellulose component of such composites by oxidation with ozone was reported to result in greater strength improvements. They concluded that the strength increase was due to crosslinking of chitosan with the carbonyl groups of cellulose.

2.3 DYNAMIC MECHANICAL ANALYSIS OF POLYMERIC MATERIALS

2.3.1 Thermomechanical Properties: A General Overview

The viscoelastic response of polymers results in deformation which inherently is influenced by temperature and rate of deformation[130-139]. Such a dependence can be illustrated by a thermomechanical spectrum **(Figure 2-9).** Thermomechanical properties are influenced by several factors which are collectively called the polymer parameters. These factors include chemical structure and composition, topology, rheology, molecular weight, additives, and morphology[131,139] . A brief discussion is presented in the following paragraphs.

A thermomechanical spectrum may comprise several distinct zones namely: a glassy region, a glass-to-rubber transition zone, an entanglement zone, a rubbery plateau, a viscous flow and melting transition **(Figure 2-10)**[130-139]. The shape of the spectrum provides vital molecular and macroscopic level information on structure-property relationships. The regions of the spectrum shown by a particular polymer are

dictated in large part by its morphology. Over a large range of temperature (or frequency), polymers typically exhibit a number of transitions which are assigned to specific molecular relaxations. One such relaxation is the glass transition, often accompanied by several decades change in the modulus or stiffness of the material in question. On a molecular scale, the glass transition (T_g) corresponds to the occurrence or onset of large scale cooperative motions which give rise to maximum energy dissipation. The temperature dependence of this transition is influenced by the balance between intermolecular and intramolecular forces. For example, dipolar intermolecular interactions cause an increase of T_g because of greater energy necessary to disrupt the inter-chain forces. The magnitude of intramolecular interactions is also influenced by chain rigidity. For example, polyimides, which are characterized by rigid backbones, tend to show very high T_gs as opposed to polyethylene with flexible backbone chains. The breadth of the T_g is dictated by such factors as network structure, heterogeneity vs homogeneity etc. For instance, highly crosslinked systems show broad glass transitions[131,139]. In the glassy state, polymers generally exhibit very limited molecular motions. Typically, internal energy is insufficient to give rise to large scale motions. On the other hand rotation of specific side groups give rise to glassy-state transitions (sub-T_gs). Such transitions have important consequences on impact properties[140]. Polymers with characteristically broad sub-T_gs have useful impact properties. Above the T_g, the polymer responds to perturbations or stresses as a viscoeleastic response giving rise to a rubbery region. The length of the rubbery region is largely influenced by topology, i.e.

linear, branched or crosslinked as depicted in **Figure 2-10**. The rubbery region can be extended indefinitely by enough chemical crosslinks[130,131,141].

Uncrosslinked amorphous polymers show viscous flow when the chains have acquired sufficient energy to disentangle on the time scale of stress application or perturbation. Therefore, the molecular weight has a significant influence on the temperature of disentanglement and viscous flow.

Additives or fillers can have a significant influence on the thermomechanical spectrum. For example, plasticizers pervade and decrease inter-chain interactions, thus facilitating molecular motions. This is reflected in the lowering of T_gs[130]. The amount of additive incorporated into a polymer can have repercussions on whether it is stiff, compliant, elastomeric etc. For example the T_g of PVC can be lowered from 85 to -30 C by the addition of a plasticizer. PVC may thereby become a soft material at room temperature[136].

Semicrystalline polymers exhibit high moduli below T_g due to the higher modulus of the crystals compared to the amorphous component. Such crystallites act as physical crosslinks providing an elevated modulus prior to eventual melt down. The degree of crystallinity influences the level of modulus drop that occurs in the glass-to-rubber transition region. Semicrystalline polymers generally show modulus of 10^{10} to 10^7 Pa as opposed to 10^9 to $10^6/10^5$ Pa typical of amorphous polymers[141].

2.3.2 Principles of Dynamic Mechanical Thermal Analysis

2.3.2.1 Theoretical Considerations

The fundamental principle underlying dynamic mechanical testing of polymers involves applying a small sinusoidal stress to the polymer, and monitoring the strain response[130-139,141,142].

This strain response is often expressed as complex modulus, E*, which is divided into two components, namely storage modulus (E') and loss modulus (E''). The storage modulus measures the energy stored per cycle of strain, and this is associated with the stress in phase with the strain **(Figure 2-11).** The loss modulus is a measure of the energy lost per cycle, and this is associated with the stress 90^{o} out of phase with the strain (**Figure 2-11**). The phase angle, δ, has two theoretical limits; 0^{o} for a perfectly elastic material (described as a Hookean material) and 90^{o} for a perfectly viscous material (described as a Newtonian fluid). Generally, polymers exhibit an intermediary behavior of the two extremes. The relative importance of viscous and elastic behavior is expressed by a parameter called tan δ. This measures the energy dissipation per cycle of stress. Below the glass transition temperature polymers exhibit limited molecular motions and are characterized by little energy dissipation reflected by small tan δ values. On the other hand above the T_g, molecuar mobility is so rapid near the liquid state such that relaxation times of the polymer chains no longer coincide with the applied stress. This is reflected in little dissipation, giving rise to an elastic as opposed to viscous behavior[130-139,142]. At the T_g the time constants for molecular relaxation coincide with

the applied stress, and correspond to maximum energy dissipation. In a practical sense, the magnitude and breadth of tan δ indicate the temperature range over which a polymer can absorb energy of given frequency[130-139,142].

In mathematical terms the stress and strain response from DMTA measurements take the form

$$\varepsilon = \varepsilon_o \sin\omega t$$

$$\sigma = \sigma_o \sin(\omega t + \delta)$$

where ω is the angular frequency (2πf), t is the period, δ is the phase angle, σ_o and ε_o are the maximum stress and strain amplitudes. The expression for the applied stress may be written in terms of addition formula as

$$\sigma = \sigma_o \cos\delta \sin\omega t + \sigma_o \sin\delta\cos\omega t$$

The ratio of stress to strain gives expressions, below, for the storage (E') and loss (E") moduli as depicted **(Figure 2-12)**.

$$E' = \sigma_o/\varepsilon_o\cos\delta \text{ and } E'' = \sigma_o/\varepsilon_o\sin\delta$$

In terms of complex notation, $\varepsilon = \varepsilon_o \exp(i\omega t)$, therefore the ratio of stress to strain produces the following equation;

$$\sigma / \varepsilon = [\sigma_o / \varepsilon_o] \exp(id)$$

By Euler expansion the above equation can be expressed as

$$\sigma / \varepsilon = [\sigma_o / \varepsilon_o]\cos\delta + i\sin\delta$$

Consequently, the complex modulus and loss tangent can be written as

$$E^* = E' + iE''$$

$$\tan\delta = E'' / E'$$

Dynamic mechanical analysis can be conducted in either bending, shear or tensile modes at frequencies of 0.01 to 100 Hz (depending on instrument type). Strain amplitudes are typically on the order of tenths of microns. This ensures linear viscoelastic behavior. Generally thin polymeric films are supported on an inert substrate. The substrates are often steel plates, glass fiber braids which show no sagging and relaxations with temperature. Polymeric films as thick as 150-200 Å have been studied with accurate results[141,142].

2.3.2.2 Cure and Thermal Analysis with DMTA

The DMTA has proven to be a valuable tool to measure cure, gelation and vitrification times of thermosetting resins. For example, Young et al.[143] studied a series of phenolic resins used for impregnation using DMTA in isothermal mode. They obtained quantitative information on relative cure speed, melting range, gel point etc. Myer et al.[144] measured the extent of cure of resoles during constant heating rate in the dynamic mode. In a related study, Geimer and Christiansen[145] related the cure response of resoles to bond strength under isothermal DMTA experiments. Additionally, Hoffman[146], and Toffey[147] have utilized the DMTA to describe the cure characteristics of epoxy and polyurethane resins, respectively. Modulus-temperature behavior and phase transitions of thermoplastic adhesives have been studied using the DMTA by several scientists[148-150].

The most elaborate description of cure behavior of thermosetting resins via the DMTA is that reported by Provder et al.[151]. They related the changes in modulus during dynamic cure to the fractional extent of cure according to the following equation

$$F(t,T) = \frac{G(t,T) - G_1}{G_2 - G_1}$$

where G_1, G(t,T) and G_2 are modulus readings at the onset of cure, at a given time and temperature during the cure process, and after the cure process has ceased, respectively. The above expression can be described by a general n^{th} order rate expression as follows

$$\frac{dF}{dt}(t,T) = k(T)[1 - F(t,T)]^n$$

where n is the order of reaction, the rate constant k(T) takes on the form

$$k(T) = \frac{1}{\phi}\frac{dF(t,T)}{dT}[1 - F(t,T)]^{-n}$$

where φ is the heating rate, dT/dt, and [dF(t,T)]/dT is the rate of change of degree of cure with respect to temperature.

Generally, the rate constant varies with temperature in an Arrhenius expression as

$$lnk(T) = lnA - \frac{E}{RT}$$

A is the Arrhenius frequency factor, E is the activation energy, R is the gas constant.

$$InA - \frac{E}{RT} = In\frac{1}{\phi}\frac{dF(t,T)}{dT}\left[1 - F(t,T)\right]^{-n}$$

These equations can be related as above. The order of reaction (n), the only unknown value in the above equation, can be determined by evaluating the linearity of the Arrhenius plot of ln k(T) versus 1/T. Thus, the mathematical expressions above permit computation of kinetic parameters under dynamic curing of a resin.

Alternatively, cure under isothermal conditions could be described using Provder et al.'s approach (detailed description is provided in chapter 3).

2.3.3 Relaxation/Thermal Transitions of Chitin and Its Derivatives

The relaxation behavior of dry chitosan films, chitin, acyl chitin and chitosan/polyimide have been studied using DMTA and related thermal methods. Kakizaki and Hideshima[152] have investigated the dielectric relaxation properties of a series of acyl chitins and native chitin. They reported that acyl chitins with acetyl, butyryl, caproyl, capryl side groups or substituents each has a β-relaxation. According to them the origin of this transition is related to local motions of the main and side chains. Additionally, they reported an γ-relaxation for all acyl chitins having side chains longer than acetyl group, and attributed it to local motion of the long side chain. Similar transitions were reported for native chitin. On the other hand there was no relationship between the frequency-temperature dependence behavior of the two materials. In an Arrhenius-type analysis they found that ΔG and ΔH of acyl chitins did not differ from each other. However, significant variation existed in their ΔS values which decreased with increased length of the side chain. This produced the conclusion that the extent of molecular rearrangement accompanying the β-relaxation decreases with increasing of

side chain length. In a related study, Ogura et al.[153] have reported a β-transition (50°C) as well as a γ-transition (-100°C) for native chitin **(Figure 2-13)**. Further, they reported γ-, β- and α-transitions for wet chitosan **(Figure 2-13)**. However, no β-transition could be detected for dry chitosan. Ratto and coworkers[154] have reported a glass transition temperature for chitosan at 90°C using DMTA at a frequency of 1 Hz **(Figure 2-14)**. On the other hand, Kaymin et al.[155] using TMA have reported 3 discrete transitions a -23, 55 and 105°C, and have assigned 105°C as the T_g of chitosan **(Figure 2-15)**. Pizzoli et al.[156] have also studied the phase transitions of chitosan using DMTA and DETA. They reported a low amplitude transition at 130°C at 3 Hz, which has been tentatively related to local motion of polysaccharide chains rather than to a glass-to-rubber transition (T_g) **(Figure 2-16)**. They also reported an γ-transition but no β-transition for chitosan. Pizzolli et al., just like Ogura et al. were able to induce a β-relaxation in chitosan by subjecting it to a high humidity environment.

2.4 CURE CHARACTERIZATION AND TIME-TEMPERATURE-TRANSFORMATION (TTT) CURE DIAGRAMS

2.4.1 Phase Transformation of Curing Systems

Thermosetting resins undergo transformation from a mobile liquid to a highly viscous liquid to an infusible and insoluble solid in a chemical process called cure. On a molecular scale, the cure process can be regarded as transformation of small molecules to large molecules of high molecular weight that undergo crosslinking or network formation[141].

During cure thermosetting resins go through three distinct phases. The precursor material (A-stage) is a liquid or solid and is soluble and fusible. The precursor passes through a B-stage at sufficiently high temperatures. Some resin systems, which are very reactive, can reach this stage at room temperature. The B-stage is characterized by chain extension and prepolymer formation to produce insoluble but swellable material[141]. The C-stage develops at higher temperatures, and the resulting material is a three dimensional network which is insoluble and infusible.

During the curing process, thermosets go through two physical or structural changes described as gelation and vitrification[157-166]. Gelation is a liquid-to-rubber transition. It depicts the transformation of the curing system from either a linear or partly branched to a crosslinked or network structure of infinite molecular weight. On the other hand, vitrification corresponds to a transition from a crosslinked rubbery to a highly crosslinked glassy state as a consequence of increasing crosslink density. It can also represent a transition from the liquid state to the uncrosslinked glassy state due to increasing molecular weight. The ability of thermosets to reach the C-stage depends on these physical changes (gelation and vitrification). For example, at vitrification the polymer chains are completely frozen in position and preclude reactive chain ends to reach each other for chemical crosslinking. This prevents full cure from being attained.

2.4.2 Time-Temperature-Transformation Cure Diagrams

The phase transformation of thermosetting resins was first described graphically by Gillham and coworkers[157-166] on the basis of time-temperature-transformation (TTT)

cure diagrams. The benefits of evaluating the cure behavior of a thermoset by thermal analysis in relation to the TTT diagram are illustrated in the following discussions.

The TTT cure diagram **(Figure 2-17)** represents the times necessary for a thermoset to gel or vitrify. It also depicts other distinct physical changes that occur during cure of a thermoset. The development of each of the physical changes and/or gelation and vitrification is controlled in large part by the time-temperature paths during the cure process, i.e., cure schedule. Three important temperatures to cure of any resin are shown; glass transition temperature of the uncured resin ($T_{g,o}$) , the temperature at which vitrification and gelation occurs simultaneously ($T_{g,g}$), and the glass transition of the fully cured material ($T_{g,\infty}$)[1]. Below $T_{g,o}$, the resin has no reactivity. The location of this temperature determines the safe storage temperature which avoids precure and which prolongs the shelf life of the resin. Below $T_{g,o}$ and $T_{g,g}$, a resin under isothermal cure will vitrify first, and this precludes gelation from ever taking place. This is an important temperature window in the sense that a material at this stage of cure is of low molecular weight, and will flow and become processable during subsequent heating. The full cure line, which distinguishes the sol/gel glass from the gel glass region **(Figure 2-17)**, represents the time at any given isothermal temperature at which a resin is ultimately cured. The determination of this line is important due to the fact meaningful structure-property relationships between different resins can only be made using fully cured materials. According to Gillham's extensive work for resins where $T_{g,\infty}$ can be obtained without degradation, curing above this temperature is the most direct

method of achieving full cure; otherwise a full cure line represents the path to follow in selecting cure schedules for ultimately cured material. Both gelation and vitrification times vary with temperature. The times to gelation decrease with increasing temperature (**Figure 2-17**). On the other hand high temperatures do not necessarily decrease the times to vitrification. As depicted **(Figure 2-17)** vitrification follows an S-shaped pattern. The maximum of the vitrification curve has been related to the opposing influences of the temperature dependence of viscosity and reaction rate constant. The minimum is due to opposing influences of the reaction rate constant and depleting concentration of reacting species. That is, at low temperatures the curing system requires a long time to go from the liquid to an uncrosslinked glassy phase due to limited molecular motions, resulting in a maximum cure time. At sufficiently high cure temperature, the time to vitrification is minimum due to greater mobility of the polymer chains. However, as $T_{g,\infty}$ is approached the long times necessary to achieve conversions indicative of vitrification produce further increase in the time to vitrification.

Thermal degradation can also occur during cure, and may be related to various chemical mechanisms including oxidation and chain scission. This degradation occurs at a rate that decreases in an exponential fashion with temperature. Consequently, the times to excessive degradation can be incorporated into the TTT cure diagram to give a line denoted as char formation **(Figure 2-17)**.

Vitrification and gelation are usually operationally defined by maxima in the tan δ curve during isothermal cure in either the torsional braid analysis or dynamic

mechanical thermal analysis. Therefore, the construction of a TTT cure diagram involves a series of isothermal cure experiments at several different temperatures (T_c), where tan δ is recorded as a function of time. After prolonged cure, the polymer is subjected to stepwise analysis, that is, it is cooled from T_c to a selected subambient temperature, say -T°C, heated from that temperature to a specified post-cure temperature, and then immediately cooled to -T°C. The first step gives the T_g after cure. The second scan from the post-cure temperature to -T°C gives the $T_{g,\infty}$ of the material. A temperature scan of the uncured resin, usually from subambient gives the value of $T_{g,o}$. Determination of $T_{g,g}$ involves plot of times to vitrification and gelation versus cure temperature, and extrapolation of the curves to a point where they coincide. **(Figure 2-18)**.

Whilst the procedures described above have been used for most thermosets with success, some thermosets do not display maxima corresponding to gelation and vitrification. And others vitrify or gel at prolonged times. For such systems Gillham and Enns[158] and Gillham and Wissanrakkit[166] have developed models for describing vitrification. These models are beyond the scope of this dissertation, and therefore are not discussed. Details of such models could be found elsewhere[158,166].

In summary, the TTT diagram provides a useful basis for understanding the cure behavior of thermosets, and permits selection of time and temperature windows so that gelation and vitrification occur in a controlled manner. It summarizes information about the thermodynamic transitions of a polymer system which form the basis for achieving predictable properties of cured materials.

The concept of the TTT cure diagam has been developed and used extensively to describe network formation. Few reports, however, are found in the literature for linear systems. For example, Aronhime and Gillham[157], and Palmese and Gillham[164] have described the curing behavior of linear free-radical polymerizable materials, and polyamic/polyimide systems, respectively. As for thermosetting resins, these linear systems displayed typical S-shaped vitrification curves.

2.4.3 Thermal Imidization of Polyamic Acid

The conversion of polyamic acid to polyimide involves a thermal treatment of thin films cast from solution. The process has been described as imidization(**Figure 2-19**)[164]. The process of thermal dehydration has most often been carried out in stages[167]. A brief discussion of the characterization of imidization is provided below. This discussion is relevant on account of the similarities between imidation and regeneration of chitin.

Various characterization procedures have been used to describe thermal imidization, including FTIR, DSC, raman spectroscopy, and TGA[168-171]. However, FTIR has received the most attention. Various scientists have developed polyamic acids from varying precursors, and have generally used the following bands to monitor the progress of imidization;

Imide I 1770-1780 cm^{-1} and 1720-1730 cm^{-1}

Imide II 1340-1400 cm^{-1}

Imide III 1110-11140 cm^{-1}

Imide IV 710-740 cm^{-1}

The imide I band at 1770-1780 cm^{-1} and the imide IV band at 710-740 cm^{-1} are mostly used for describing the kinetics of imidization. The progress of imidization has been reported to be influenced by casting solvent[169], film thickness,[172] curing temperature[169] , and chemical structure[173]. Kruez et al.[171] examined the imidization of solvent cast polyamic acid at temperatures of 160-180^{0}C. They described the process as a two-step process, with an initial fast reaction, preceeded by a significantly slower reaction. They related the two-step process to the influence of vitrification , and removal of solvent that favored suitable orientations for imidization. Activation energies reported for the first and second phase of imidization were 26 and 23 Kcal/mol.

Other methods have been used to describe imidization. For example, the process has been followed by measuring the weight loss that occurs during thermal dehydration[174]. Similar to FTIR monitoring, these studies have reported a two-stage imidization reaction. It has been observed that the glass transition of the partially imidized material is often similar to the ultimate glass transition, and that an increase of the cure temperature above the ultimate glass transition produces further imidization. This observation was interpretated on the basis of the influence of vitrification. In other studies, DSC[175],and microdielectric analysis[176] have been used. DSC analysis suggested that imidization occurred favorably at 100-250^{o}C, and that the process followed two first order reactions[175].

2.5 REFERENCES

1. Murlidhara, H.S., Maggih, S., Resources and Conservation, 1985, 11, 274
2. Muzzarelli, R.A.A., In Encyclopedia of Polymer Science and Engineering, Vol. 3, Wiley, NY, pp430-440, 1985
3. Bartnicki-Garcia, S., In Chitin and Chitosan: Sources, Chemistry, Biochemistry, Physical Properties and Applications: G. Skjak-Braek, T. Anthosen and P. Sandford, eds., Elsevier Appied Sci. NY, 1989
4. Chitin in nature and Technology, R. Muzzarelli, C. Jeuniax and G.W. Gooday, eds., Plemum Press, New York, 1986
5. Proceedings of the 2nd International Conference on Chitin and Chitosan, S. Hirano and S. Toleura, eds., Sapporo, Japan, 1982
6. Arcidiacono, S., J. Lombardi, D.L. Kaplan: in Chitin and Chitosan: Sources, Chemistry, Biochemistry, Physical Properties and Applications: G. Skjak-Braek, T. Anthosen and P. Sandford, eds., Elsevier Appied Sci., NY, 1989, pp 319-332
7. Arcidiano, S. and D.L. Kaplan, Biotechnol. Bioeng., 39, 281-286, 1992
8. Shimahara, K., Y. Takiguchi, T. Kobayashi, K. Uda and T. Sanan, in Chitin and Chitosan: Sources, Chemistry, Biochemistry, Physical Properties and Applications: G. Skjak-Braek, T. Anthosen and P. Sandford, eds., Elsevier Appied Sci., NY, 1989, pp 171-178
9. Zechmeister, Z. and Toth, G., Zoological and physiological chem., 1934, 223, 53
10. Bulawa, C.E., Annual. Rev. Microbiol, 47, 505-534, 1993

11. Richard A. Snucker, Biochem. Sys. Ecol., 19(5), 357-369 , 1991

12. Kurita, K., Sannan, T. and Iwakura, Y, Makromol, Chem., 178, 1977, 3197-3202

13. Muzzarelli, R.A.A. and R. Rochetti, In Chitin in Nature and Technology, Muzalli, J. Jeanniauz and G.W. Gooday, eds., Plenum Press, N.Y. 1989, pp. 385-388

14. Varum, K.M. Anthosen, M.W., Ottoy, M.H. Grasdalen, H. and O. Smidsrod: In Advances in Chitin and Chitosan, C.J. Brine, Sanford P.A. and J.P. Zikakis, eds., Elsevier Applied Sci., NY, pp. 127-129, 1991

15. Rudall, K.M., and W. Kenchington, Biological Revies, 49, 597-636, 1973

16. Rudall, K.M., J. Polym. Sci. Part C: Polym. Symp. No 28, 83-102, 1969

17. Minke, R., and J. Blackwell, J. Mol.Biol. 120, 167, 1978

18. Blackwell, J Biopolymer, 7, 281, 1969

19. Gardener, K.H., and Blackwell, J., Biopolymer, 14, 1581, 1975

20. Kurita, K., Tomita, K., Tada, T., Ishii, S., Nishimura, S., Shimoda, K., J. Polym. Sci., Part A. Polymer chemistry, vol. 31, 485-491, 1993

21. Allan, G.G., Fox, J.R., and Kong, N., In Proceedings of the 1st Int. Conf. on Chitin and Chitosan, Muzzarelli, R.A.A., and E.R. Parisher, eds., Cambridge, MA, pp64-78, 1978

22. Brine, C.J., In Proceedings of the 1st int. Conf. on Chitin and Chitosan, Muzzarelli, R.A.A., and E.R. Parisher, eds., Cambridge, MA, pp509-516, 1978

23. Hepburn, H. R. and H.D. Chandler, In Proceedings of the 1st int. Conf. on Chitin and Chitosan, Muzzarelli, R.A.A., and E.R. Parisher, eds., Cambridge, MA, pp124-143, 1978

24. Anderson, C. G., N. D. Pablo, and C.R. Romo, In Proceedings of the 1st int. Conf. on Chitin and Chitosan, Muzzarelli, R.A.A., and E.R. Parisher, eds., Cambridge, MA, pp5-10, 1978

25. Ohashi, E., and T. Koriyama, Anal. Chimica Acta, 262, 19-25, 1992

26. Retnakaran, A., In Chitin in Nature and Technology, Muzzarelli, R.A.A., C. Jeuniaux and G.W. Godday, eds., Plenum Press, NY pp147-163, 1986

27. Griaud-Guille, M.M. Chanzy, H., and Vuong, R., J., Struct. Biol. 103, 232-240, 1990

28. Herth, W., J. Ultrastruct. Res., 68, 16-27, 1979

29. Herth, W., M. Mulisch and P. Zugenmaier, In Chitin in Nature and Technology, Muzzarelli, R.A.A., C. Jeuniaux and G.W. Godday, eds., Plenum Press, NY, pp107-120, 1986

30. Reyes, F., M.J. Martinez, J. Catatayud, and R. Lahoz, In Chitin in Nature and Technology, Muzzarelli, R.A.A., C. Jeuniaux and G.W. Godday, eds., Plenum Press, NY, pp99-102, 1986

31. Vincendon, M., and J.C. Roux, In Chitin and Chitosan: Sources, Chemistry, Biochemistry, Physical Properties and Applications: G. Skjak-Braek, T. Anthosen and P. Sandford, eds., Elsevier Appied Sci. NY, 1989, pp. 169-174

32. Takai, Z., and Tokura, K., In Chitin and Chitosan: Sources, Chemistry, Biochemistry, Physical Properties and Applications: G. Skjak-Braek, T. Anthosen and P. Sandford, eds., Elsevier Appied Sci. NY, pp169-174 1989

33. Focher, B., P.L. Beltrame, A. Naggi, G. Torri, Carbohydrate Polymers, 12, 405-418, 1990

34. Rigby, G.W., US patent 2,072,771, 1936

35. Horowitz, S.T., Roseman, S., Blumenthal, H.J., In Chitin, Muzzarelli, R.A.A., ed., Pergamon Press, NY, pp96, 1977

36. Peniston, Q.P. and Johnson, E.L., In Chitin, Muzzarelli, R.A.A., ed., Pergamon Press, NY, pp98, 1977

37. Pelletier, A., I. Lemire, Sygusch, J., Chornet, E. and Overend, R.P., Biotech. and Bioeng., Vol. 36, 310-315, 1990

38. Domard, A., and Rinaudo, M., Int. J. Biol. Macromol., 5, 49-53, 1983

39. Araki, Y., and Ito, E., Eur. J. Biochem., 55, 71-73, 1975

40. Kafetzopoulos, D., Martinou, A. and Bouriotis, V., Proc. Natl. Acad. Sci. USA, Vol 90, pp2564-2568, 1993, Applied Biological Sciences.

41. Battista, O.A., Microcrystalline Polymer Sci., McGraw Hill, NY, 1975

42. Dunn et al., US patent 3,847,897, 1974

43. Austin, P.R. and C.J. Brine, US patent 4,286,087, 1979

44. Struszczyk, H., Polish patent, 109,210, 1979

45. Kurita, K., Kamiya, M., and Nishimura S., Carbohydrate Polymers, 16, 83-92, 1991

46. Aiba, S., Int. J. Biol. Macromol, Vol. 11, 249-52, 1989

47. Domszy, J.G., and Roberts, G.A.F., Makromol. Chem. , 186, 1671-77, 1985

48. Sannan, T., Kurita, K., K. Ogura and Y. Iwakura, Polymer, 19, 458-459, 1978

49. Miya, M., R. Iwamoto, S. Yoshikawa and S. Mima, Int. J. Biol. Macromol., 2, 323-324, 1980

50. Moore, G.K., and G.A.F. Roberts, Int. J. Biol. Macromol., 2, 115-116, 1980

51. Alasdair, B., Michael, D., K.B., A., Taylor, and G.A.F. Robers, Int. J. Biol. Macromol., 14, 166-169, 1992

52. Lal, G.S., and Hayes, E.R., J. Anal. Appl. Pyrol., 6, 183-193, 1984

53. Aiba, S., Int. J. Biol. Macromol., 8, 173-176, 1986

54. Domard, A., Int. J. Biol. Macromol., 9, 333-336, 1987

55. Alonso, I.G., C. Peniche-Covas, J.M. and Nieto, J. Thermal. Anal., 28, 189-195, 1983

56. Broussiqnac, P., Chim. Ind., Genie, chim, 99, 1241, 1968

57. Rutherford, F.A. and Austin P.R., In Proc. 1st Symp. on Chitin and Chitosan, Cambridge, MA, p182, 1978

58. Hayes, E.R., and D.H. Davies, In Proc. 1st Symp. on Chitin and Chitosan, Cambridge, MA, p406, 1978

59. Moore, G.K., and G.A.F. Roberts, In Proc. 1st Symp. on Chitin and Chitosan, Cambridge, MA,, p421, 1978

60. Raymond, L., Morin, F.G. and Marchessault, R.H., Carbohydrate Research, 246, 331-336, 1993

61. Frederic, N., Basora, N., Chornet, E., Vidal P.F., Carbohydrate Res. 238, 1-9, 1993

62. Nanjo, Fk. Katsumi, R., and Sakai, Kazuo, Analytical Biochemistry, 193, 164-167, 1991

63. Rathke, T.D. and Hudson, S.M., J. Polym. Sci., Polym. Chem., ed., 31 (3), 749-753, 1993

64. Muzzarelli, R.A.A., Tafani, F. Scarpini, and G., Laterza, G., J. Biochem. Biophys. Methods, 2, 299, 1980

65. Wu, A.C.M., Methods Enzymol, 161, Part B, 447-452, 1988

66. Muzzarelli, R.A.A., C. Lough, and Emanuelli, M. Carbohydrates Res, 164, 433-442, 1987

67. Wang, W., S. Bo, S. Li, and Qin W., Int. J. Biol. Macromol. 13, 281-285, 1991

68. Rinaudo, M. and Donard, A. , Int. J. Biol., Macromol, 5, 1983, 49-52

69. Donard, A. and Rinaudo, M., In Chitin and Chitosan: Sources, Chemistry, Biochemistry, Physical Properties and Applications: G. Skjak-Braek, T. Anthosen and P. Sandford, eds., Elsevier Appied Sci. NY, pp71-86, 1989

70. Gamzazade, A.I., Pavlova, S.S.A., and Rogozhin, S.V., Acta Polym., 8, 420-424, 1985

71. Roberts, G.A.F., and J.G. Domzy, Int. J. Biol. Macromol., 4, 1982, 374-377

72. Aruchami, M., Gowri, N. and Sundara, R.G., In Chitin in Nature and Technology, pp263-268

73. Trudel, J. and Asselain, A. Anal. Biochem., 189, 249-253, 1986

74. Davis, L.L., Biochemistry, 23, 1065-1073, 1984

75. Bartnicki-Garcia, S. In Advances in Chitin and Chitosan, Skjaki, Braek, G., Anthonsem, T. and Sandford, P., eds., Elsevier, Essex, UK, pp. 23-35

76. Cabib, E., Adv. Enzymol., 59, 59-101, 1987

77. Ahtakara, A., Y. Uchida and M. Mitsutomi, in 1st Proceedings on Chitin/Chitosan, pp. 587-605

78. Berkely, R.C.W., in 1st Proceedings on Chitin/Chitosan, pp. 570-577

79. S. Hirano, M., Yohyashi, K., Murae, H., Tsuchida S., and T. Nishida, In Applied Bioactive Polymeric Materials, (C.G. Gebelein, C.E. Carraher, Jr. And V.R. Foster eds) Plenum Press, NY 1988, pp. 45-59

80. Ohtakara, A., Izume, M. and Mitsutomi, M., Agric. Biol. Chem., 52 (12) 3181-3182, 1988

81. Aiba, S., Int. J. Biol. Macromol., 15, 421-245, 1993

82. Yabuki, M., In Chitin and Chitosan: Sources, Chemistry, Biochemistry, Physical Properties and Applications: G. Skjak-Braek, T. Anthosen and P. Sandford, eds., Elsevier Appied Sci. NY, pp197-206, 1989

83. Osswald, W.F., McDonald, R.E., Randall, P.N., Shapiro, J.P., and Mayer R.T., Analytical Biochem., 204, 40-46, 1992

84. Tokura, S., and Azuma, I., In industrial Polysaccharides: Genetic engineering, Structure-property Relationships and Applications., Yaplan M., ed., Elsevier Sci. Publishers, Amsterdam, pp347-362, 1987

85. Tokura, S., Nishi, N., Nishimura, S., and Ikeuchi, Y., In chitin, chitosan, and related enzymes., Zikakis, J.P., ed., Academic Press, Orlando, Florida, pp218-241, 1984

86. Sashiwa, H., Saimoto, Shigemasa, H., Ogawa, R., and Tokura, S., Int. J. Biol. Macromol., 12, 295-296, 1990

87. Kurita, K., Yoshino, H. Nishimura, S., and Ishii, S., Carbohydrate Polym., 20, 239-245, 1993

88. Aiba, S., Int. J. Biol. Macromol., 14, 225-288, 1992

89. Sensland, C., and Matttiasson, B., Biotech. Bioeng., 34, 389-393, 1989

90. Allan, C.R., and Hadwiger, L.A., Exp. Mycol., 3(3), 285-287, 1979

91. Balassa, L.L., and prudden, J.F., In Proc. 1st Symp. on Chitin and Chitosan, Cambridge, MA, pp296-305, 1978

92. Malette, W.G., Quigley, H.J., and Adiches, E.D., In Chitin in Nature and Technology., Muzzarelli, R.A.A., Jeuniaux, C., and Gooday, G.W., eds., NY, Plenum Press, pp435-442, 1986

93. Suzuki, K., Ogawa, Y., Hashimoto, K., Suzuki, S., and Suzuki, M., Microbiol. Immunol>, 28, 903-912, 1984

94. Hirano, S.K., Tobetto, M., Hasegawa, M., and Matsuda, N., J. Biomedical Mat. Res., 14, 477-486, 1988

95. El-Ghouth et al. J. Food Process. Preser. Vol. 15, No. 5, 359-68, 1991

96. Hirano, S., Agric. Biol. Chem., 42(10) 1939-1940, 1988

97. Making Paper Better with Shrimps., Pulp and Paper Int., 27, No. 2, 33, 1985

98. Kobayashi et al., In Proc of the 2nd Conf. on Chitin and Chitosan, pp239-43, 1982

99. Allan, G.G., In Mat. Res. Soc. Symp., Vol 197, pp239-243, 1990

100. Makhlouf, L., and Pikulik, I.I., Nordic Pulp and Paper Res. J., No. 3, 99, 1991

101. East, G.E., and Qin, Y., J. Appl. Polym. Sci. Vol 50, 1773-1779, 1991

102. Wei, Y.C., Hudson, S.M., Mayer, J.M., and Kaplan, D.L., J. Polym. Sci., Part A, 30, 2187-2193, 1991

103. Hosokawa, J., Nishiyama, M., Yoshihara, K., and Kubo, T., Ind. Eng. Chem. Res., 29, 800-805, 1990

104. Hosokawa, J., Nishiyama, M., Yoshihara, K., Kubo, T., and Terabe, A., Ind. Eng. Chem. Res., 30,788792, 1991

105. Isogai, A., and Atalla, R.H., Carbohydrate Polym. 19, 25-28, 1992

106. Wu, A.C.M., Bough, W.A., Holmes, M.R., and Perkins, B.E., Biotech. Bioeng. 20, 1957-1968, 1978

107. Seo, T.T., Kanbara, T., and Iijima, T., J. Appl. Polym. Sci., 36(6), 1443-1451, 1988

108. Muzzarelli, R.A.A., Natural Chelating Polymers, Pergamon Press, Toronto, pp85-95, 1973

109. Tsezos, M., Biotech. Bioeng., 25, 2025-2040, 1988

110. Koyama, Y., and taniguchi, A., J. Appl. Polym. Sci., 31, 1951-1954, 1986

111. Ogawa, K., Oka, K., Miyanishi, T., and Hirano, S., In Chitin, Chitosan and Related Enzymes, Zikakis, J.P., ed. Academic Press, Inc. pp327-346, 1984

112. Maruca, R., Suder, B.J., Wightman, J.P., J. Appl. Polym. Sci., 27, 4827-4837, 1982

113. Kurita, K., Sannan, T. and Iwakura, Y., J. Appl. Polym. Sci., 23, 511-515, 1979

114. Muzzarelli, R.A.A., Tanfani, F., and Scarpini, G., Biotech. Bioeng., 22, 885-896, 1980

115. Muzzarelli, R.A.A., Chitin, Pergamon of Canada Ltd, Toronto, Canada, 1977

116. Hirano, S., Agric. Biol. chem., 42 (10), 1939-1940, 1978

117. Roberts, G.A.F., and Taylor, K.E., Makromol. Chem. 190(5), 951-960, 1989

118. Lim, F., and Sun, A.M., Science, 210, 908-910, 1980

119. Nakatsuka, S., and Andrary, A.L., J. Appl. Polym. Sci., 44, 17-28, 1992

120. Muzzarelli, R.A.A., Carbohydrate Polym., 3, 53-75, 1983

121. Tokunaga, M., Jpn. Kokai Tokkyo Koho JP 63,175,186., 1988

122. Aizawa, Y. and Noda, T., Jpn. Kokai Tokkyo Koho JP 63,189,859., 1988

123. Austin, P.R., Brine, C.J., US Patent, 4,029,727, 1978

124. Tokura, S., Nishi, N., and Noguchi, J., Polym. J., 11, 781, 1979

125. Unitika Ltd., US Patent, 4,431,601., 1982

126. Koyama, Y., and Taniguchi, A., J. Appl. Polym. Sci., 31, 1951, 1986

127. Richards, F.M., and Knowles, J.R., Int. Mol. Biol., pp231, 1968

128. Draget, K.I., Varum, K.M.E., Moen, H.G., and Smids, O., Biomaterials, vol. 13, 9, 1992

129. Muzzarelli, R.A.A., Barontini,G., and Rocchetti, R., Biotech. Bioeng., 18, p1445, 1976

130. Ferry, J.D., Viscoelastic Properties of Polymers, Univer. of Wis. Madison, 1980

131. Ward, I.M., Mechanical Properties of Solid Polymers, 2nd Ed., John Wiley & Sons, NY, 1983

132. Aklonis, J.J., and Macknight, W.J., Introduction to Polymer Viscoelasticity, John Wiley & Sons, Inc., New York, 1983

133. Read , B.E., and Dean, G.D., The Determination of Dynamic Properties of Polymers and Composites, Adam Hilger, Ltd., Bristol, 1978

134. McCrumm, N.G., Read, B.E., and Williams, G., Anelastic and Dielectric Effects in Polymeric Solids, John Wiley & Sons, Inc., New York, 1967

135. Koenig, J.L., Chemical Microstructure of Polymer Chains, John Wiley & Sons, Inc., New York, 1980

136. Rudin, A., The Elements of Polymer Science and Engineering: An Introductory Text for Engineers and Chemists, Academic Press, Inc., New York, 1982

137. Hiemenz, P.C., Polymer Chemistry: The Basic Concepts, Marcel Dekker, Inc., New York, 1984

138. Nielsen, L.E., Mechanical Properties of Polymers and Composites, Vol. 1, Marcel Dekker, Inc., New York, 1974

139. Nielsen, L.E., Mechanical Properties of Polymers and Composites, Vol. 2, Marcel Dekker, Inc., New York, 1974

140. Hartmann, B., Lee, G.F., J. Appl. Polym. Sci., 23, 3639-3650, 1979

141. Turi, E.A., Thermal Characterization of Polymeric Materials, Academic Press, Inc., New York, 1981

142. Wetton, R.E., In Developments in Polymer Characterization, Dawkins, J.V., ed., Elsevier, New York, 1986, p179-221

143. Young, R.H., Kopf, P.W., and Salgada, O., Tappi, 64(4), 127-130, 1981

144. Myers, G.E.,Christiansen, A.W., Geimer, Follensbee, R.L., Koutsky, J.A., J. Appl. Polym. Sci., 43, 237-250, 1991

145. Geimer, R.A., and Christiansen, A.W., Proc. of the Adhesives and Bonded Wood Products Symp. Seattle, Washington, 1991

146. Hoffmann, K. Ph.D. Dissertation, Virginia Tech., 1991

147. Toffey, A. MS Thesis, Virginia Tech., 1993

148. Mizumachi, H., Mokuzai Gakkaishi, 2594), 289-295

149. Rials, T., and Glasser, W. G., J. Appl. Polym. Sci., 37, 2399-2415, 1989

150. Motohashi, K., Tomita, B., Mizumachi, H., and Sakaguchi, H. Wood Fiber Sic., 16(1), 73-85, 1979

151. Provder, T., Holsworth, R.M., and Grentzer, T.H., In Adv. Chem. Ser., 203, ACS., Washington, D.C., 1981

152 Kakizaki, M., and Hideshima, T., In Advances in Chitin and Chitosan, Brine, C.J., Sandford, P.A., and Zikakis, eds., Elsevier Applied Sci, NY, p165-171, 1991

153. Ogura, K., Kanamoto, T., Itoh, M., Hajima, M., and Tanaka, K., Polymer Bulletin, 2, 301-304, 1980

154. Ratto, J.N., Chen, C.C., and Blumstein, R.B., J. Appl. Polym. Sci., 59, 1451-1461, 1996

155. Kayim, I.F., Ozonlinya, G.A., and Plisko, Y.A., Polym. Sci., U.S.S.R., 22, 171-177, 1980

156. Pizzoli, M., Ceccorulli, G., and Scandola, M., Carbohydrate Res., 222,205-213, 1991

157. Aronhime, M.T., and Gillham, J.K., Adv. Polym. Sci., 78, 83-112, 1986

158. Enns, J.B. and Gillham, J.K., J. Appl. Polym. Sci., 28, 2567-2591, 1983

159. Aronhime, M.T., and Gillham, J.K., Adv. Polym. Sci., 56, 35-47, 1984

160. Babayevsky, P.G., and Gillham, J.K., J. Appl. Polym., 17, 2067-2088, 1973

161. Scheneider, N.S., Sproise, J.F., Hagnauer, G.L. and Gillham, J.K., Polym. Eng. Sci., 19(4), 304-312, 1979

162. Wisanrakkit, G., and Gillham, J.K. ACS Polym. Mater. Sci. and Eng. Prep., 56, 87-91, 1987

163. Gillham, J.K., British Polym. J., 17(2), 224-226, 1985

164. Palmese, G.R., and Gillham, J.K., J. Appl. Polym. Sci., 34, 1925-1939, 1987

165. Gillham, J.K., and Enns, J.B., ACS Polym. Mater. Sci. and Eng. Prep., 59, 851-858, 1988

166. Wisanrakkit, G., and Gillham, J.K. ACS Polym. Mater. Sci. and Eng. Prep., 59, 969-975, 1988

167. Jones, J.I., Ochynski, F.W., and Rackley, F.A., Chem. Ind. 1686, 1962

168. Dinehart, R.A., and Wright, W.W., Die Makromol. Chemie., 143, 189, 1971

169. Frayer, P.D., In Polyimides: Synthesis, Characterization and Applications, Mittal, K.L., ed., Vol. 1. Plenum Press, pp273

169. Ishida, H., and Wellinghoff, S.T., Macromolecules, 13, 826, 1980

171. Kreuz, J.A., Endrey, A.L., Gay, F.P., and Sroog, C.E., J. Polym. Sci., Part A-1, Vol. 4, 2607-2616, 1966

172. Dine-Hart, R.A., and Wright, W.W., J. Appl. Sci., 11, 609, 1967

173. St. Clair, A.K., and St. Clair, T.L., Polym. Prep., 27(2), 406, 1986

174. Numata, S., Koji, F., and Kinjo, N., In Polyimides: Synthesis, Characterization and Applications, Mittal, K.L., ed., Vol. 1. Plenum Press, pp259

175. Navarre, M., In Polyimides: Synthesis, Characterization and Applications, Mittal, K.L., ed., Vol. 1. Plenum Press, pp429

176. Day, D., and Senturia, S., In Polyimides: Synthesis, Characterization and Applications, Mittal, K.L., ed., Vol. 1. Plenum Press, pp249

Table 2-1. Occurrence and Sources of Chitin[1]

Marine animals	Insects	Microorganisms
Annelida	Scorpion	Green algae
Molluska	Spiders	Yeast
Coelenterata	Cockroaches	Fungi (cell wall)[2]
(Crustaceans)	Beetles	Mycelia Penicillium[2]
Lobster[1]		Brown algae
Crabs[1]		Ascomycedes
Shrimps[1]		Chytridiaceae
Prawn[1]		
Krill[1]		

[1] Current commercial source

[2] Potential commercial source

Table 2-2. Sources and Properties of Chitin

Source	Type	Properties	Ref
Crustaceans	Crab shell and tendon	α-chitin: $M_w = 1.036 \times 10^6$	21
	Blue crab	N/A	22
	Shrimp/Prawn	α-chitin	23
	Krill shell	N/A	24
Squid (mollusk)	Loligo pen	β-chitin: $M_v = 2.5 \times 10^6$	21
	Todares pacificus	β-chitin	25
Insects	Cuticle	α-chitin	26
	Locust apodemes	α-chitin	23
	Ovipositors	N/A	27
Centric diatoms	Thalassiosira fluviatilis	β-chitin	28
Protozoa	Eufolliculina uhligi	β-chitin	29
Fungi	*Mucor rouxii*	α-chitin	3
	Aspergillus nidulans	N/A	30

N/A ; not available

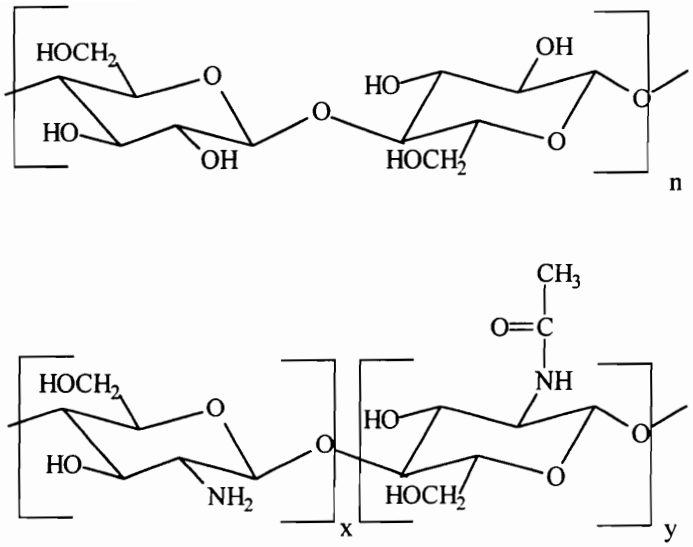

Figure 2-1. Chemical structures of cellulose (top), chitin, and chitosan (bottom). These polysaccharides differ only at the C-2 position. Acetamide, amino and hydroxyl group at C-2 position for chitin, chitosan and cellulose, respectively. y>>x for chitin, and x>>y for chitosan.

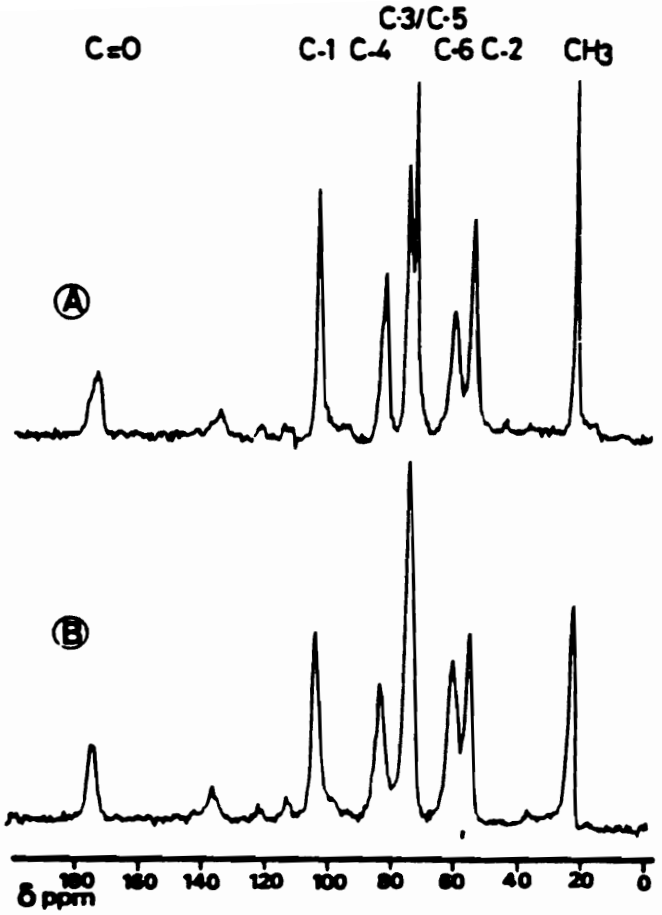

Figure 2-2. Solid state CP/MAS ^{13}C NMR spectra of chitin; (A) α-chitin and (B) β-chitin[31].

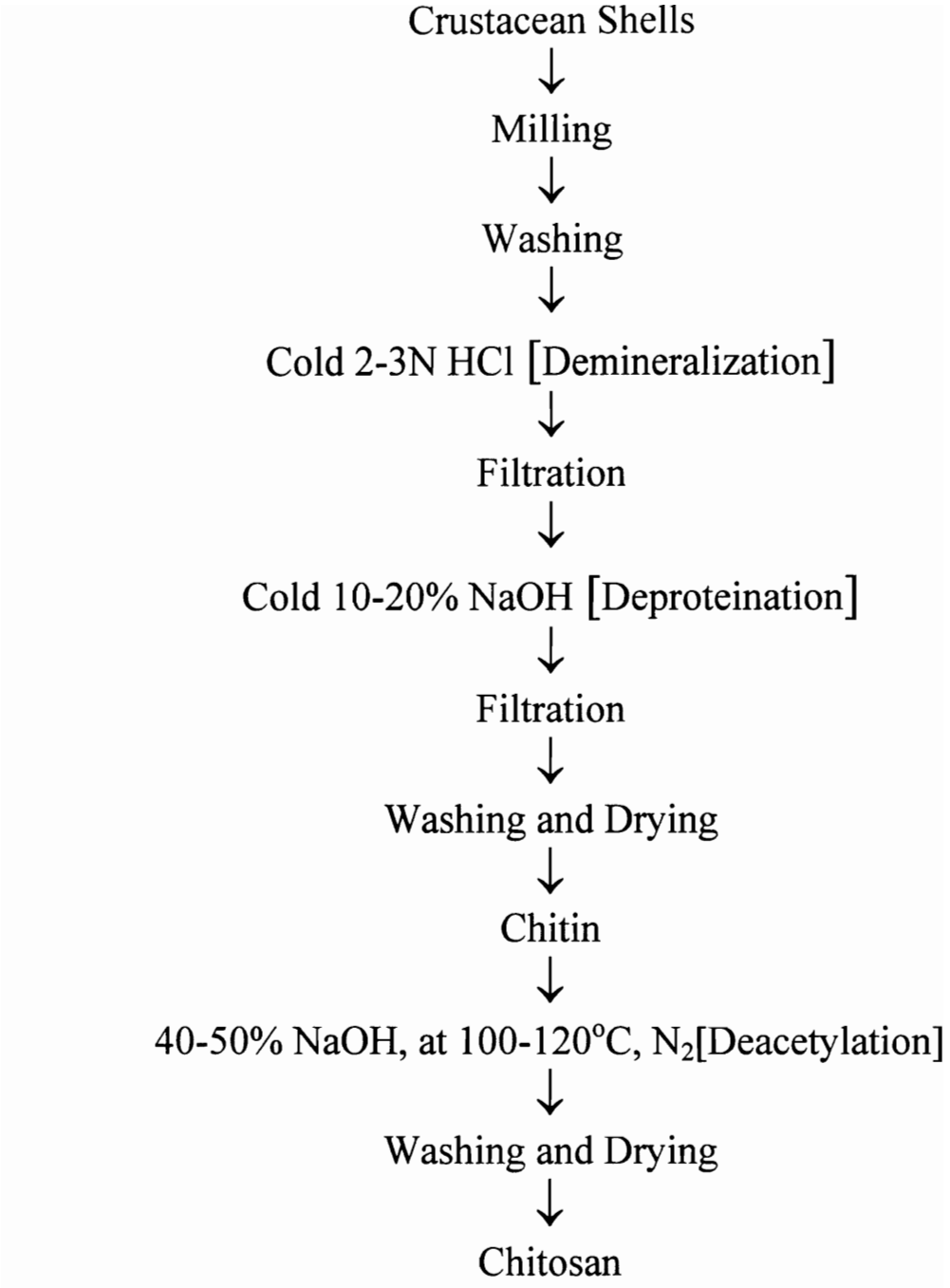

Figure 2-3. Commercial isolation of chitin and preparation of chitosan.

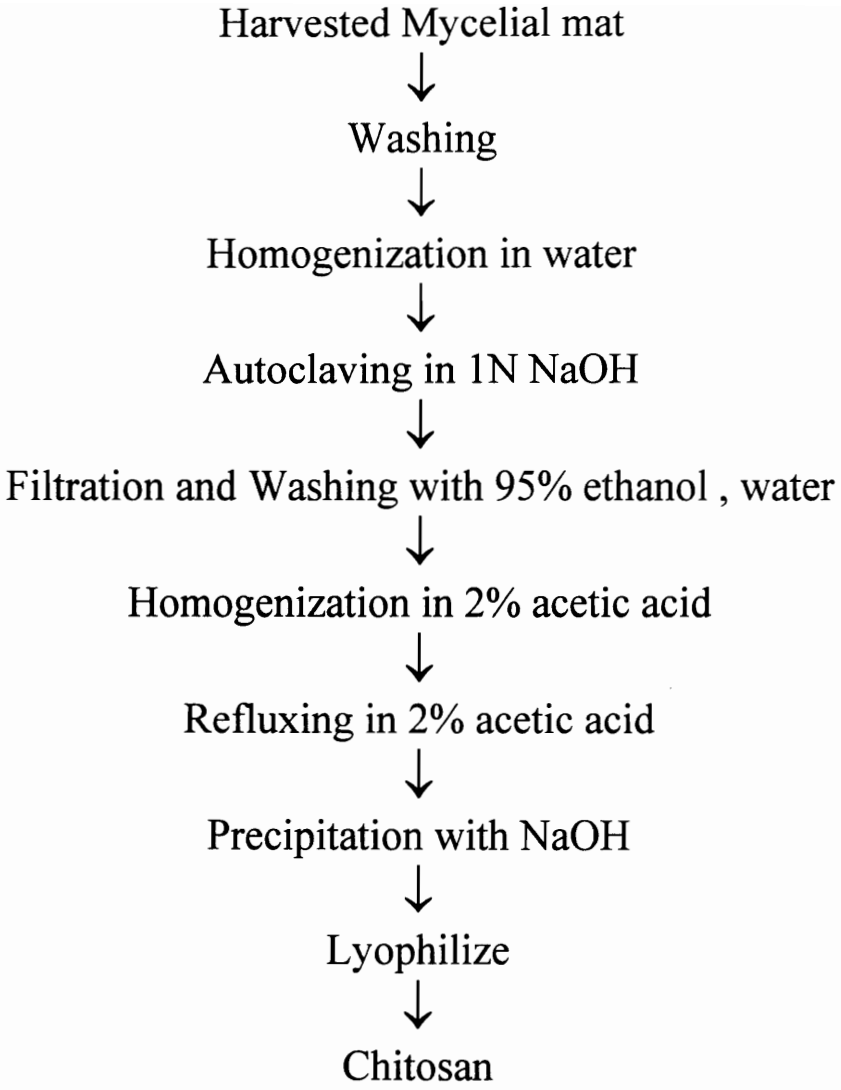

Figure 2-4. Extraction of chitosan from fungal cell walls[7]. This procedure is currently not practiced commercially.

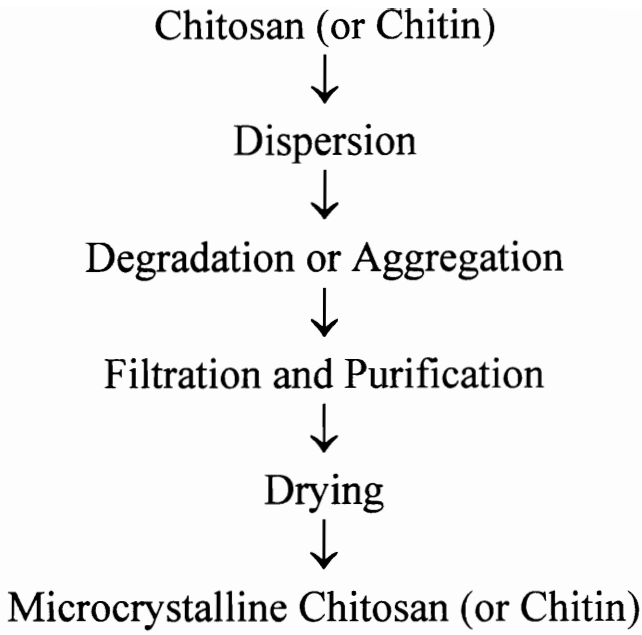

Figure 2-5. Preparation of microcrystalline chitin and chitosan. Dispersion involves dispersing chitosan or chitin in dilute organic acid or a mixture of phosphoric acid and methanol, respectively. Following dispersion, microcrystalline chitosan can be prepared in one of two ways, namely degradation or aggregation. Degradation involves heating the dispersed material at 70°C for 3h. Aggregation involves coagulation of the dispersed chitosan in an alkaline bath. Microcrystalline chitin is prepared by the degradation method only[42,48].

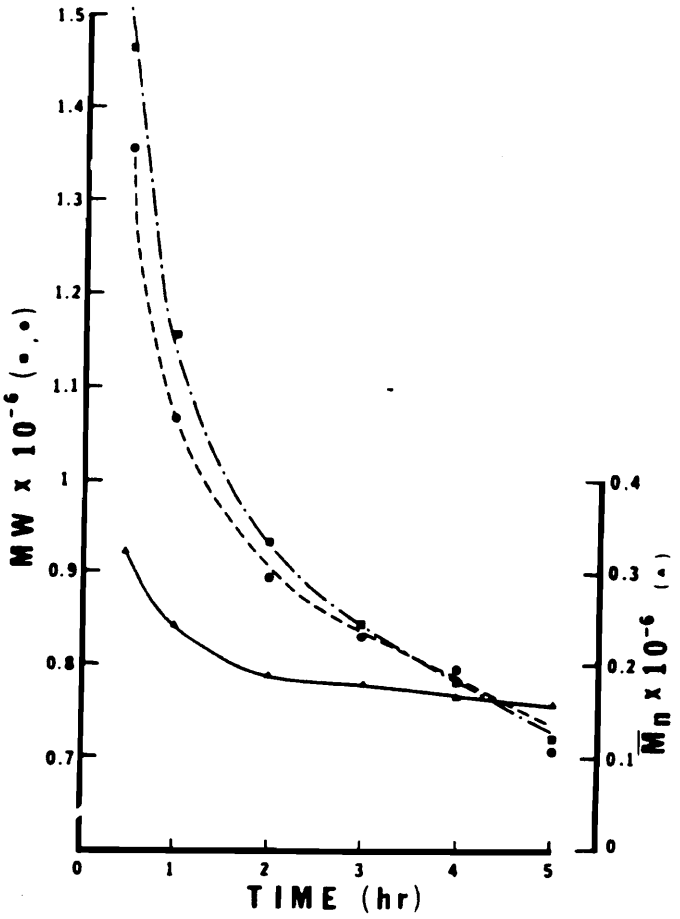

Figure 2-6. Molecular weight distribution of chitosan products with different times of deacetylation. The solvent was 2% acetic acid with 0.1M sodium acetate. M_w (squares) and peak molecular weight (circles) refer to the left y-axis; M_n (triangles) refer to the right y-axis[67].

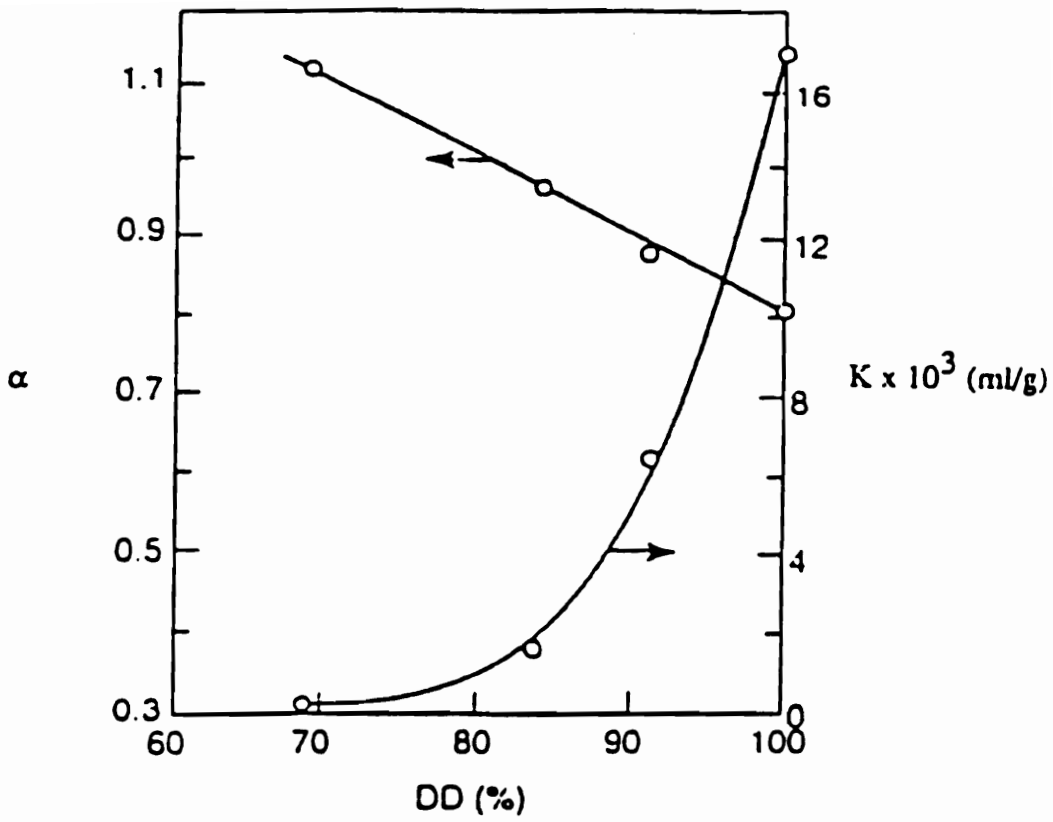

Figure 2-7. Dependence of Mark-Houwink constants, K and a (α) on the degree of deacetylation (DD)[67].

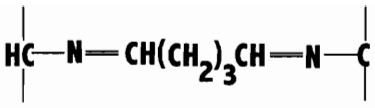

1

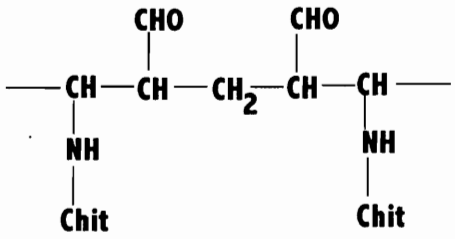

2

Figure 2-8. Chemical structures of products formed by the gelation of chitosan and glutaraldehyde reaction mixture. One school of thought favors 1 (Schiff base) and the other favors 2 (Michael adduct) as the principal structure formed by the gelation of the above reaction mixture[117,127,129].

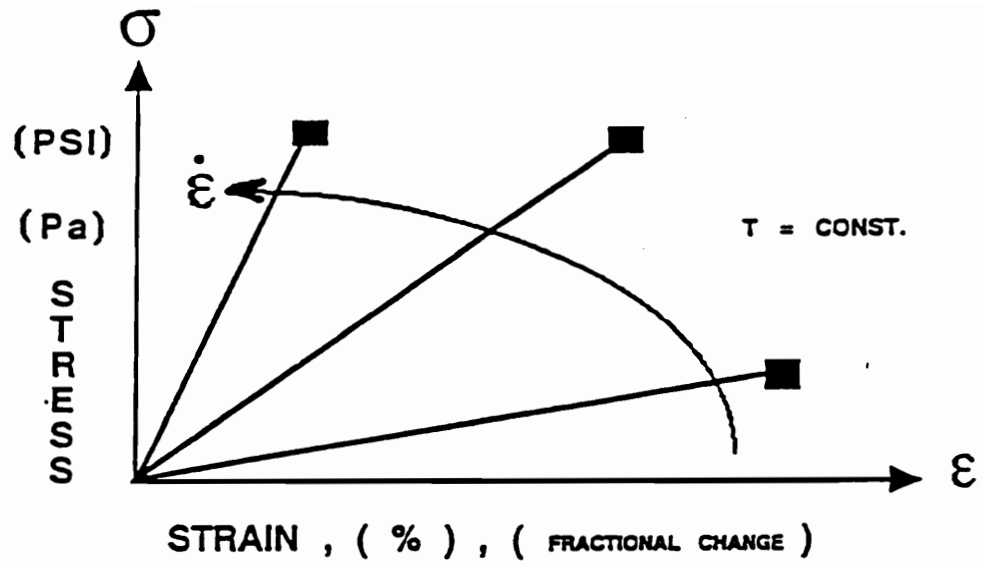

Figure 2-9. Rate and temperature dependence of mechanical properties of polymers. ε and T represent strain rate and temperature, respectively[130].

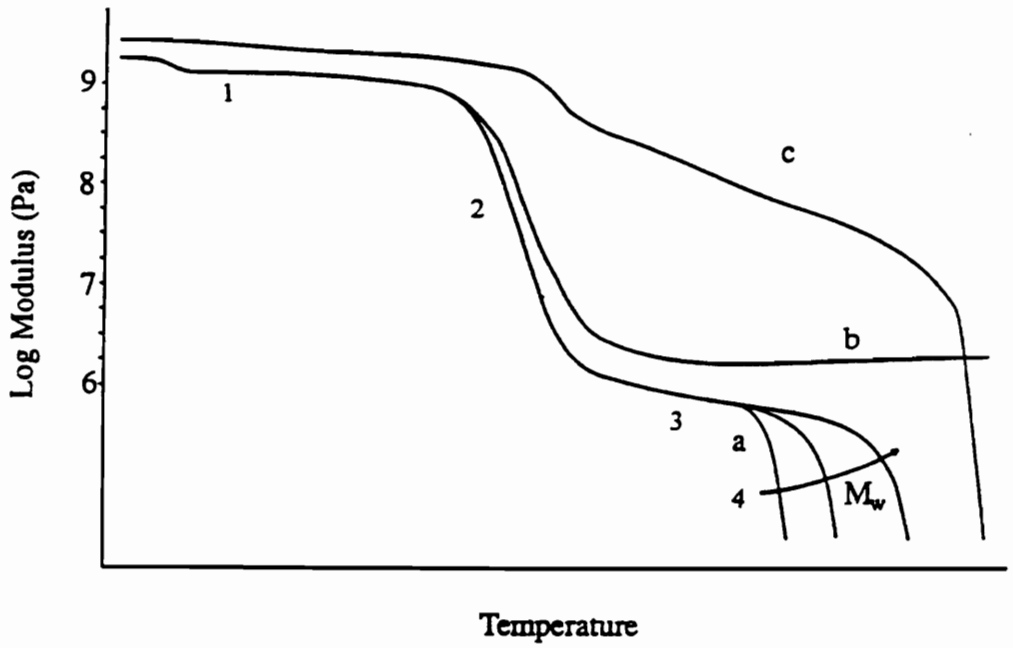

Figure 2-10. A schematic thermomechanical spectra showing modulus variation with temperature and the various phase changes under dynamic conditions. a: uncrosslinked and amorphous polymer of different molecular weight; b: crosslinked and amorphous polymer; and c: semicrystalline polymer. 1, 2, 3,4 represent glassy, glass transition, rubbery, viscous flow regions, respectively[130].

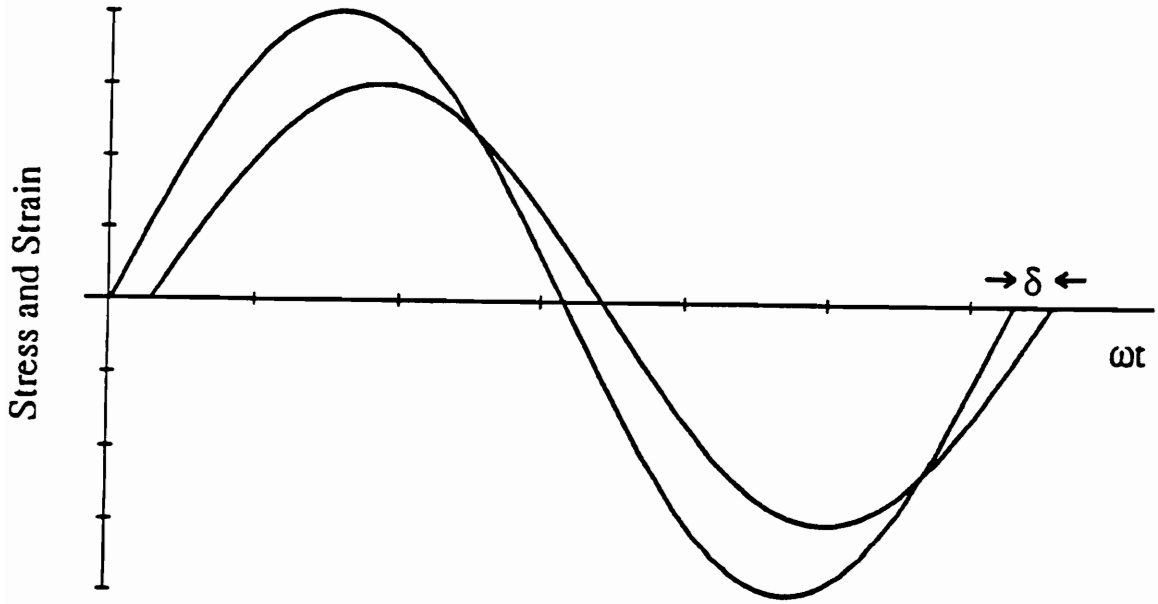

Figure 2-11. A schematic viscoelastic response showing the variation of an applied stress and the corresponding strain response. The phase shift, δ, denotes the extent of damping due to molecular motion[130].

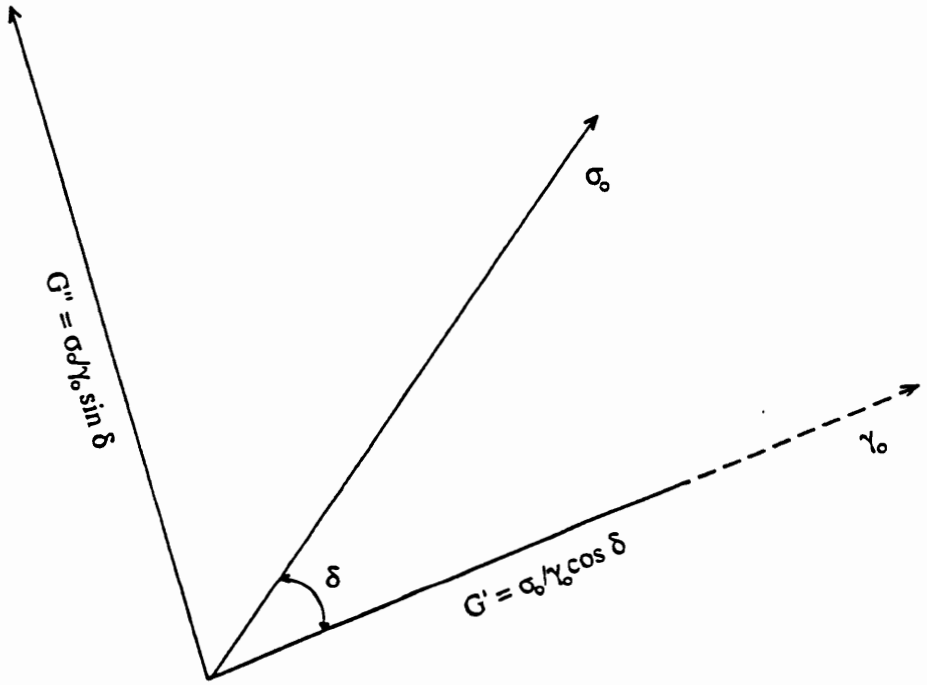

Figure 2-12. A schematic representation of rotating vector showing the storage and loss moduli vectors and the separation by a phase angle, δ[130].

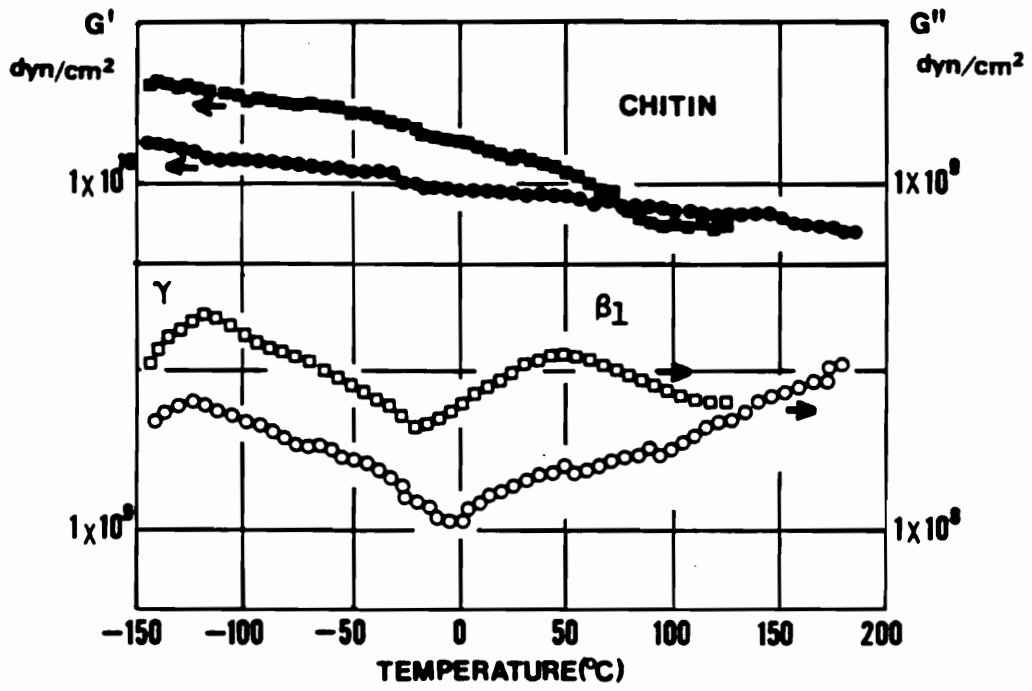

Figure 2-13. Temperature dependence of the complex shear modulus for chitin. G' (•) and G" (O) for dry sample, and G' (■) and G"(□) for wet sample[153].

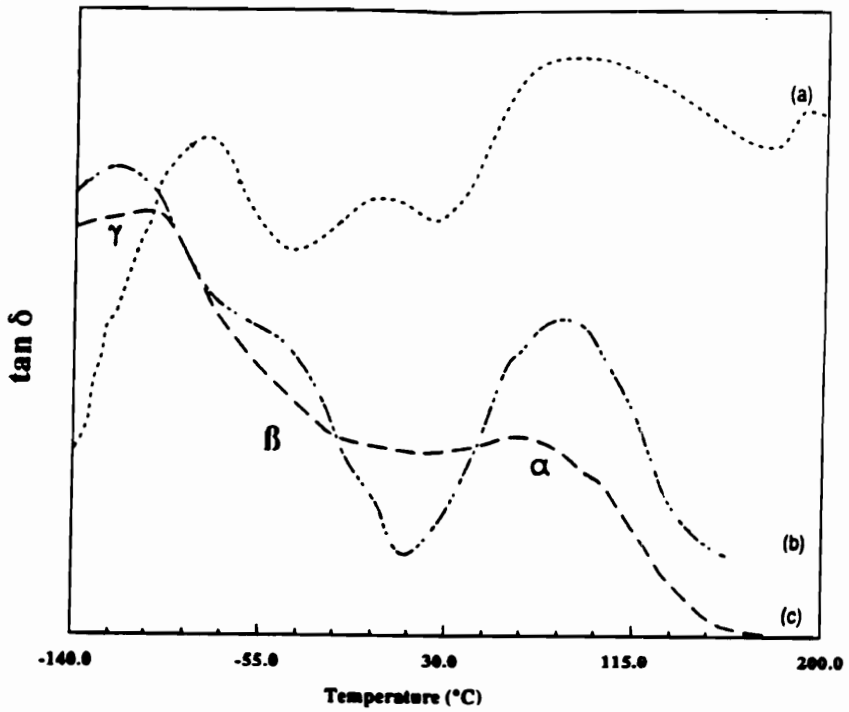

Figure 2-14. DMA data (E") of chitosan. A T_g of 90°C is detected for chitosan.[153].

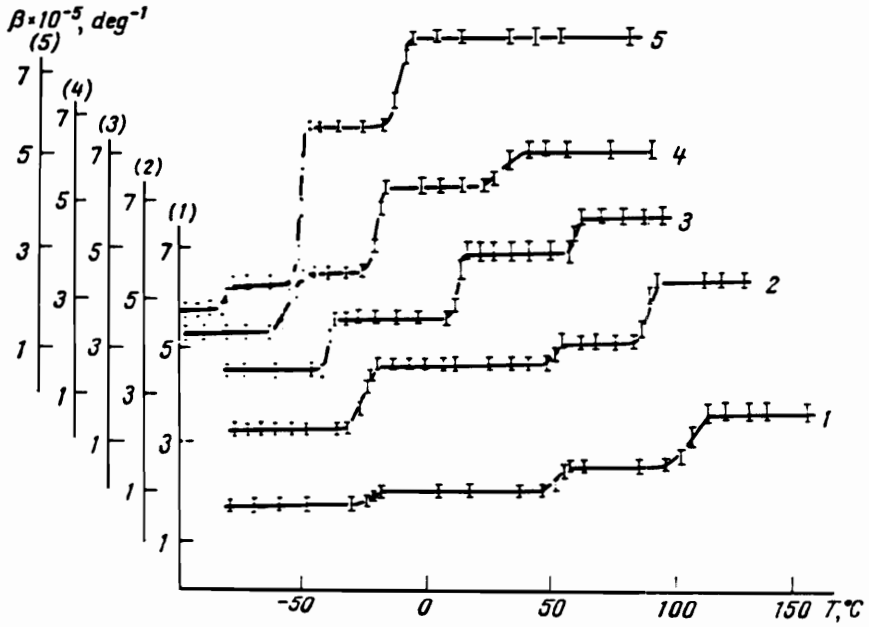

Figure 2-15. Temperature dependence of linear thermal expansion coefficient for dry chitosan (1) and for chitosan containing 3.2 (2), 10.5 (3), 16.4 (4), 39.3% glycerin (5). The step transition at 105°C is considered as the T_g of chitosan[155].

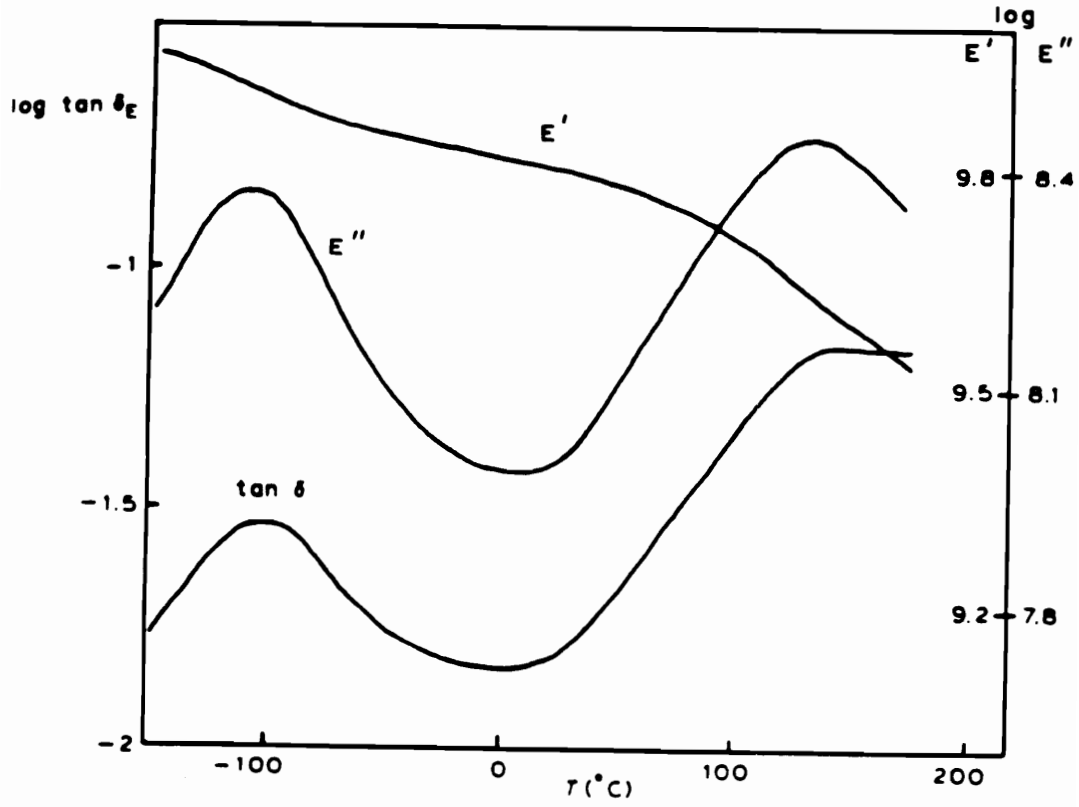

Figure 2-16. DMTA spectrum of dry chitosan. The transition at 130°C is tentatively considered as due to local motion of polyssacharide chains[156].

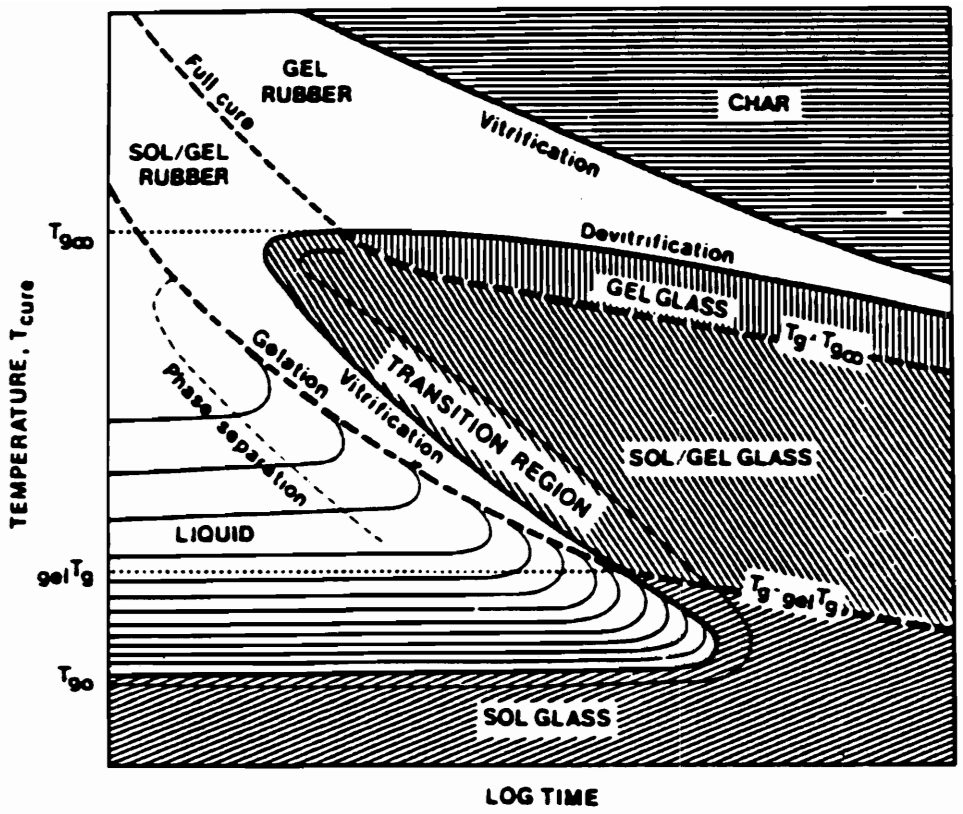

Figure 2-17. A schematic TTT cure diagram. The diagram depicts the various physical changes that characterize network formation.

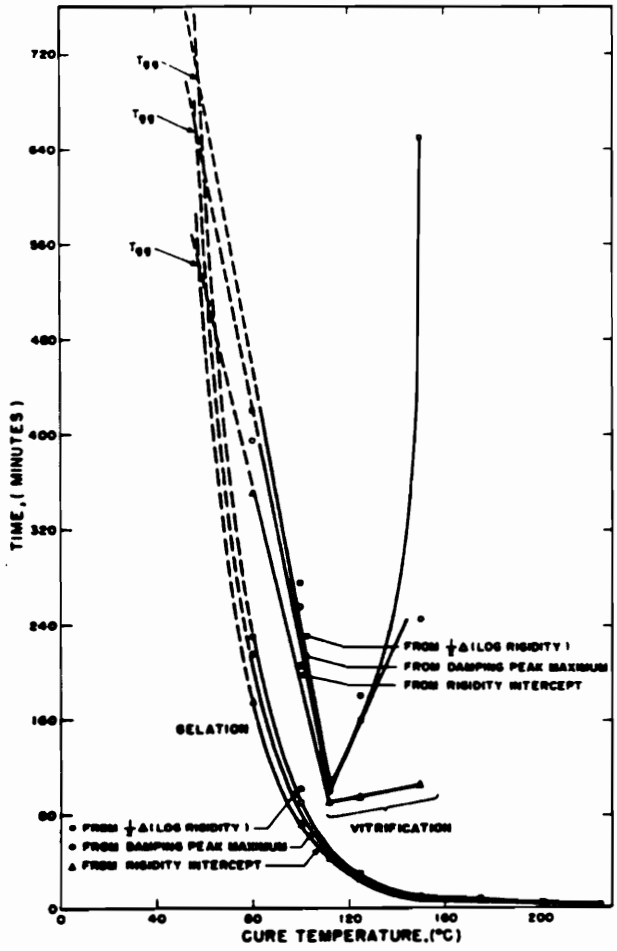

Figure 2-18. Time to gelation and time to vitriification vs. isothermal cure temperature. This diagram is useful for determining the temperature at which gelation and vitrification coincide, denoted as $T_{g,g}$ in the TTT cure diagram[160].

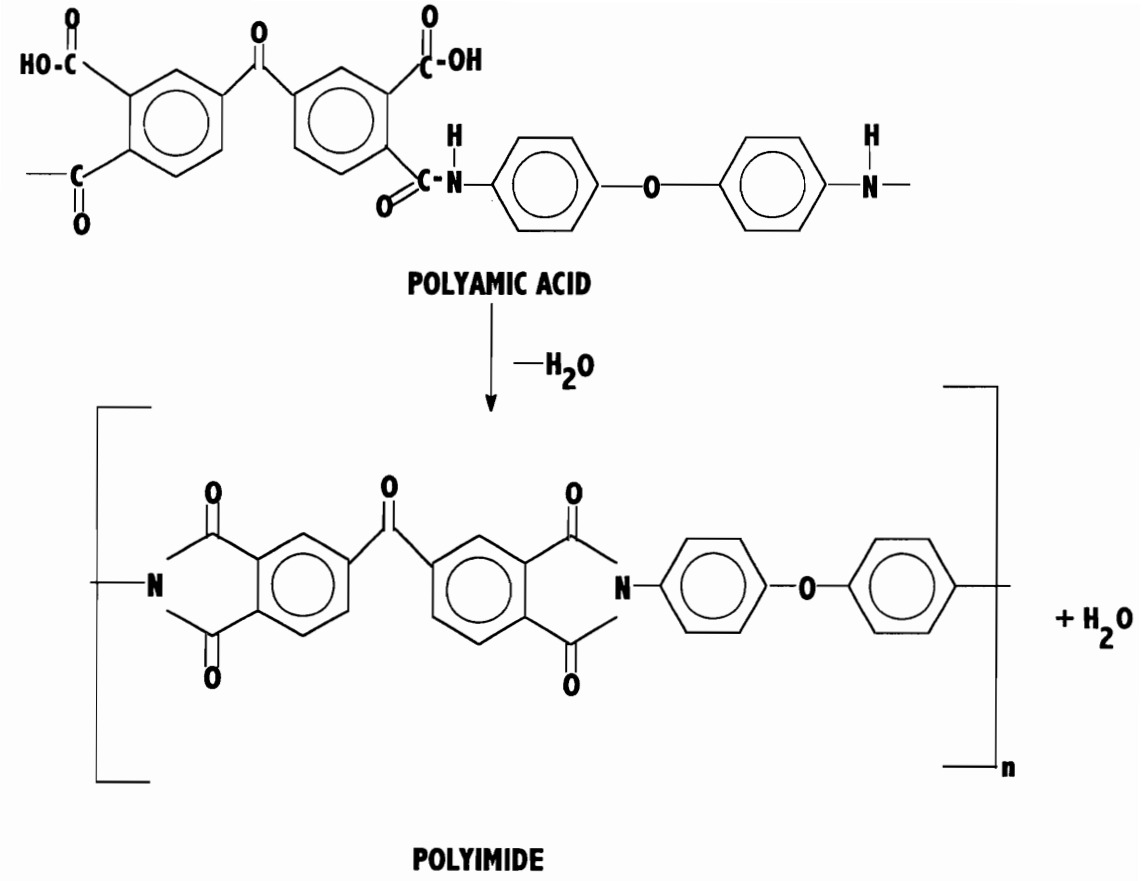

Figure 2-19. A chemical scheme of the thermal dehydration of polyamic acid to polymide, referred to as imidization[164]. This is a parallel process to regeneration of chitin from chitosonium acetate.

CHAPTER 3[1]

CHITIN DERIVATIVES. I. KINETICS OF THE HEAT-INDUCED CONVERSION OF CHITOSAN TO CHITIN

3.1 ABSTRACT

The water-soluble solids comprised of the ionic complex between chitosan and acetic acid, chitosonium acetate, are converted into chitin by heating. The thermally-induced conversion of a water-soluble chitosonium acetate in film-form into a water-insoluble chitin film was examined by thermal analysis (DMTA, TGA, DSC, and TMA) and by solid state ^{13}C -NMR spectroscopy. Results indicate that tan δ-transitions occur at increasingly high temperatures, and over progressively wider temperature ranges, as the transformation progresses. Likewise, the storage modulus, log E', increases as the chitosonium acetate film undergoes "cure" and converts to chitin. Cure kinetic parameters are obtained using the model proposed by Provder et al. modified for glass transition temperature (T_g). The results suggest the existence of two sequential first order reactions, an initial and a late cure reaction, having activation energies of approximately 15 and 21 kcal/mol, respectively.

---

[1] Published in J. Appl. Polym. Sci. Vol. 66, 75-85, 1996. The original manuscript was co-authored by Ackah Toffey, Gamini Samaranayake, Charles E. Frazier, and Wolfgang G. Glasser (in that sequence).

3.2 INTRODUCTION

Chitin is the principal structural polymer of the exoskeleton of crustaceae as well as of insects[1]. It serves nature as a mechanically strong barrier polymer with significant oxygen diffusivity[1]. Chitin is well-recognized by polymer chemists as an attractive linear poly(anhydro N-acetyl glucose amine[2-4]. Unfortunately, chitin is notoriously insoluble in all common organic solvents with the exception of dimethyl acetamide (DMAc)/LiCl[5]. Because of its insolubility, chitin is usually converted to chitosan by alkaline hydrolysis. Chitosan, the deacetylated poly(glucose amine), is readily soluble in dilute acetic acid from which it is usually regenerated by treatment with alkali. The water-soluble ionic complex of chitosan and acetic acid, chitosonium acetate, can be handled like any other soluble linear polymer. It can be cast into films[6-8], spun into fibers[9], precipitated into particles from suitable non-solvents which revert the ionized ammonium groups back into amine functionality, and crosslinked to produce chitosan fibers[10]. In addition, chitosan blends with cellulose have been advocated as biodegradable films[11, 12]. However, the integrity of chitosan films or fibers is more easily compromised than chitin since chitosan remains soluble, and more susceptible to moisture-attack. Thus, a procedure which converts chitosan to chitin holds great promise for the industrial utilization of this abundant biobased material.

The objectives of this paper are to present evidence in support of the conversion of the ionic complex of chitosan, chitosonium acetate, to chitin by heating, and to describe the kinetic parameters underlying the conversion. This regeneration of chitin,

the restoration of insolubility, and the recreation of characteristics usually found in thermosetting network polymers, can be likened to the process of cure.

3.3 MATERIALS AND METHODS

3.3.1 Materials

The chitosan used in the preparation of chitosonium acetate was obtained from Sigma Chemicals, St. Lious, MO. This chitosan was obtained by deacetylation of chitin from crab shells, and it had a degree of deacetylation of 89.3% (manufacturer's specification). Glacial acetic acid obtained from Aldrich Chemicals, Milwaukee, WI was used as the solvent for chitosan.

3.3.2 Methods

3.3.2.1 Chitosonium Acetate Film Preparation

The preparation of chitosonium acetate films involved a two-stage process. In the first stage, about 100 g of chitosan was dissolved in 7 L of 10% aqueous acetic acid and stirred for about 24 hrs to obtained a clear, highly viscous solution. This solution was cast into films in large rubber trays from which solvent evaporated. The dried films were then pulverized to obtain powderous chitosonium acetate. In the second stage 9.5 g of powderous chitosonium acetate were dissolved in 400 mL of water with stirring until clear solution was obtained. This was cast as films in flat petri dishes followed by solvent evaporation and drying at room temperature for two weeks. Films were produced, the thickness of which ranged from 0.5 to 1.2 mm. Attempts to use vacuum drying resulted in warped films. Samples for thermomechanical analysis were preheated

in an oven at temperatures of 80°C, 100 °C, 120 °C, 130 °C , and 140 °C for periods ranging from 5 mins to 48 hrs.

3.3.2.2 Differential Scanning Calorimetry (DSC)

A DSC from Perkin Elmer, model DSC 4, connected to a temperature controller and interfaced to a thermal analysis data station (TADS) was used to assess whether or not the dried chitosonium acetate films contained residual moisture. A freshly-cast or well-dried film was sealed in an aluminium pan and heated at a rate of 10°C/min. All experiments were done under a purge of dry nitrogen.

3.3.2.3 Dynamic Mechanical Thermal Analysis (DMTA)

Dynamic mechanical thermal analysis of chitosonium acetate films was performed with a Polymer Laboratory DMTA. Samples were tested by bending in a single cantilever mode, at a heating rate of 2.5°C/min, an oscillation amplitude of 0.4 mm and a frequency of 1hz. Typical sample dimensions were 8 × 5 × 1.1 mm. A nitrogen purge at a rate of 25 cm^3/min was used during data collection. The glass transition temperature was taken as the maximum in the tan δ curve.

3.3.2.4 Thermomechanical Analysis (TMA)

A TMA from Perkin-Elmer, model TMS-325 was used to determine the glass transition temperature (T_g) of heat-treated samples. All experiments were done using the thermal expansion probe and a loading weight of 5 g. The samples were 0.65 mm thick. TMA experiments involved two stages. The first stage addressed the determination of T_g of the partially cured material, where the material is scanned to a temperature well

above the glass transition. This treatment gave a fully cured or converted material (supported by DMTA). The second stage involved scanning of the fully-cured material to determine the ultimate T_g associated with each isothermal temperature.

3.3.2.5 Thermogravimetric Analysis (TGA)

A Perkin-Elmer TGA-2 was used to assess the weight loss with heat treatment. All samples were in powderous form, and were heat treated under a purge of dry nitrogen. Heat treatment involved dynamic (at a heating rate of 5°C/min) and isothermal mode (at 110° for 6hrs)

3.3.2.6 CP/MAS NMR Spectroscopy

Solid state NMR experiments were carried out on a Bruker MSL-300 at a resonance frequency of 75.47 MHz for ^{13}C nuclei. The proton spin-lock field strength was approximately 56 KHz. Powderous chitosonium acetate, untreated and heat treated were loaded into a zirconium oxide rotor. The magic angle was set using the KBr method, and the rotor was spun at 5 KHz. The Hartmann-Hahn match was established with adamantane. Standard phase cycling was used to obtain the spectra. Cross-polarization contact time was 1ms. A delay time of 3.75s was used between successive pulses, and 1000 scans were accumulated for each experiment. Signal assignments were based on literature values.

3.4 RESULTS AND DISCUSSION

3.4.1 Thermal Analysis

The process of cure has been described by Gillham[13] in terms of the so-called time-temperature-transformation (TTT) diagram (**Figure 3-1**). The TTT diagram provides an illustration of the morphological changes a thermosetting network polymer undergoes in response to time at isothermal cure temperature. The process commences with "gelation," the formation of an infinite polymer network. Gelation precedes vitrification which is described as the moment when the rising glass transition temperature of the network undergoing cure reaches the isothermal cure temperature. Gelation and vitrification are two events in a cure process which convert a low modulus liquid into a high modulus infinite network. Transitions of the damping behavior, tan δ or loss modulus, log E", of the DMTA spectrum can be used to analyze the cure process[14]. Typical DMTA spectra of an amine-cured epoxy at two isothermal cure temperatures are shown (**Figure 3-2**)[14]. Two distinctive transitions associated with gelation and vitrification are observed. At the onset of cure, the liquid-state resin exhibits low damping. Damping increases as the resin becomes rubbery, and it declines again after gelation due to restrictions on chain mobility. Damping exhibits a second maximum as the rubbery material transforms to the glassy state, in a similar fashion as the glass to rubber transition. Thus, gelation and vitrification are thermal events which give rise to distinctive transitions by dynamic mechanical thermal analysis

(**Figure 3-2**)[14]. Both gelation and vitrification occur after a short time exposure at the higher temperature. This observation is always true of the time to gelation; however the time to vitrification is dependent on the relative values of the isothermal cure temperature and the ultimate T_g of the fully-cured polymer. When a moisture-free chitosonium acetate film is exposed to isothermal cure conditions in a dynamic mechanical thermal analysis (DMTA) instrument, changes in tan δ and log E' are recorded (**Figure 3-3**). The tan δ-transitions occur after shorter time periods when heated at 140°C as compared to 100°C; and the storage modulus rises more rapidly at the higher temperature. Both transitions reveal a distinctive separation into two sub-events which overlap each other and which form a broad overall transition (**Figure 3-3**). Whereas it is difficult to ascribe these transitions and/or modulus increases to either gelation or vitrification as in thermosets, it is apparent that there is a heat-induced transformation of the material which takes a two-step process. The pattern of the DMTA spectrum is typical of the cure behavior of a thermoset (**Figure 3-2**).

When a chitosonium acetate film is scanned by DMTA from a temperature of -110°C to various elevated temperature levels, tan δ-transitions are observed which are located at progressively higher temperatures in addition to being progressively smaller in height and broader in width (**Figure 3-4**). This indicates a shift of T_g to higher temperatures as the temperature range over which the sample is scanned increases. This phenomenon is consistent with the cure behavior of thermosets. A similar pattern is observed during sequential heat treatments of chitosan films[15]. The rising glass

transition temperature is attributed to the removal of residual moisture which plasticizes the material. In the case of chitosonium acetate, loss of residual moisture is evidently not responsible for the rising glass transition temperature. DSC studies suggest loss of residual moisture from a freshly-cast chitosonium acetate film. This is evident in a DSC thermogram, where there is a well-resolved endotherm at 100°C due to evaporation of residual moisture (**Figure 3-5**). A similar, but well-dried material did not indicate any trace of residual moisture. This is supported by the absence of an endotherm at 100°C (**Figure 3-5**).

Likewise, chitosonium acetate films preheated for four hours, each, at different temperature levels, reveal tan δ-transitions which occur at progressively higher temperatures and which diminish in size and slightly broaden in width (**Figures 3-6**). A similar trend of declining peak height is observed for samples heated at a constant isothermal temperature of 110°C for varying periods. In this case the rise in glass transition temperature is paralleled by an increase in storage modulus after the glass-to-rubber transition region, and this suggests further transformation of a partially transformed material (**Figure 3-7**). A similar trend has been observed with an amine-cured epoxy[14]. This supports the assertion that the thermally-induced transformation of chitosonium acetate can be likened to the cure reaction of a thermoset.

When powderous chitosonium acetate is exposed to heating by thermo-gravimetric analysis (TGA), a progressive loss of mass is recorded even below ca. 250°, the temperature at which chitin and chitosan begin to thermally degrade (**Figure 3-8a**).

Isothermal heating at 110°C results in a gradual loss of mass over prolonged periods of time without ever reaching an equilibrium level. However, mass loss approaches 9% after 6 hrs., a value comparable to the theoretical loss of mass for the conversion of chitosonium acetate to chitin,i.e., 8.1% (**Figure 3-8b**).

3.4.2 NMR Spectroscopy

The analysis of chitin, chitosan, and chitosonium acetate following different levels of heat treatment (**Figures3-9 to 3-14**) reveals signals representing, among others, acetyl functionality. The N-acetyl group of chitin raises signals at 23 ppm (CH_3-group), and at 173 ppm (N-acetyl CO-functionality)(**Figure3-9**). Following deacetylation, both peaks disappear from the ^{13}C -NMR spectrum (**Figure 3-10**). Chitosonium acetate raises signals at 23 ppm (CH_3 group), and at 179 ppm (acetate-CO carbon) (**Figure 3-11**). Solid chitosonium acetate partially preheated raises signals at 23 ppm, at 173 and at 179 ppm (**Figure 3-12**). When this partially "cured" chitosonium acetate film is treated with mild, cold alkali so as to neutralize ionically bound acetate groups, the remaining solids display a CO-carbon signal at 173 ppm (**Figure 3-13**). The transition the CO-carbon signals undergo in response to severity of heat treatment are illustrated (**Figure 3-14**). The signal at 179 ppm representing CO-acetate functionality gradually reverts to a signal centered at 173 ppm representing N-acetyl CO functionality. Intermediate levels of conversion represent two distinct peaks which change in proportion in relation to heat treatment. These changes point to chitosonium acetate to chitin transformation.

Using acetic acid solutions of chitosan and finely suspended cellulose powder, Hosokawa et al. formed strong composites by heating[11]. Carbonyl enrichment of the cellulose component of such composites by oxidation with ozone was reported to result in strength improvements. The conclusion of this study was that the strength increase supposedly was due to crosslinking of chitosan with the carbonyl groups of cellulose. However, when similar experiments were repeated by the same authors with acids other than acetic acid, no strength increase was observed[11]. If the strength improvements were due to crosslinking, similar observations should have been made with acids other than acetic acid. This is because other acids would not hinder crosslinking. An alternate explanation is that there was a thermally triggered transformation of the ionic complex of chitosan to chitin, which was manifested in an improvement of strength.

3.4.3 Kinetic Considerations

The process of cure has been kinetically described by Provder et al. in terms of modulus change[16]. Extent of cure, F, was reported to be a function of modulus, G, for samples having been cured at time t and temperature T,

$F_{(t,T)} = G_{(t,T)} - G_{(0)} / G_{(\infty)} - G_{(0)}$ (Equation 1)

where $G_{(0)}$, $G_{(t,T)}$, $G_{(\infty)}$ are the modulus at the onset of cure, the modulus at a given time and the ultimate modulus of the material, respectively. Using this definition of extent of cure, a kinetic rate constant describing a first order cure process is derived from

$-\ln (1 - F) = k_{(T)} t$ (Equation 2)

where **t** represents time and **k** represents rate constant. Using this first order rate equation, and adapting it to the more sensitive changes in T_g as opposed to modulus, a modified form of the model of Provder et al. can be formulated

$$F_{(t, T)} = T_{g\,(t, T)} - T_{g,(0)} / T_{g\,(\infty)} - T_{g\,(0)} \quad \text{(Equation 3)}$$

where $T_{g,(0)}$, $T_{g,\,(t,\,T)}$ and $T_{g,\,(\infty)}$ are the glass transition temperature at the onset of cure, at a given time under isothermal cure, and at full cure, respectively.

The first order rate equation (equation 2) can be expressed in Arrhenius form,

$$\ln k_{(T)} = \ln A - E/RT \quad \text{(Equation 4)}$$

from which the activation energy, E, for a reaction can be derived in the usual manner.

Changes in glass transition temperature, determined by TMA, over time for isothermal cure experiments conducted at different temperatures (**Figure 3-15**) show a progressive rise with cure temperature, similar to the behavior of thermosets. The ultimate T_g of fully-cured chitosonium acetate was taken as the average of values determined for the various isothermal temperatures, and this was determined to be 189°C. The T_g of unheated chitosonium acetate was determined to be 57°C. The rise in T_g can be expressed in terms of conversion (or extent of cure) according to equation 3 (**Figure 3-16**). Using the relationship between extent of conversion and time at different isothermal cure temperature (Equation 2), results emerge (**Figure 3-17**) which indicate two sequential cure reactions both of which follow first order kinetics. The initial, fast reaction has an activation energy of 15 kcal mol^{-1} and the second, late reaction reveals an activation energy of 21 kcal mol^{-1} (Figure 3-18).

These results suggest that chitosonium acetate is capable of undergoing a transformation to chitin by heating, an amidization process, and that the process involves two sequential first order reactions. This pattern of amidization is similar to the reported heat-induced transformation of polyamic acid to polyimide, an imidization process, in which imidization proceeds by an initial fast reaction, followed by a substantially slower reaction[17, 18]. In contrast to the amidization process, however the activation energies of the imidization reaction were reported to be insignificantly different, i.e., 26 ± 3 kcal/mol and 23 ± 7 kcal/mol for the initial, fast and later, slow reactions, respectively[18]. The higher activation energies for the imidization process over amidization may be related to higher energy barriers associated with the ring closure that occurs in imidization with the loss of water. In the imidization process, the T_g of the material continually rises as conversion proceeds. Molecular motion is frozen in or restricted when the rising T_g becomes equal to and/or well above the imidization temperature such that attainment of suitable conformation necessary for imidization is not possible. However, when the imidization temperature is raised to a value above the ultimate T_g of a corresponding fully-cured (and therefore fully-imidized) material further imidization is possible. Therefore, it has been suggested that the existence of two sequential cure reactions could be related to restrictions on chain mobility. It would be expected, contrarily to the activation energies reported for the imidization process, that the slow, late reaction should be associated with a higher energy barrier, i.e activation energy. This is because it would require a much higher activation energy to rearrange

the polymer chains which are supposedly frozen in position to suitable conformations necessary for imidization to occur. This expectation is consistent with the activation energies of amidization reported in this study, i.e., a lower activation energy for the fast, initial reaction compared to the slow, late activation energy. Other studies suggest that the cure of amine-cured epoxy is considerably retarded once vitrification is reached, i.e., when the rising T_g becomes equal to the cure temperature. This is attributed to restrictions on chain diffusion necessary for the cure reaction to proceed [19]. Thus, it is reasonable to postulate that the existence of two sequential reactions involved in chitosonium acetate to chitin transformation has to do with limitations on chain mobility. Further work to substantiate this postulate is presented in chapter 5.

3.5 CONCLUSIONS

1. Chitosonium acetate spontaneously converts to chitin at elevated temperatures. Thus, chitin is regenerated from a chitosan-acetic acid complex.
2. Chitosonium acetate to chitin transformations give rise to modulus and T_g-changes, which can be likened to the behavior of thermosets.
3. T_g-changes can be used to describe the kinetics of chitosonium acetate-to- chitin transformations.
4. Two first-order rate equations, which adequately describe the chitosonium acetate-to-chitin transformation, suggest two distinct reaction phases, an initial phase with an activation energy of 15 kcal mol^{-1} and a late phase with an activation energy of 21 kcal mol^{-1}.

5. The transformed material behaves in several respects like a thermoset, especially in terms of T_g and modulus rise with time, and tan δ-decline.

3.6 ACKNOWLEDGEMENT

This is to thank Mr. Jianwen Ni, Department of Wood Science and Forest Products, Virginia Tech, for his assistance with the solid state NMR spectroscopy.

3.7 REFERENCES

1. Encyclopedia of polymer science and engineering, vol 3,. Wiley, NY, pp430-40.

2 Balassa, L.L., and Prudden, J.F., in: Proceedings of the first International Conference on Chitin and Chitosan, Muzzarelli, R.A.A. and Pariser, Eds., MIT, Cambridge, MA, 1978.

3. Sapelli, P.L., in: Chitin in nature and Technology, Muzzarelli, R.A.A., Ed., 1986.

4. Nakajima, M., Atsumi, K., K., Miura, K., and Kanamaru, H., Jpnese J Surg.,16, 418, 1986.

5. Rutherford, F.A., and Austin, P.R., In: Proceedings of the first International Conference on Chitin and Chitosan, Muzzarelli, R.A.A. and Pariser, Eds., MIT, Cambridge, MA, 1978.

6. Averbach, B.L., in: Proceedings of the first International Conference on Chitin and Chitosan, Muzzarelli, R.A.A. and Pariser, Eds., MIT, Cambridge, MA, 1978.

7. Hepturn, H.R., and Chandler, H.D., in: Proceedings of the first International Conference on Chitin and Chitosan, Muzzarelli, R.A.A. and Pariser, Eds., MIT, Cambridge, MA, 1978.

8. Mima, S., Miya, M., Iwamoto, R., and Yoshikawa, S., J. Appl. Poly. Sci., Vol. 28, 1909-1917, 1983.

9.East, G.E., and Qin, Y., J. Appl. Poly. Sci., Vol. 50.1773-1779, 1993.

10. Wei, Y.C., Hudson, S.M., Mayer, J.M., and Kaplan, D.L., J. Polym. Sci., Part A, 30, 2187-2193, 1992.

11. Hosokawa, J., Nishiyama, M., Yoshihara, K., and Kubo, T., Ind. Eng. Chem. Res., 29, 800-805, 1990.

12. Isogai, A., and Atalla, R.H., Carbohydr. Polym., 19, 25-28, 1992.

13. Gillham, J.K., in: Structural Adhesives, Kinloch, A.J., Ed.,Elsevier Applied Sci. Pub., 1986.

14. Hofmann, K. , and Glasser, W.G., Thermochimica Acta, 166, 169-184, 1990.

15. Pizzoli, M., Ceccorulli, G., and Scandola, M., Carbohydrate Research, 222, 205-213, 1991.

16.Provder et al. ,In: Polymer Characterization, Craver, C.D., Ed., 1981.

17. Numata, S., Fujisaki, K., and Kinjo, N., In: Polyimides: Synthesis, Characterization and Applications, Vol. 1, Mittal, K.L., Ed. Plenum, N.Y., 1984.

18. Kreuz, J.A., Endrey, A.L., Gay, F.P., and Sroog, C.E., J. Polym. Sci., Part A-1, Vol. 4., 2607-2616, 1966.

19. Wisanrakkit, G., and Gillham, J.K., J. Appl. Poly. Sci., Vol. 41, 2885-2929, 1990.

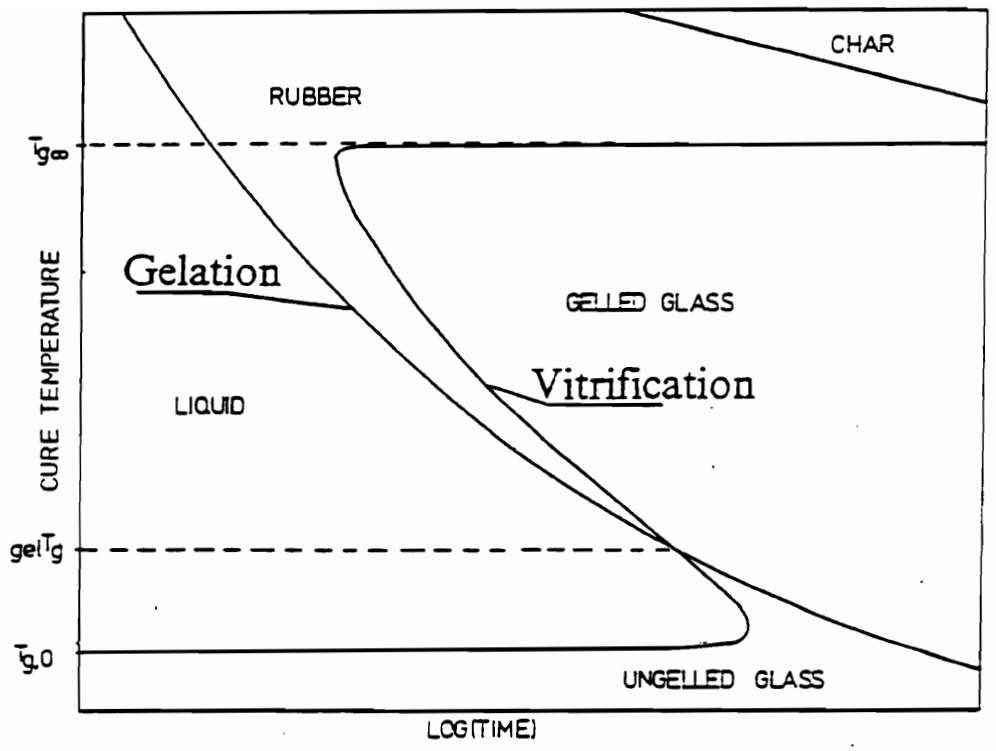

Figure 3-1. The time-temperature-transformation (TTT) cure diagram of Gillham[13] showing the various events and states associated with cure of a thermoset.

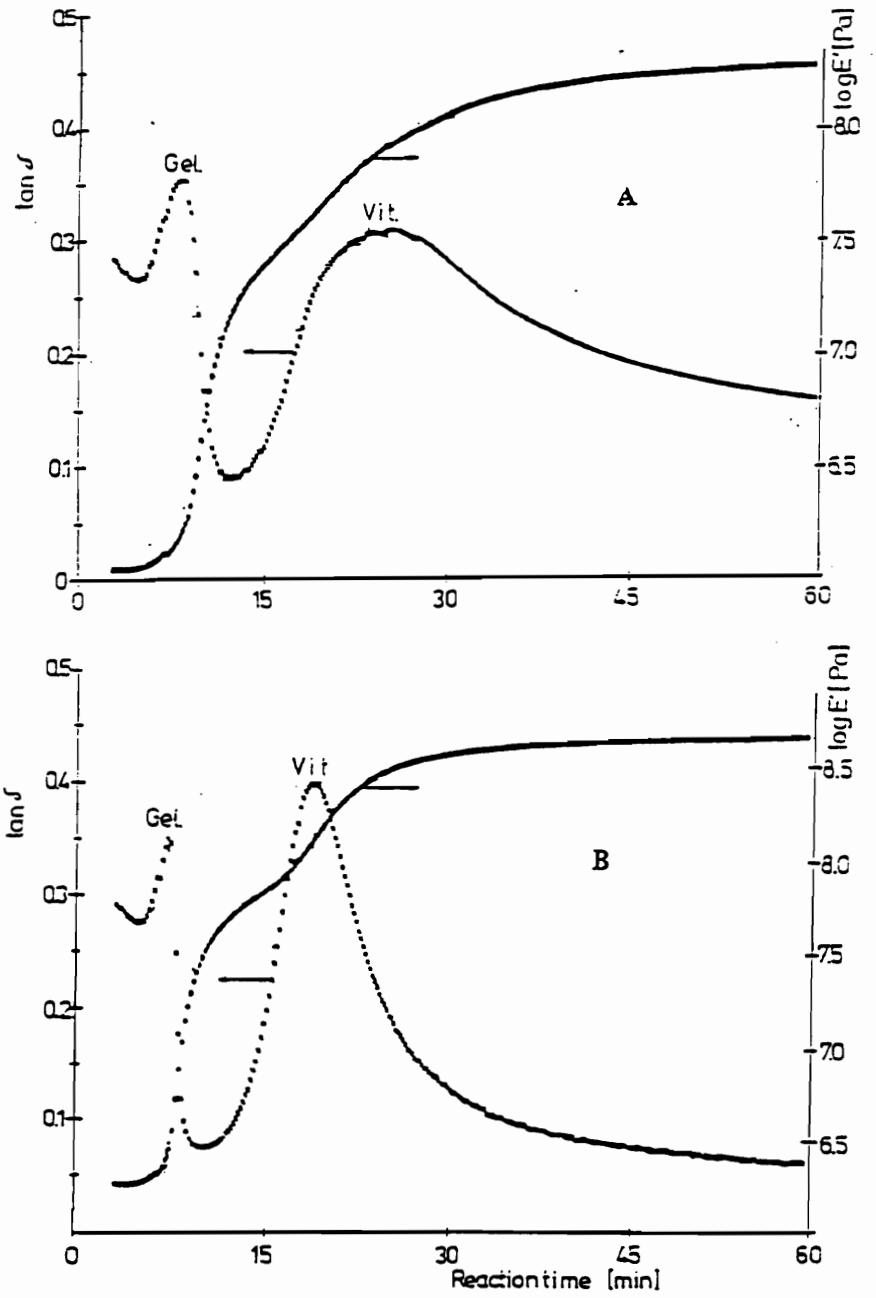

Figure 3-2. Isothermal cure profiles of an amine-cured epoxy resin at two temperatures (A: 130°C , B: 140°C). The tan δ curves give distinct transitions identified with gelation and vitrification. The times to both gelation and vitrification were shorter at the higher temperature[14].

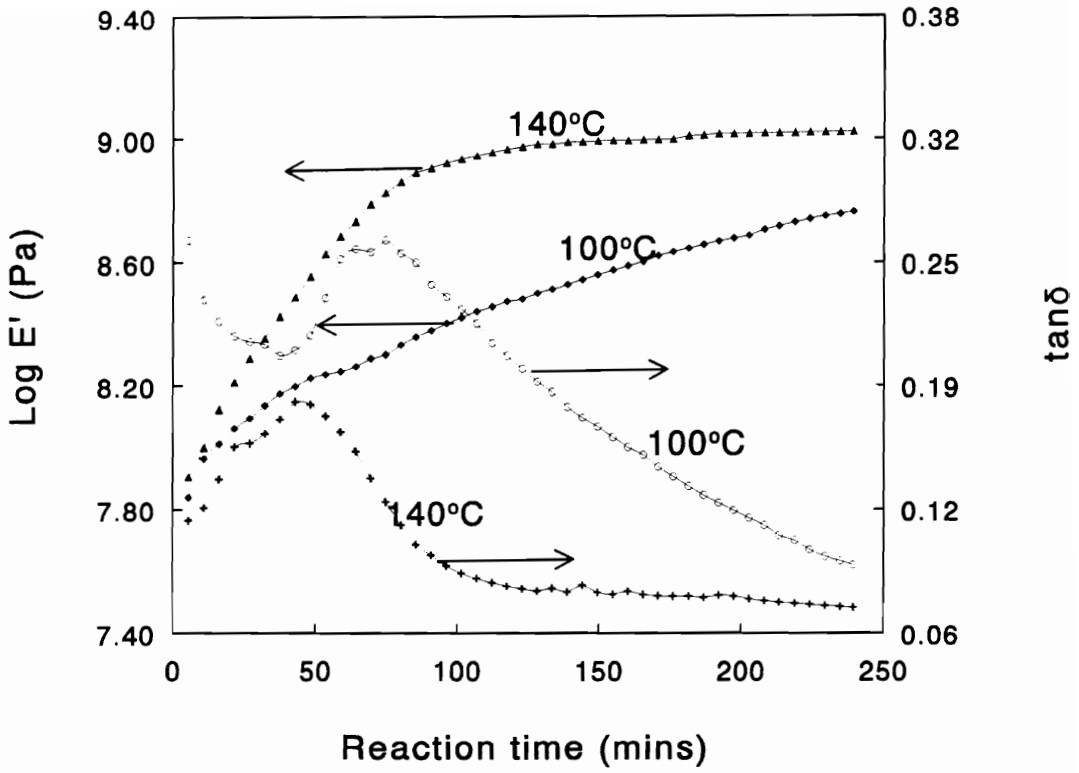

Figure 3-3. Isothermal cure profiles of chitosonium acetate (ChAc) at two temperatures, 100°C and 140°C. The storage modulus shows a progressive increase with time, and the tan δ shows two overlapping transitions.

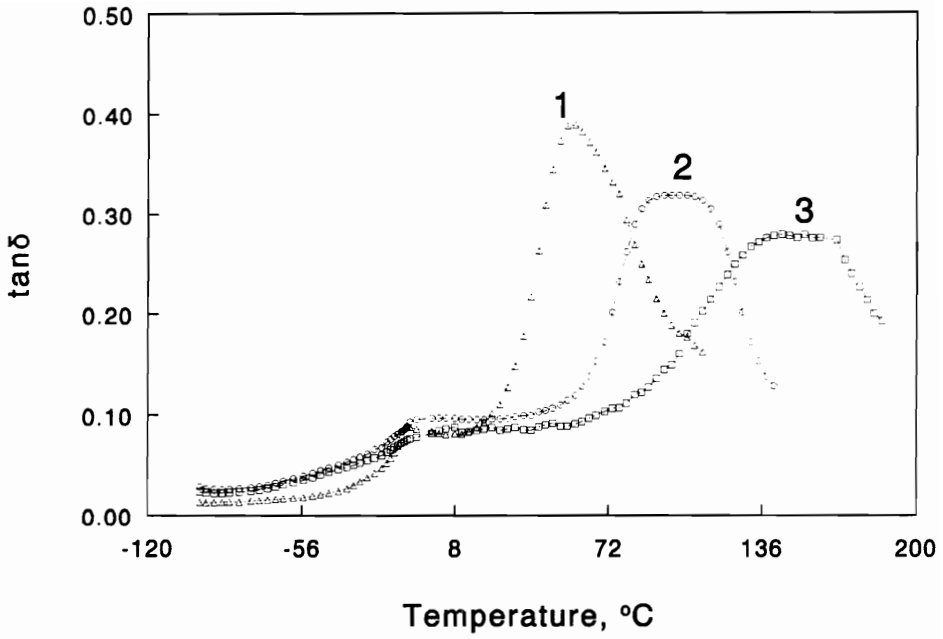

Figure 3-4. DMTA spectra of chitosonium acetate subjected to sequential heat treatments. There is a progression of T_g to higher value with each scan, and a corresponding decline in peak height. 1, 2, and 3 represent 1st, 2nd, and 3rd scans, respectively.

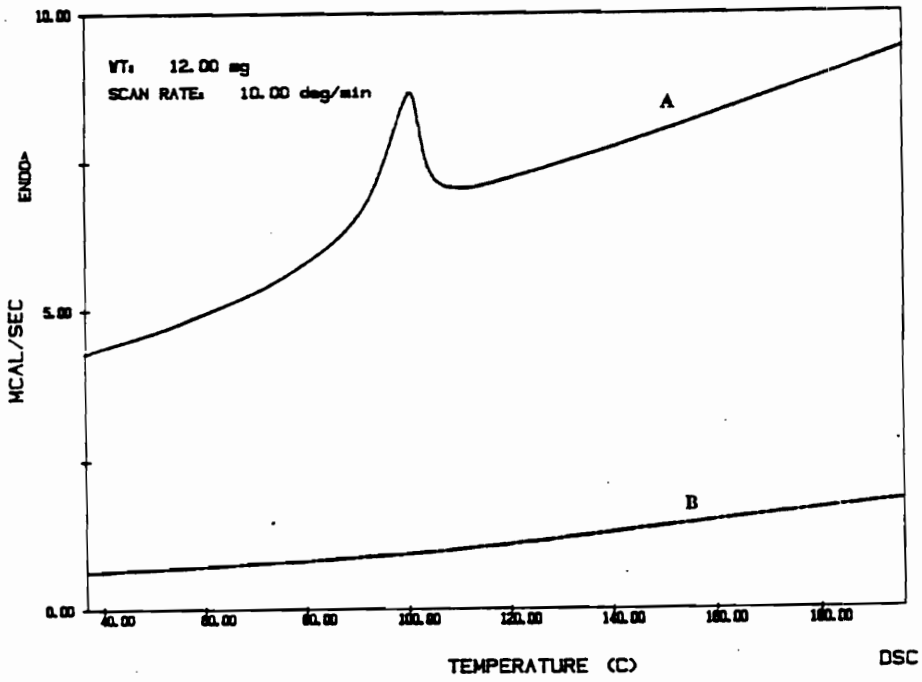

Figure 3-5. A differential scanning thermogram of a freshly-cast (A), and dried (B) chitosonium acetate films. A well-resolved endotherm due to the loss of residual moisture is apparent at 100°C for A.

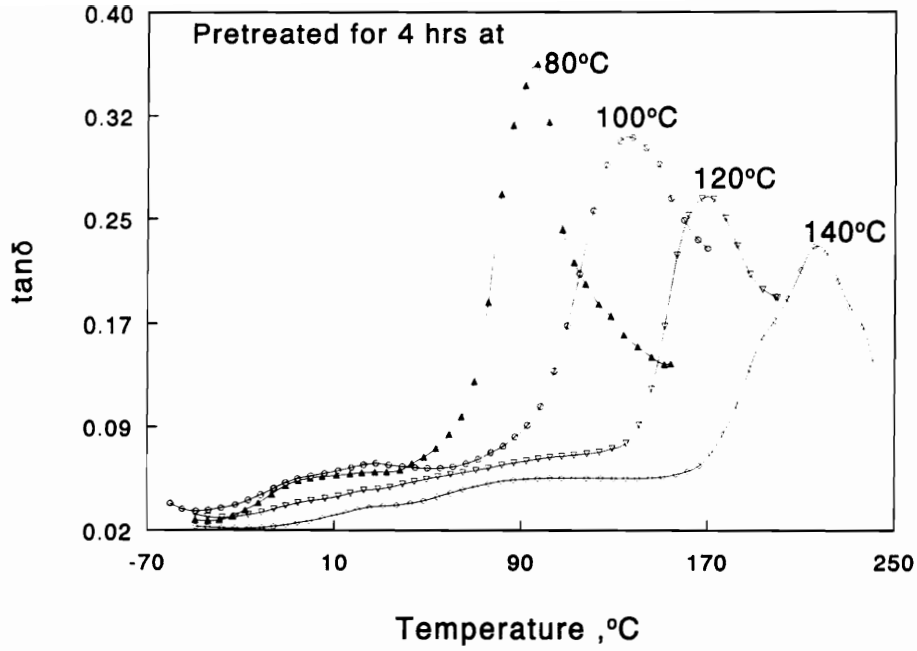

Figure 3-6. Dynamic scan of chitosonium acetate heat treated at various temperatures for 4 hrs. As the temperature is raised, there is a progression of T_g to higher values, and a decline of the peak height of the transition. This is a behavior which parallels that of a thermoset at different crosslink densities.

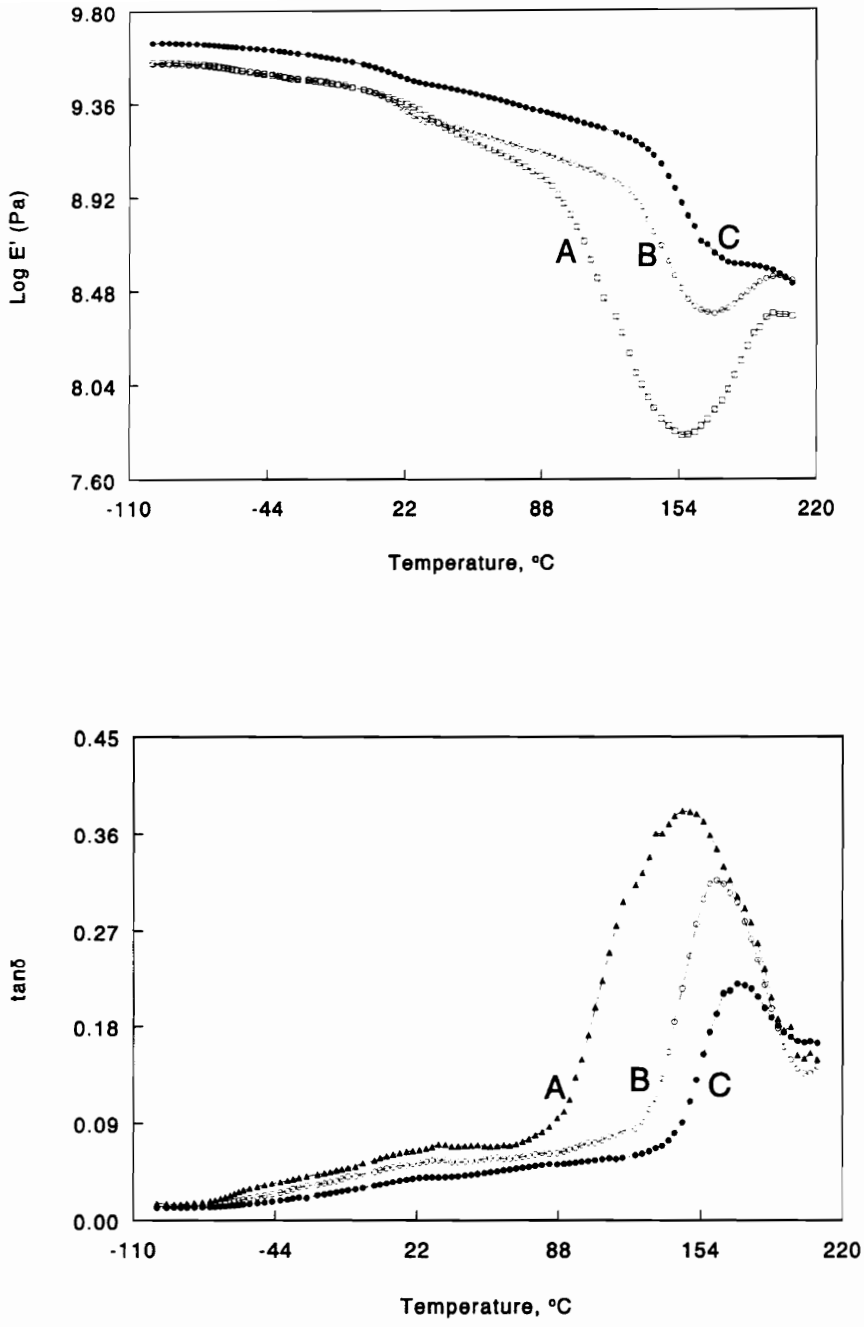

Figure 3-7. Top: Storage modulus profile of chitosonium acetate heat treated at 110°C for various periods; Bottom: Damping profile of same material. A, B, and C represent 2hr, 4hr, and 12hrs of heat treatment at 110°C.

(a)

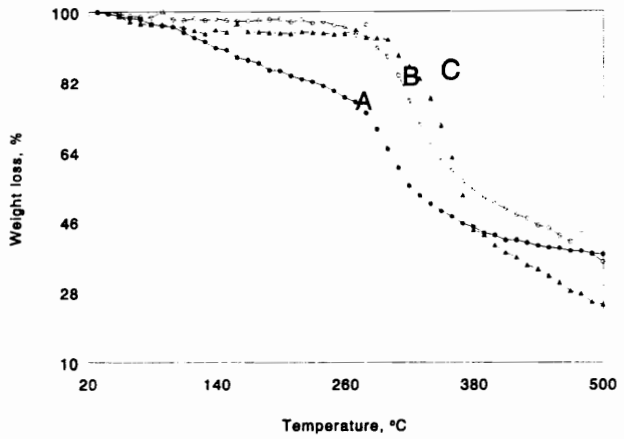

(b)

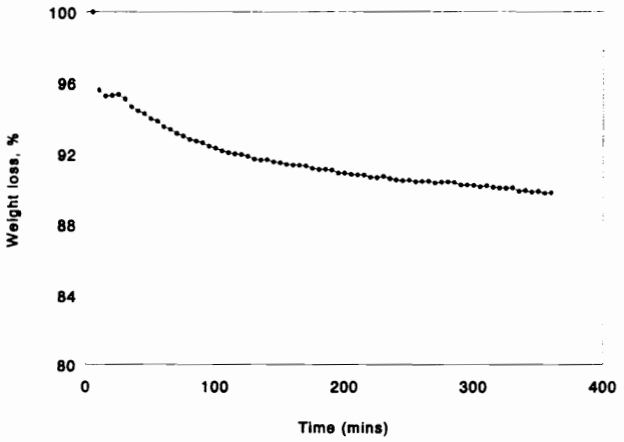

Figure 3-8 (a) Relative stability of chitosonium acetate (A), heat treated chitosonium acetate (B), and native chitin (C). The degradation profile of heat treated chitosonium acetate mirrors that of native chitin, and supports the assertion that there is a thermally triggered conversion of chitosonium acetate to chitin. Figure 3-8 (b). Thermogravimetric analysis spectrum of powderous chitosonium acetate at an isothermal temperature of 110°C. The loss of weight never attains an equilibrium; but, it is approximately equivalent to the theoretical weight loss expected in the conversion of chitosonium acetate to chitin.

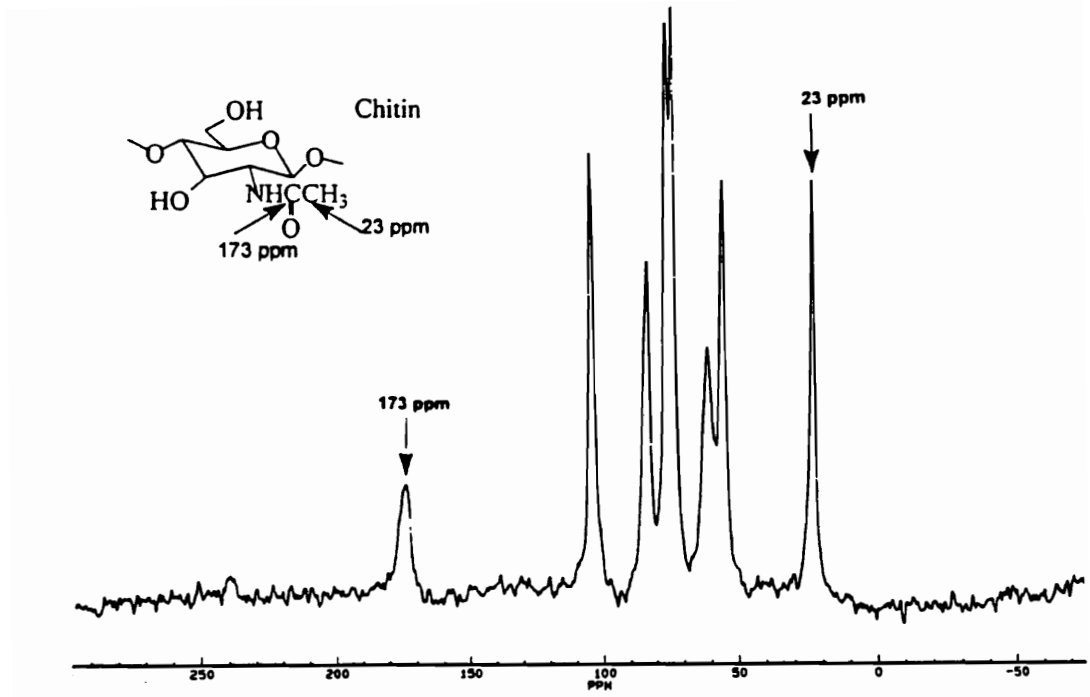

Figure 3-9. CP-MAS ^{13}C-NMR spectrum of chitin. The peaks at 23 and 173 ppm are identifiable as methyl (CH_3) and N-acetyl carbonyl groups, respectively.

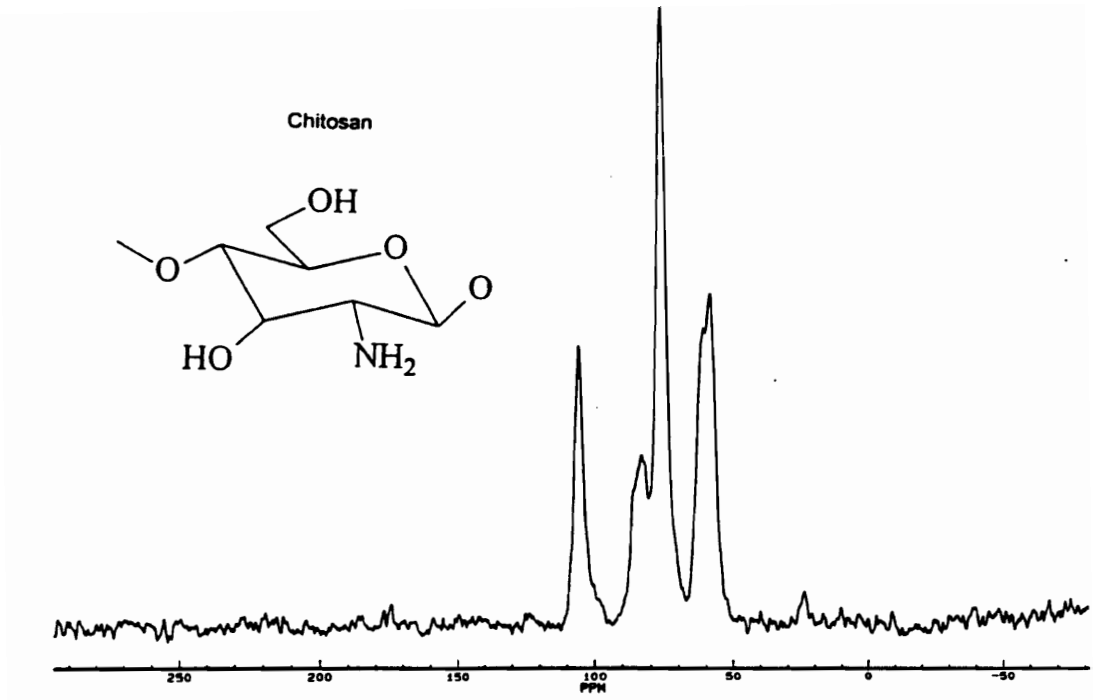

Figure 3-10. CP-MAS ^{13}C-NMR spectrum of chitosan. Both the methyl and N-acetyl carbonyl peaks disappear due to deacetylation.

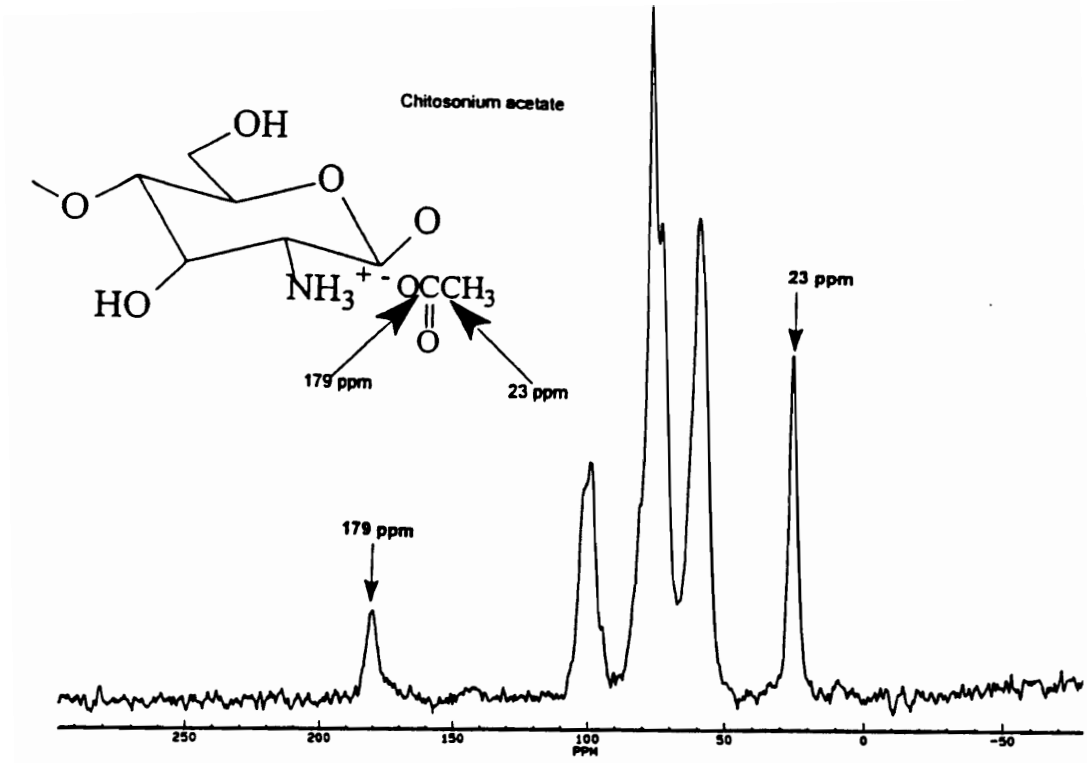

Figure 3-11. CP-MAS ^{13}C-NMR spectrum of chitosonium acetate. The peaks at 23 and 179 ppm are identifiable as methyl (CH_3) and ionic N-acetate carbonyl groups, respectively.

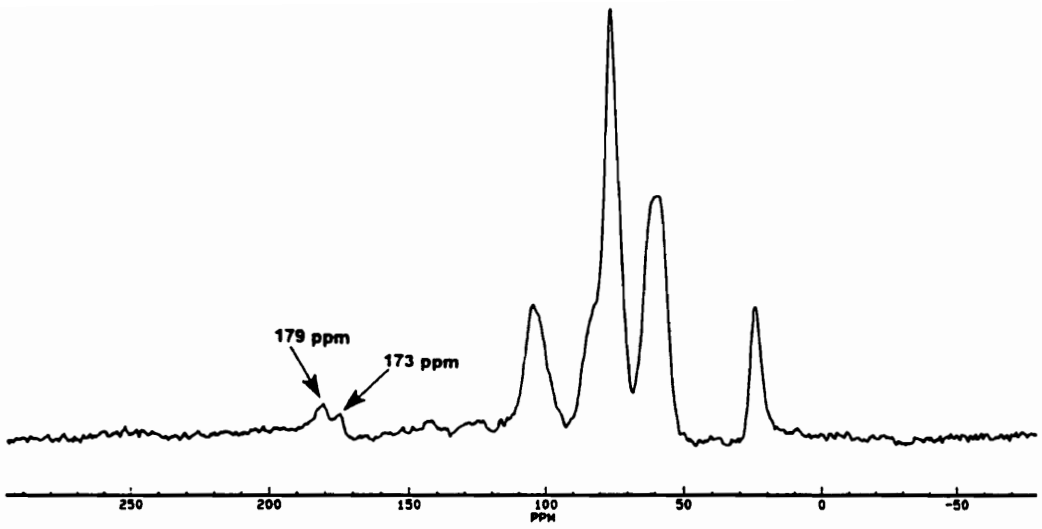

Figure 3-12. CP-MAS ^{13}C-NMR spectrum of chitosonium acetate which is subjected to heat treatment at 100°C for 12 hrs. Both the N-acetate and N-acetyl carbonyls are discernible.

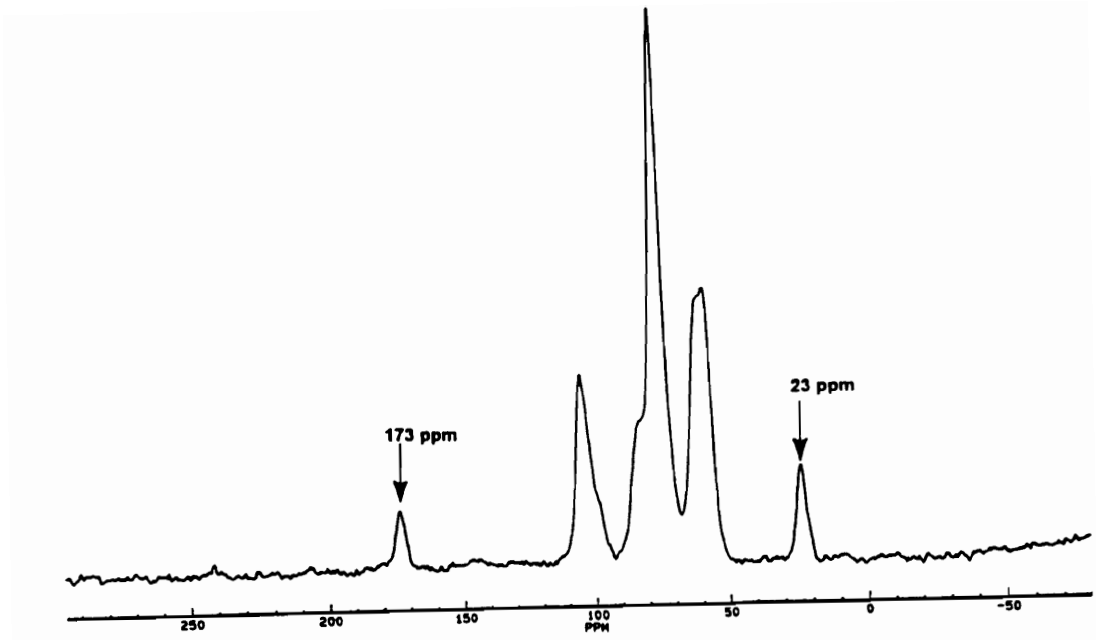

Figure 3-13. CP-MAS ^{13}C-NMR spectrum of chitosonium acetate which is subjected to heat treatment at 100°C for 12 hrs, followed by treatment with cold alkali. The N-acetate carbonyl at 179 ppm disappears as a result of this treatment, only leaving the N-acetyl carbonyl at 173 ppm.

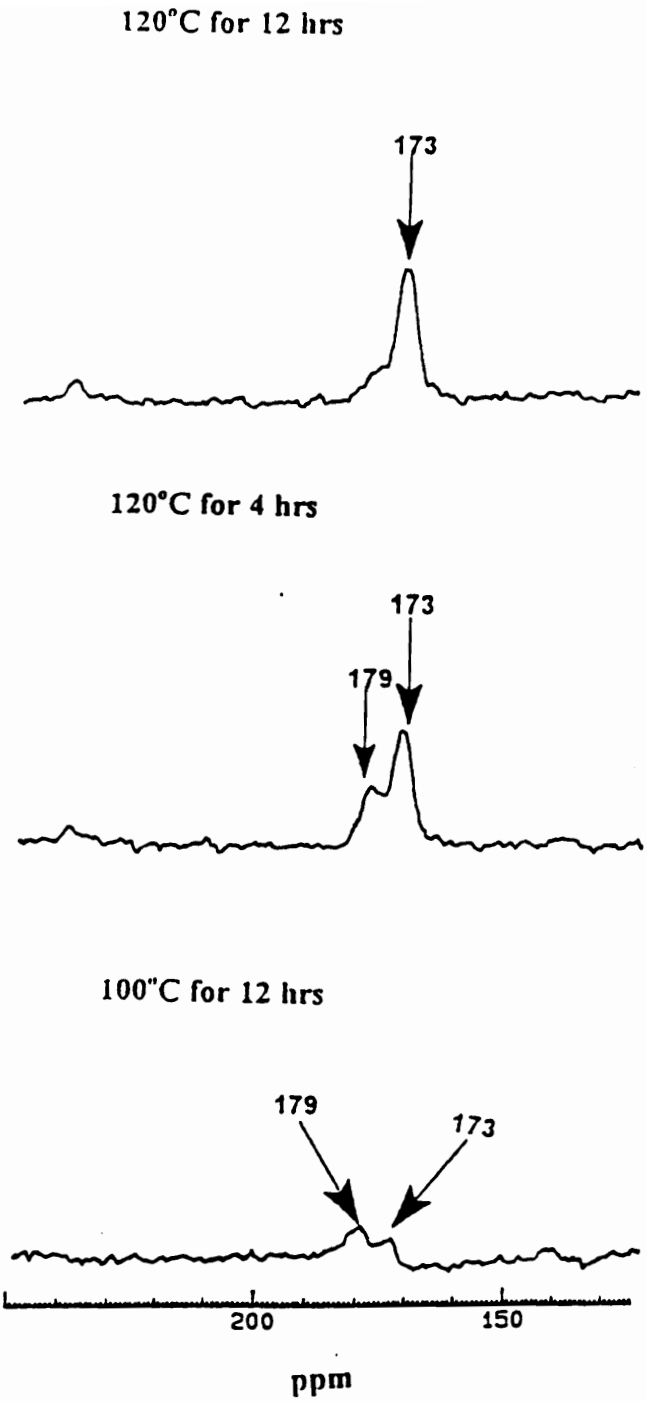

Figure 3-14. CP-MAS ^{13}C-NMR spectra of chitosonium acetate which is subjected to different severity of heat treatment. There is a progressive disappearance of the N-acetate carbonyl peak at 179 ppm with increasing severity of heat treatment.

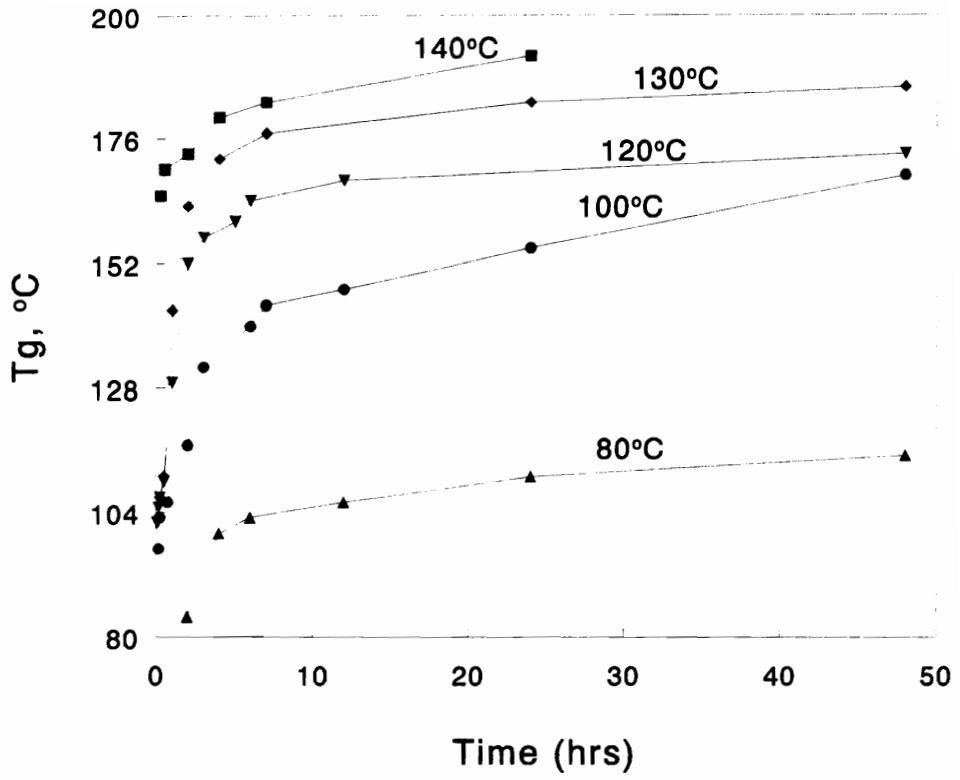

Figure 3-15. Glass transition temperature variation with time at various isothermal cure temperatures. This figure is transformed, according to equation 3, to conversion variation with time. The initial, $T_{g,o}$, and maximum glass transition temperatures, $T_{g,\infty}$, were determined as 57 and 189°C, respectively.

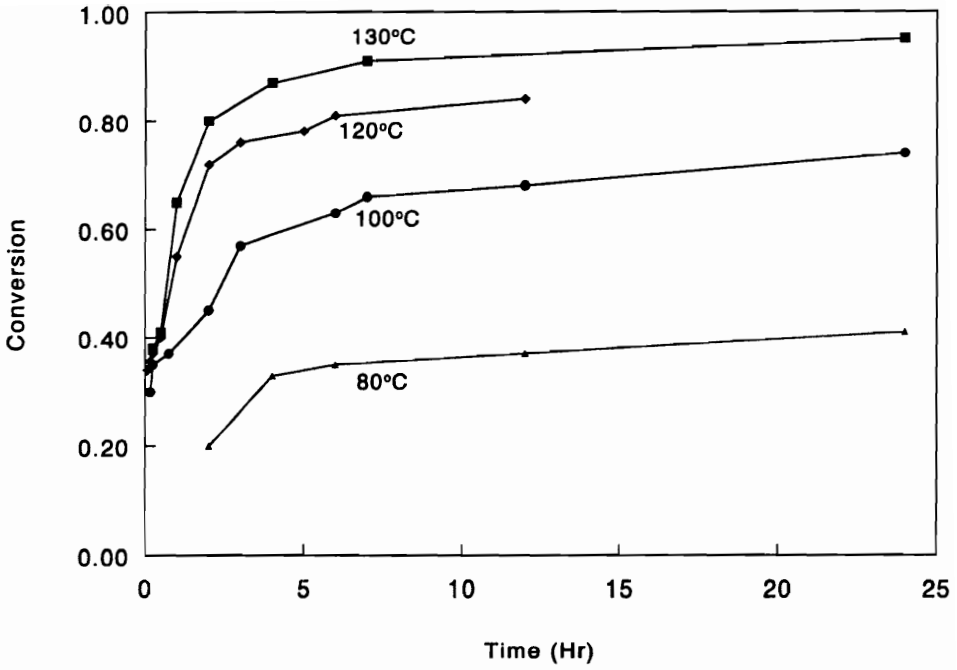

Figure 3-16. Conversion, calculated using equation 3, with time at various isothermal temperatures.

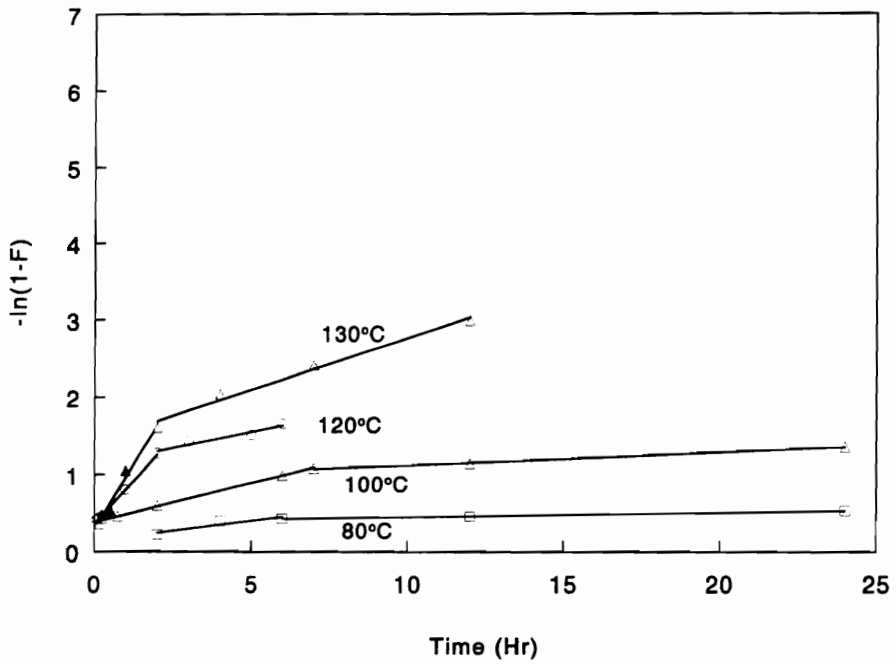

Figure 3-17. First order plot of chitosonium acetate to chitin transformation according to equation 2. There is a change in slope of each line after prolonged heat treatment. This trend suggests that two sequential steps are involved in the chitosonium acetate to chitin transformation.

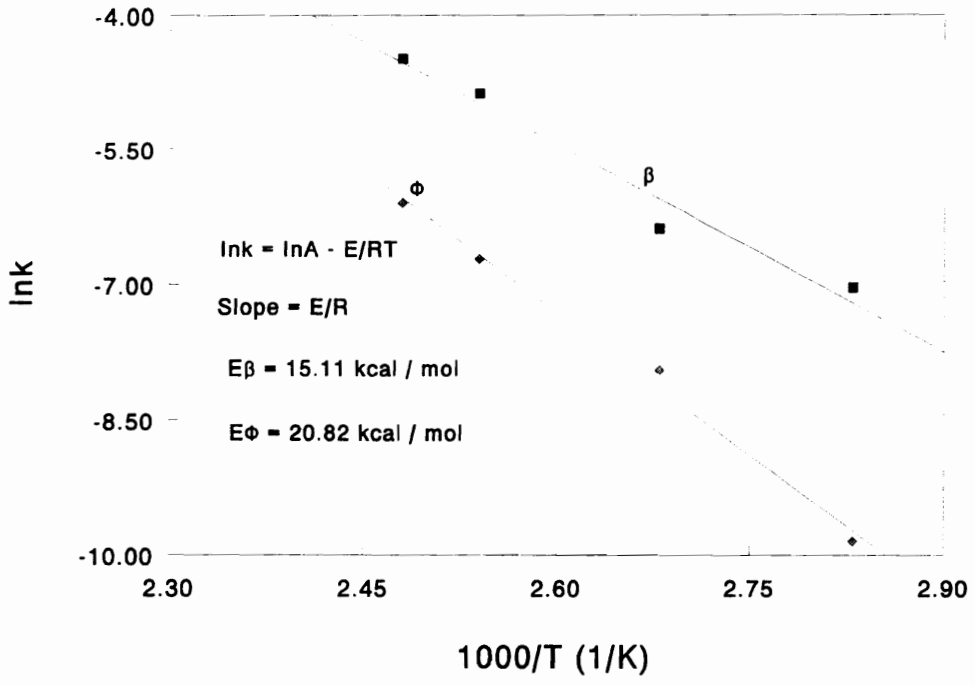

Figure 3-18. Arrhenius plot of rate constants versus temperature for activation energy determination of the amidization reaction involved in the transformation of chitosonium acetate to chitin. The activation energy is determined from the slope of the line according to equation 4. β: First step reaction, Φ: second step reaction. Eβ and EΦ are the corresponding activation energies.

CHAPTER 4

CHITIN DERIVATIVES. II. TIME-TEMPERATURE-TRANSFORMATION CURE DIAGRAMS

4.1 ABSTRACT

The transformation of the ionic complexes of chitosan with acetic and propionic acid, chitosonium acetate and chitosonium propionate, into chitin or the respective homolog of amidized chitosan has been described on the basis of time-temperature-transformation (TTT) cure diagrams. The time to vitrification at various isothermal cure temperatures (T_c) was determined using dynamic mechanical thermal analysis. The time to full cure was derived using a T_g–T_c–cure time relationship according to the method of Peng and Gillham as well as by an extrapolation procedure. Consequently, TTT-cure diagrams describing the above transformation include full cure and vitrification curves. As in thermosets, this transformation displays an S-shaped vitrification curve, and the time to full cure increases with decreasing cure temperature. The time to full cure is very remote from the time to vitrification and this is due to the tendency of vitrification to prevent full cure from being attained. The activation energy for vitrification of chitosonium acetate and chitosonium propionate derived from an Arrhenius equation are similar. This suggests that the same mechanism governs glass formation in acetate and propionate chitosan homologs.

Additionally, the morphology of amidized chitosan and native chitin was examined using X-ray diffraction and FTIR analysis. X-ray diffraction results indicate that amidized chitosan is an amorphous material. On the other hand, native chitin is

crystalline. FTIR suggests the existence of hydrogen-bonded amide groups in native chitin but not in amidized chitosan. This difference in morphology between amidized chitosan and native chitin is accounted for in terms of the influence of glass formation in the former.

4.2 INTRODUCTION

The transformation of a thermosetting resin from the liquid state into the solid state involves polymerization and crosslinking. This is technically referred to as cure[1]. The process of cure is often accompanied by several chemo-rheological events. These include modulus (stiffness) build-up and T_g-increase with isothermal cure time, as well as gelation and vitrification. Both gelation and vitrification give rise to characteristic peaks in the tan δ-curve of a typical dynamic mechanical thermal analysis (DMTA) spectra[2]. In a previous article we reported on the kinetics of the heat-induced transformation of the ionic complex of chitosan with acetic acid, chitosonium acetate, to chitin[3]. The process was described as amidization curing of chitosonium acetate. This description was on the basis that N-acetate is converted to the N-acetyl (amide) when exposed to isothermal conditions. Also, since this transformation is accompanied by a modulus rise as well as a T_g-increase, it was likened to the process of cure of network-forming resins. However, the amidization curing process differs from crosslinking in terms of chemical and structural changes. Whereas the latter involves chemical reactions between various functional groups which form a three-dimensional network, the former involves thermal dehydration with the formation of a linear polymer closely

resembling the starting material. Nonetheless, the chemo-rheological transformations involved in both processes are similar.

The time-temperature-transformation (TTT) cure diagram has evolved as a useful framework to understanding the cure behavior of thermosetting resins[4]. It represents the times necessary to achieve gelation and vitrification at various isothermal cure temperatures **(Figure 4-1)**. In terms of practical significance, it assists in the selection of time and temperature schedules to achieve a material of certain physical properties. $T_{g,0,}$ included in the TTT cure diagram represents the T_g of the uncured resin and is considered as the safe storage temperature to avoid premature crosslinking. $T_{g,\infty}$ is the ultimate T_g of the network polymer. For polymers which do not show substantial degradation above $T_{g,\infty}$, selection of cure temperatures above $T_{g,\infty}$ represents an effective means of achieving a fully-cured polymer.

Palmese and Gillham have studied the conversion of polyamic acid to polyimide using the concept of the TTT-cure diagram[5]. This conversion is referred to as imidization curing of polyamic acid. The process involves thermal dehydration of polyamic acid to the imide **(Figure 4-2)**. These authors suggest that the process does not involve gelation since the resulting polyimide is a linear system, closely resembling the starting material. Consequently, they were able to develop a TTT-cure diagram that depicts only the vitrification and full-cure curves. Like thermosetting resins, a description of imidization in relation to the TTT-cure diagram is useful in so far as it permits selection of time and temperature windows so that vitrification and full cure

occurs in a predictable manner. The imidization curing of polyamic acid reported by Palmese and Gillham is similar to the amidization curing of chitosonium acetate, i.e., both processes involve thermal dehydration (**Figures 4-2 and 4-3**). More importantly the two processes were found to follow a two-stage transformation scheme; i.e., imidization and amidization both were observed to proceed by an initial fast reaction followed by a substantially slower reaction.

The usefulness of the TTT-cure diagram cannot be overemphasized, yet it has received no attention in evaluating the cure behavior of biobased resins. To date only one report is found in the literature dealing with a description of the cure behavior of biobased resins on the basis of the TTT-cure diagram[14]. This is a study carried out in our laboratory. The close resemblance of amidization to imidization and network formation provides a scenario for understanding amidization on the basis of the TTT-cure diagram as well as for extending the concept to biobased polymer research.

During cure, thermosetting resins go through three distinct phases. The precursor material (A-stage) is a liquid or solid and is soluble and fusible[1]. The precursor passes through a B-stage at sufficiently high temperatures. Some resin systems, which are very reactive, can reach this stage at room temperature. The B-stage is characterized by chain extension and prepolymer formation to produce insoluble but swellable material[1]. The C-stage develops at higher temperatures, and the resulting material is a three dimensional network which is insoluble and infusible. The ability of thermosets to reach the C-stage depends on gelation and vitrification. For example, at vitrification the polymer chains are

completely frozen in position and preclude reactive chain ends to reach each other for chemical crosslinking. Different morphologies develop at each of these phases with implications on the end-use properties. Therefore, it implies that the morphology that develops during cure is influenced by both gelation and vitrification. During the transformation of chitosonium acetate to regenerated chitin vitrification is suspected to occur very early in the process[3]. This will likely prevent chain alignment and ordering and thus develop a morphology different from native chitin.

The intent of this paper is to describe the amidization curing of the ionic complexes of chitosan with acetic and propionic acid, chitosonium acetate and chitosonium propionate, respectively on the basis of TTT cure diagrams. Also the influence of vitrification on the phase transition (morphology) of amidized chitosan is investigated.

4.3 MATERIALS AND METHODS

4.3.1 Materials

The chitosan used for this study was obtained from Sigma Chemicals, St Louis, MO. This chitosan is derived from crab shells by alkaline hydrolysis (deacetylation). The extent of deacetylation is specified by the manufacturer as 89.3%. Glacial acetic acid and propionic acid were used as solvents for chitosan. Both solvents were obtained from Aldrich Chemicals, Milwaukee, WI. Both chitosan and the acids were used as received from the manufacturer.

4.3.2 Methods

4.3.2.1 Chitosonium Acetate/Propionate Film Preparation

The preparation of chitosonium acetate and chitosonium propionate films involved dissolution of 57 g of chitosan in 2 L of 10% aqueous acetic acid and propionic acid, respectively, followed by vigorous stirring for 24 h. The resulting solutions were centrifuged to remove suspended matter. About 150-250 mL of each solution was poured into evaporation dishes and left in a laboratory hood for solvent evaporation at room temperature for two days. After the second day each evaporation dish was covered with perforated aluminium foil. The aluminium-covered dishes were left for a period of one week for further solvent evaporation. This was followed by vacuum drying at room temperature for 24 h. It was necessary to leave the films "glued" to the evaporation dishes to avoid warping of the films during vacuum drying. The films produced had a thickness of 0.2-1.4 mm depending on the initial volume of solution. Residual solvent content was less than 2% as measured by TGA.

4.3.2.2 Cure Monitoring by Dynamic Mechanical Thermal Analysis

Amidization curing of chitosonium acetate and propionate was monitored using a Polymer Laboratory DMTA. Samples in the form of circular disks produced from films using a paper puncher were tested in shear mode under isothermal cure conditions of 80 to 190°C. Rectangular samples of dimensions 8 × 5 × 1.1 mm were also tested using similar isothermal conditions but in bending mode. Further, samples in the form of rectangular bars of similar dimensions preheated in an oven at isothermal

temperatures of 80 to 190°C for varying cure times were tested under dynamic conditions in bending mode at a heating rate of 2.5°C/min. Both modes of testing employed oscillation amplitudes of 0.4 mm and frequencies of 1 Hz as well as a nitrogen purge of 25 cm^3/min. Samples tested in bending were oscillated in a single cantilever fashion.

4.3.2.3 X-ray Diffraction Analysis

The morphology of amidized chitosan, native chitin, chitosan, and chitosonium acetate was examined using X-ray diffraction analysis. This was carried out using a Scintag PTS XDS 2000 instrument. Measurements were executed from 5 to 60° with irradiation conditions of 30 kV and 25 mA, and scanning rate of 2°/min of diffraction angle 2θ. Native chitin, chitosan, chitosonium acetate and amidized chitosan were mounted on the instrument holder with the aid of scotch tape. All samples were in powderous form. The degree of cystallinity of chitosan and native chitin was determined by ratioing the crystalline peak area of the diffractogram and the total peak area (crystalline and diffuse background area).

4.3.2.4 FTIR Analysis

FTIR measurements were performed at room temperature using a Nicolet FTIR instrument. Native chitin and amidized chitosan were each blended with KBr in a ratio of 1:6 (sample:KBr) and pressed into small, clear discs in an FTIR sample holder. Each disc thus obtained was mounted immediately for analysis.

4.3.3 Data Interpretation

The process of cure typically give rise to gelation, the formation of an infinite polymer network. Gelation precedes vitrification which corresponds to the point when the rising glass transition temperature of the curing system becomes equal to the isothermal cure temperature. In a typical DMTA spectrum gelation and vitrification are thermal events which give rise to distinctive transitions in the tan δ curve[2]. Therefore, the construction of the vitrification or gelation curve in a TTT cure diagram involves a series of isothermal cure experiments at several different temperatures (T_c), where tan δ is recorded as a function of time, and plotted as T_c vs vitrification or gelation time on a log scale.

Sometimes the TTT cure diagram is constructed to include a full cure curve. This curve aids in the selection of time and temperature paths to achieve full cure[5,15]. This is particularly important considering that meaningful structure-property relationships of two polymers can be deduced when they are fully-cured. Peng and Gillham[15] have related T_gs of epoxy networks toT_cs by a linear equation as follows

$$T_g = A + BT_c \qquad (1)$$

where A is a constant influenced by cure time, and B is a constant independent of cure time. Under the assumption that these networks are fully-cured when T_g reaches $T_{g,\infty}$, they obtained the temperatures for full cure to be reached in a specified time, $T_{\infty(t)}$ by recasting equation (1) as

$$T_{g,\infty} = A + B\,T_{\infty(t)} \qquad (2)$$

Alternatively, the times to full cure can be derived by extrapolation of T_g vs. T_c- curves to $T_{g,\infty}$.

The activation energy for vitrification provides a basis for evaluating the influence of structure on glass formation. Peng and Gillham[15] as well as Palmese and Gillham[5] have described the times to vitrification in an Arrhenius fashion to derive the apparent activation energies for vitrification. The time to achieve a specified extent of cure (p) was reported to be an inverse function of the isothermal cure temperature (T_c) necessary for attaining p,

$$\ln t = (E / R)1 /T_c + \ln g(p) \qquad (3)$$

where E and R are activation energy and universal gas constant, respectively and g is a constant that depends on p.

Equation (3) assumes that cure reactions are not influenced by vitrification-related diffusion. However, in most cases reactions are influenced by polymer chain diffusion, particularly beyond vitrification. Nonetheless, a recast of equation (3) as

$$\ln t_{vit} = (E_{vit} / R)1 /T_c + \ln g(p_{vit}) \qquad (4)$$

with p_{vit} as the extent of cure at vitrification, produces a linear relationship between the times to vitrification ($\ln t_{vit}$) and the cure temperature (T_c). Consequently, the activation energy for vitrification (E_{vit}) can be derived by plotting $\ln t_{vit}$ vs T_c.

4.4 RESULTS AND DISCUSSION

4.4.1 Phase Transformation of Chitosonium Acetate/Propionate

When chitosonium acetate or chitosonium propionate films are exposed to isothermal cure temperature of 140°C in a DMTA operated in a single cantilever bending mode two transitions are observed in the loss tangent **(Figure 4-4)**. These transitions are within the vicinity of each other giving a more or less single, broad transition. On the other hand, when similar samples are tested at the same temperature in a shear mode, a single, well-defined peak is obtained **(Figure 4-5)**. In both cases there is an increase of modulus with time. Generally, a network forming polymer gives two distinctive transitions in the loss tangent under isothermal exposure. These transitions are attributed to gelation and vitrification. This attribute is related to the fact that the reactive polymer exhibits low damping in the liquid phase, but damping rises with time as the material becomes rubbery. This rise becomes limited once the material has gelled on account of restriction on chain mobility, therefore giving a characteristic peak in the loss tangent. The polymer displays a second transition as it transforms from a rubbery phase to a glassy phase, similar to the glass-to-rubber transition[2]. In the case of chitosonium acetate or chitosonium propionate no gelation is expected since the final product (amidized chitosan) remains a linear polymer although "physical gelation" is possible by the formation of ordered aggregates (crystalline regions) or physical entanglements. However, since (a) there is no distinct crystallinity (as explained in a latter section) observed; and (b) there is only a shoulder of the loss tangent, the initial

peak in bending is attributed to a phenomenon inherent to clamping rather than a molecular reorganization, and the single loss tangent peak in shear (the peak at log 3.3 sec), as well as the second loss tangent peak in bending (the peak at approximately log 3.3 sec) are identified as the phase transformation of chitosonium acetate or chitosonium propionate from the rubbery state to the glassy state, i.e., vitrification. This identification is on the basis that both bending and shear testing are capable of detecting vitrification[2,5] and that both peaks are in the vicinity of each other. Presumably the first peak observed in bending is due to another phenomenon, probably not related to a molecular reorganization that occurs just prior to extensive thermal dehydration. Shear testing may not have been sensitive to such changes. Palmese and Gillham have also observed single peaks at various temperatures in torsional braid analysis of the thermal dehydration of polyamic acid similar to the single peaks observed in shear testing of chitosonium acetate or propionate, and assigned them to vitrification. They have also indicated that no gelation peak is expected[5].

When unheated chitosonium acetate or chitosonium propionate films are exposed to dynamic conditions in a DMTA operated in a single cantilever bending mode two transitions are observed in the loss tangent. These occur at 10°C and 82°C, and -5°C and 77°C for acetate and propionate, respectively **(Figure 4-6)**. The high temperature transition as opposed to the low temperature transition is accompanied by an appreciable decline in modulus (not shown). Ratto et al. have observed a subambient transition at -55°C in chitosan films and have described it as a β-relaxation[16]. The

β-transition observed in chitosan films was associated with limited change in modulus. Therefore, the low temperature transition in both acetate and propionate films, which also is accompanied by a negligible change of modulus, corresponds to a β-relaxation. The high temperature transition is displayed as the uncured films undergo a glass-to-rubber transition. This assignment is supported by the observed decline of modulus typical of the T_g-region. Thus, the high temperature transition is described as the T_g of the uncured acetate or propionate designated as $T_{g,o}$ in the TTT-cure diagram.

4.4.2 TTT Cure Diagrams for Amidized Chitosan

4.4.2.1 Glass Transition Temperature of Partially-Amidized Salts

After prolonged (12 h) exposure of chitosonium acetate and chitosonium propionate to a temperature of 120°C the T_gs of the partially-amidized chitin increase with cure temperatures (T_cs) (**Figure 4-7**). These T_gs are higher than the T_cs as depicted by the $T_g = T_c$ line **(Figure 4-7)**. The rate of T_g increase with cure temperature is pronounced at low temperatures, but levels off at cure temperatures close to the ultimate T_g ($T_{g,\infty}$) of amidized chitosan **(Figure 4-7)**. $T_{g,\infty}$ was determined as 189 and 163°C for chitin regenerated from acetate and propionate, respectively **(Figure 4-7)**. As depicted in **Figure 4-4** or **4-5** vitrification occurs well under 12 h. This implies that the T_gs of the partially-amidized chitosan should have been equal to T_cs, i.e., the T_g vs T_c relationship should have corresponded to the $T_g = T_c$ line. This is because vitrification, operationally defined as the point when the T_g of the curing system becomes equal to T_c, freezes all reactions, such that no T_g-increase is expected even after prolonged cure beyond

vitrification. The fact that the T_gs of the partially-amidized chitosan are higher than the T_cs can be accounted for by one of two reasons, or both. Either additional amidization occurs even after the material has vitrified, or further amidization is promoted in the course of T_g measurement effectively driving the measured T_g to higher values, or both. The leveling off of T_gs at T_cs close to $T_{g,\infty}$ might be related to the fact the material may nearly be fully-cured.

4.4.2.2 Vitrification Curves

Isothermal curing was conducted at several temperatures ranging from 80 to 190°C to derive the times to vitrification of chitosonium acetate or chitosonium propionate. The times to vitrification obtained as the maximum in the tan δ-curve were used to construct a TTT cure diagram. Representative isothermal spectra are shown **(Figures 4-8)**. The time to vitrification of chitosonium acetate and chitosonium propionate shows a decrease with increasing cure temperature between 100 and 150°C, and 80 and 140°C, respectively **(Figure 4-9)**. The time to vitrification tends to increase beyond 150°C and 140°C for acetate and propionate, respectively. In the case of chitosonium acetate, temperatures between 100 and 150°C constitute the central portion of the S -shaped patten of the vitrification curve. The corresponding temperatures for chitosonium propionate are 80 and 140°C. Temperatures beyond 150°C and 140°C constitute the upper shoulder of the vitrification curve for acetate and propionate, respectively, whilst temperatures between 100 and 80°C, and their respective $T_{g,o}$s form the lower shoulder. The S-shaped character of the vitrification curves can be explained

on the basis of the following; at low temperatures, the curing system requires a long time to go from the rubbery phase to the glassy phase due to limited molecular motions, resulting in a maximum vitrification time. At sufficiently high cure temperature, the time to vitrification is minimal due to the greater mobility of the polymer chains. However, as $T_{g,\infty}$ is approached, the long times necessary to achieve conversion indicative of vitrification produce further increase in the time to vitrification.

4.4.2.3 Time to Full Cure

The experimental data of T_g for both N-acetyl and N-propyl homologs of amidized chitosan plotted as T_g vs T_c for several cure times shows an increase with cure time as well as with cure temperature **(Figure 4-10)**. Values of B calculated according to equation (2) are nearly constant with an average value of 1.0 and 0.892 for acetate and propionate, respectively **(Table 4-1)**. On the other hand the constant A varies with cure time. Times to full cure calculated according to equation (2) and incorporated into the TTT cure diagrams decrease with increasing cure temperature **(Figure 4-11)**. Likewise the values of the times to full cure calculated by the extrapolation procedure also decrease with increasing cure temperature. There is close correlation of the full cure curves derived by the method of Peng and Gillham and the extrapolation procedure **(Figure 4-11)**. These results suggest that the two procedures for constructing the full cure curve of a typical TTT cure are applicable to amidization. It must be emphasized that full cure as used here does not imply a completely amidized chitosan; it merely

implies that amidized chitosan has attained the maximum T_g ($T_{g,\infty}$). Studies described in chapter 5 suggest that even at $T_{g,\infty}$ amidized chitosan is not completely substituted.

The time required to achieve full cure **(Figure 4-11)** is much delayed beyond vitrification. This is not a surprising observation. Vitrification of chitosonium acetate or propionate occurs very early in the amidization process so the tendency of the material to achieve full cure is opposed by the tendency of vitrification to freeze all reactions. The large time difference between full cure and vitrification indicates that the influence of vitrification dominates the tendency to reach full cure.

A schematic TTT cure diagram constructed for the amidization curing of chitosonium acetate and chitosonium propionate using experimentally-determined times to vitrification and full cure suggests an S-shaped vitrification curve **(Figure 4-12)**.

4.4.2.4 Activation Energy for Vitrification

The times to vitrification of chitosonium acetate and propionate, determined by DMTA for isothermal cure experiments conducted at several cure temperatures (T_c) show a linear relationship with T_c when plotted in Arrhenius fashion according to equation (4) **(Figure 4-13)**. E_{vit}-values determined from the slopes of Figure 4-13 are lower than the apparent activation energies for full cure **(Table 4-2)**. The activation energies for vitrification of chitosonium acetate and chitosonium propionate are similar **(Table 4-2)**. This similarity suggests that the same mechanism is responsible for glass formation in the two materials. The activation energy for full cure is expected to be higher than E_{vit}. This is because the material vitrifies very early in the process, such that

the tendency of the material to achieve full cure is opposed by the tendency of vitrification to freeze all reactions; consequently, there is a higher energy barrier to the progress of amidization. This effect is well demonstrated by the large time difference between the vitrification and full cure curves in the TTT cure diagram **(Figure 4-11)**.

4.4.4 Influence of Vitrification on the Morphology of Amidized Chitosan

When amidized chitosan is exposed to irradiations in X-ray diffraction analysis it gives a diffuse type of diffractogram with no peaks characteristic of crystalline regions. On the other hand native chitin gives an intense peak identifiable with crystalline materials **(Figure 4-14)**. Chitosan exhibits a similar diffractogram pattern as native chitin Chitin and chitosan have 39% and 18% degrees of crystallinity, respectively. Chitosonium acetate gives a characteristic diffuse diffractogram as in amidized chitosan **(Figure 4-14)**.

When native chitin and amidized chitosan are examined by FTIR the former displays bands at 3439, 3263 and 3103 cm^{-1} **(Figure 4-15)**. On the other hand amidized chitosan displays only a band at 3439 cm^{-1} **(Figure 4-15)**. These bands can be described as non-hydrogen bonded NH groups, hydrogen bonded NH groups, and neighboring hydrogen bonded amide groups, respectively, according to the work of Miyake[17] as well as Trifan and Terenzi[18].

Extensive hydrogen bonding of hydroxyl groups, as well as the amide groups present in chitin are responsible for the crystalline morphology of chitin. Miyake[17] as well as Trifan and Terenzi[18] have reported that the amide groups in polyamides are

hydrogen bonded and provide the polymer chains an ordered alignment such that a crystalline morphology is produced. Additionally, these authors have observed an increasing extent of hydrogen bonding with increasing concentration of amide groups. On this basis it is reasonable to expect that increasing the severity of heat treatment for producing amidized chitosan should lead to more hydrogen bond formation; this is because more amide groups are produced. The fact that no hydrogen bonding occurs with the amide groups of amidized chitosan may suggest that the groups are not within the vicinity of each other. The concept of TTT cure diagram has shown that vitrification occurs very early in the transformation of chitosonium acetate to chitin. Presumably, once vitrification occurs, the resulting immobilization of the polymer chains prevents the chains to move into vicinities favorable for hydrogen bonds to form, let alone alignment of chains for formation of an ordered morphology. Beside amide groups, the presence of hydroxyl groups should give rise to extensive hydrogen bonding and consequently a crystalline morphology provided suitable alignment of polymer chains is present. The diffractogram of chitosonium acetate indicates that it is amorphous. It is suspected that solvation of chitosan by acetic acid/water disrupts hydrogen bonds present in chitosan. Possibly hydrogen bonds, due to hydroxyl group interactions, are not reformed during the transformation of chitosonium acetate to amidized chitosan. This may be related to the influence of vitrification as well. Based on this discussion we suspect that vitrification, which occurs early in the amidization process, prevents amidized chitosan from achieving a crystalline morphology.

4.5 CONCLUSIONS

(1) The transformation of chitosonium acetate and chitosonium propionate to N-acyl homologs of chitin gives rise to characteristic tan δ peaks and these are typical of vitrification.

(2) The glass transition temperatures of partially-amidized and vitrified chitin are always higher than the cure temperatures. This suggests that amidization occurs even after the material has vitrified or that further amidization is promoted during T_g measurement.

(3) Isothermal cure monitoring at several temperatures can be used to describe the vitrification behavior of chitosonium acetate and chitosonium propionate on the basis of the TTT-cure diagrams. As in thermosets, the vitrification curves of the TTT-cure diagrams describing the amidization curing of these ionic complexes of chitosan are S-shaped. E_{vit} is the same during amidization of chitosonium acetae and chitosonium propionate. This similarity suggests that the same mechanism governs glass formation in the two materials.

(4) An extrapolation method, and also the theoretical method of Peng and Gillham, can be used to determine the time to full cure. The time to full cure increases with decreasing cure temperature. Full cure takes much longer than vitrification, and this is due to the tendency of vitrification to prevent full cure from being attained.

(5) Native chitin and chitosan are crystalline. Chitosonium acetate and amidized chitosan have amorphous morphologies. The amorphous character of amidized chitosan is related to the influence of vitrification.

4.6 ACKNOWLEDGEMENT

This is to express thanks to Dr. Charles E. Frazier of the Department of Wood Science and Forest Products for the valuable discussions in the course of this study. His continuous interest in this research is also greatly appreciated. Additionally, the assistance of Dr. Gamini Samaranayake of Westvaco Corporation, Charleston, is acknowledged with gratitude.

4.7 REFERENCES

1. Turi, E.A., Thermal Characterization of Polymeric Materials, Academic Press, Inc., New York, 1981

2. Hofmann, K., and Glasser, W., Thermochimica Acta, 166,169-184, 1990

3. Toffey, A., Samaranayake, G., Frazier, C.E., and Glasser, W., J. Appl. Polym. Sci., 60, 75-85, 1996

4. Aronhime, M.T., and Gillham, J.K., Adv. Polym. Sci., 78, 83-112, 1986

5. Palmese, G.R., and Gillham, J.K., J. Appl. Polym. Sci., 34, 1925-1939, 1987

6. Enns, J.B. and Gillham, J.K., J. Appl. Polym. Sci., 28, 2567-2591, 1983

7. Aronhime, M.T., and Gillham, J.K., Adv. Polym. Sci., 56, 35-47, 1984

8. Babayevsky, P.G., and Gillham, J.K., J. Appl. Polym., 17, 2067-2088, 1973

9. Scheneider, N.S., Sproise, J.F., Hagnauer, G.L. and Gillham, J.K., Polym. Eng. Sci., 19(4), 304-312, 1979

10. Wisanrakkit, G., and Gillham, J.K. ACS Polym. Mater. Sci. and Eng. Prep., 56, 87-91, 1987

11. Gillham, J.K., British Polym. J., 17(2), 224-226, 1985

12. Gillham, J.K., and Enns, J.B., ACS Polym. Mater. Sci. and Eng. Prep., 59, 851-858, 1988

13. Wisanrakkit, G., and Gillham, J.K. ACS Polym. Mater. Sci. and Eng. Prep., 59, 969-975, 1988

14. Hofmann, K., and Glasser, W., Macromol. Chem. Phys., 195, 65-80, 1994

15. Peng, X., and Gillham, J.K., J. Appl. Polym. Sci., 30, 4685-4696, 1985

16. Ratto, J.N., Chen, C.C., and Blumstein, R.B., J. Appl. Polym. Sci., 59, 1451-1461, 1996

17. Miyake, A., J. Polym. Sci., 64, 223, 1960

18. Trifan, D.S., and Terenzi, J.F., J. Polym. Sci., 28, 443, 1958

Table 4-1a. Values for A and B in equation (1) for chitosonium acetate.

	Cure time (Hr)				
	0.5	1	2	4	6
A	37	*	19.4	3.4	4.0
B 1.25	0.64	*	0.97	1.16	
R^2	0.93	*	0.99	0.97	.99

R^2 is correlation coefficient
* not determined

Table 4-1b. Values for A and B in equation (1) for chitosonium propionate.

	Cure time (Hr)				
	0.5	1	2	4	6
A	21	14.8	-11.6	1.4	8.8
B	0.6	0.73	1.01	1.06	1.06
R^2	0.99	0.97	0.97	0.98	.99

R^2 is correlation coefficient

Table 4-2. A comparison of activation energy for vitrification ($E_{A\ vit}$) and full cure ($E_{A\ ,\ full\ cure}$) of chitosonuim acetate and propionate. $E_{A\ ,\ full\ cure}$ derived from addition of the activation energies of the first and second phases of amidization reported in chapter 5.

Material type	$E_{A\ vit}$ (kcal/mol)	$E_{A\ ,\ full\ cure}$ (kcal/mol)
Acetate	13	36
Propionate	11	37

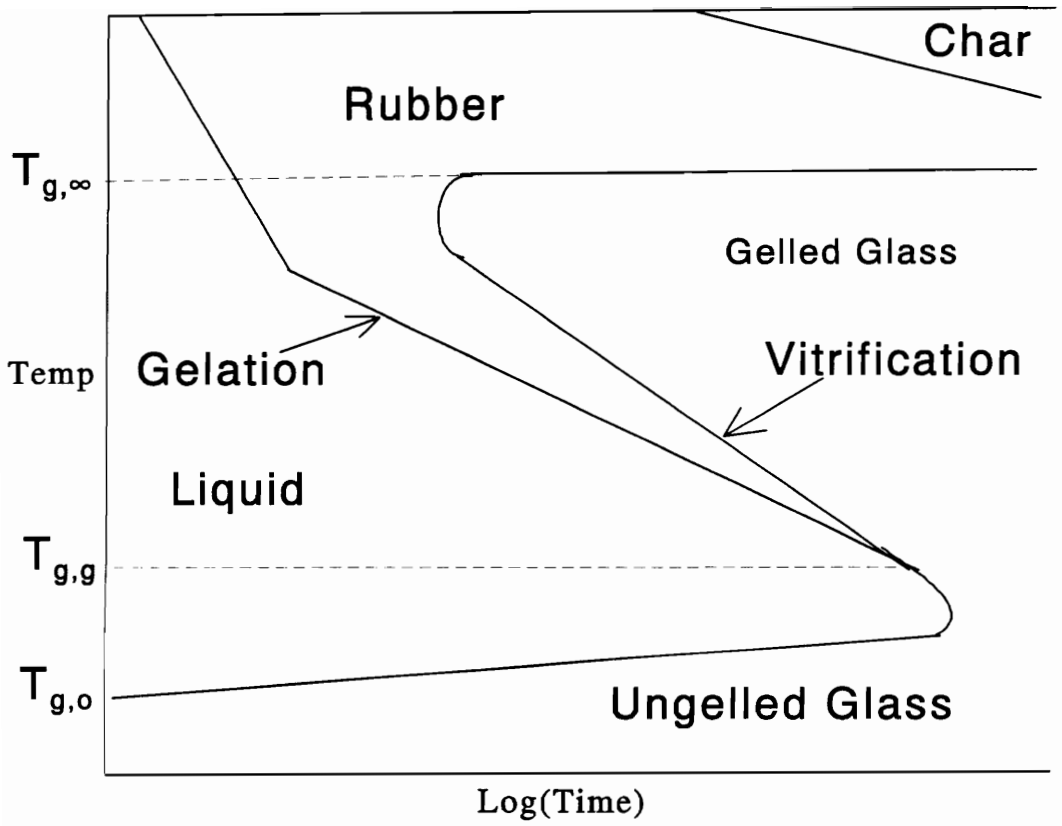

Figure 4-1. A schematic time-temperature-transformation cure diagram. The diagram depicts the times to vitrification and gelation, as well as the various physical states characteristics of the cure of a thermoset.

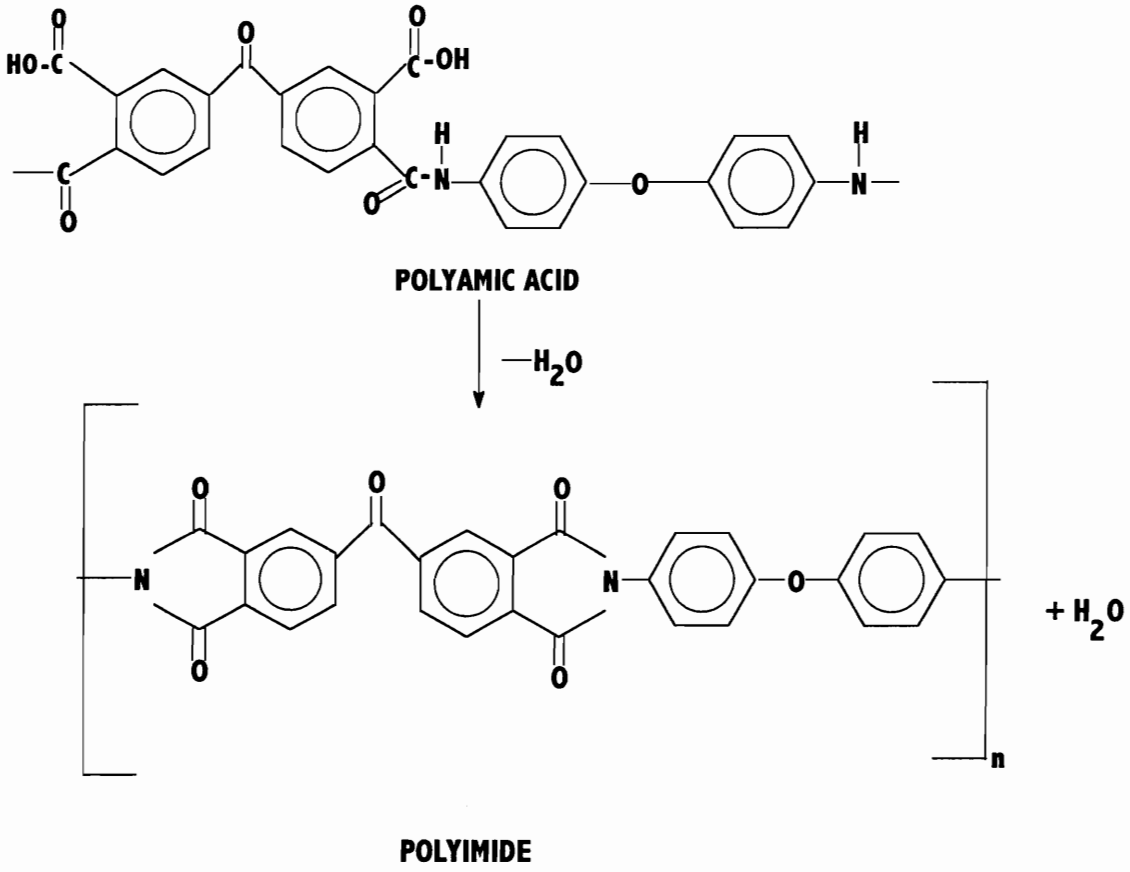

Figure 4-2. Conversion of Polyamic acid to Polyimide. The conversion involves removal of water, i.e., a thermal dehydration process.

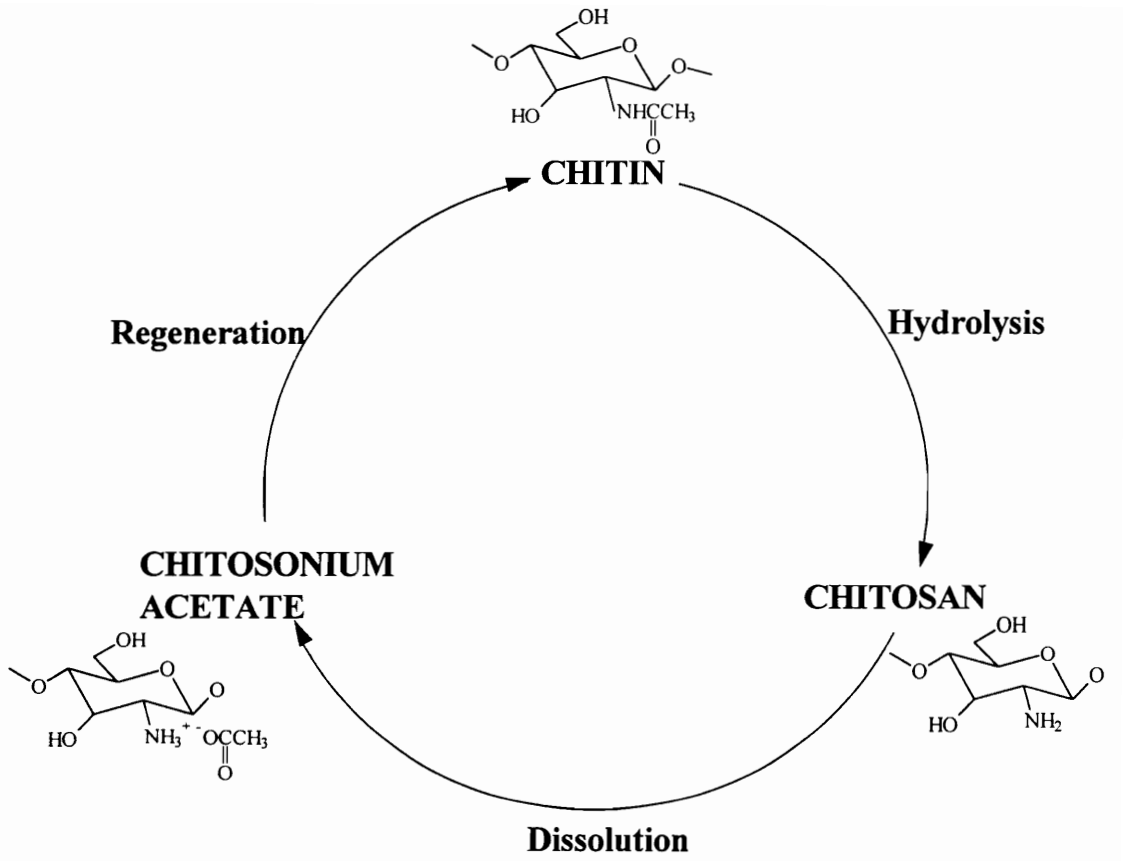

Figure 4-3. The regeneration of chitin from chitosan. This regeneration process is similar to the conversion of polyamic acid to polyimide (Figure 4-2), because the two processes involve thermal dehydration.

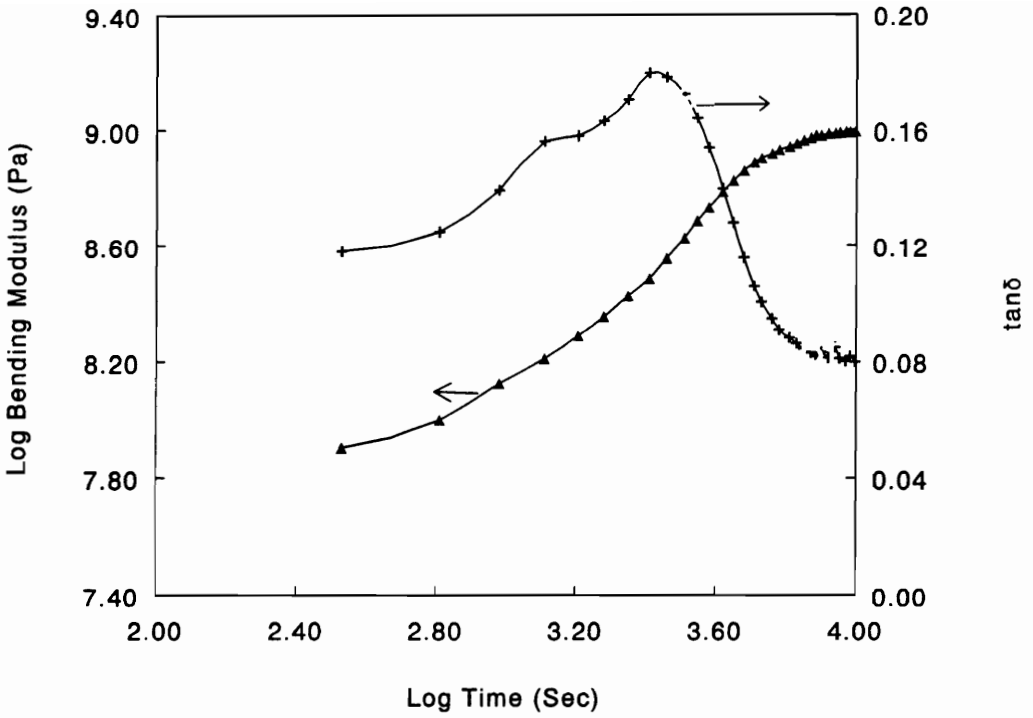

Figure 4-4. Isothermal cure (140°C) monitoring of chitosonium acetate in bending mode using DMTA. Two overlapping peaks are discernible. The first may be due some phenomenon not related to molecular reorganization that occurs during amidization and the second peak is related to vitrification. Also there is an increase in modulus with time. These observations parallel the behavior of thermosetting resins.

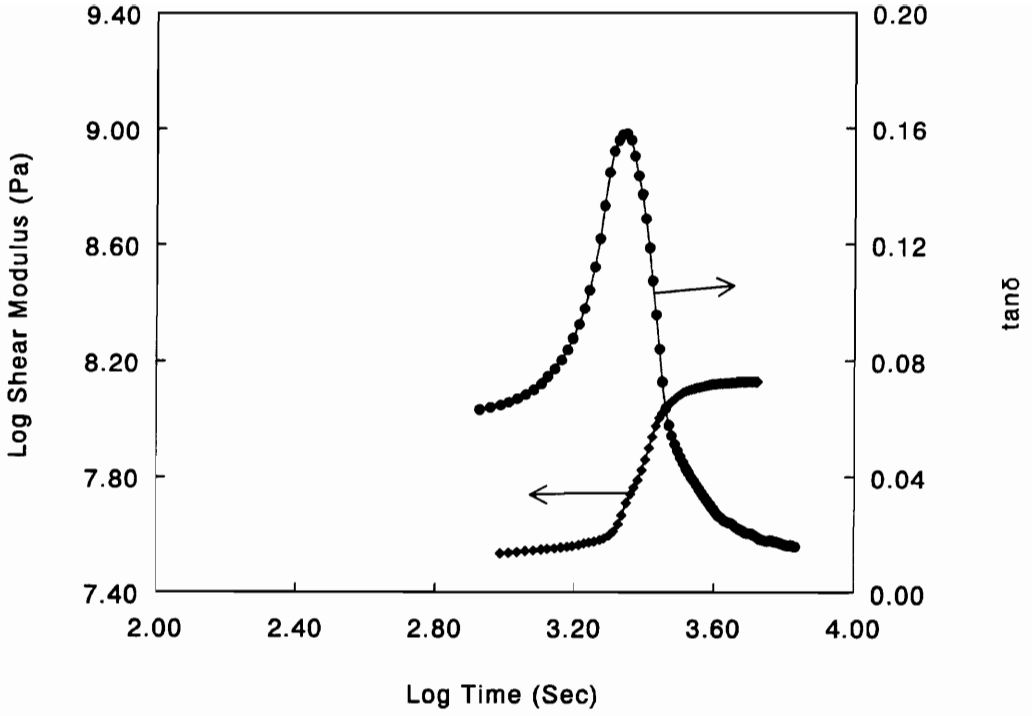

Figure 4-5. Isothermal cure (140°C) monitoring of chitosonium acetate in shear mode using DMTA. A well-resolved peak is discernible and is assigned to vitrification. Also there is an increase in modulus with time. These observations parallel the behavior of thermosetting resins.

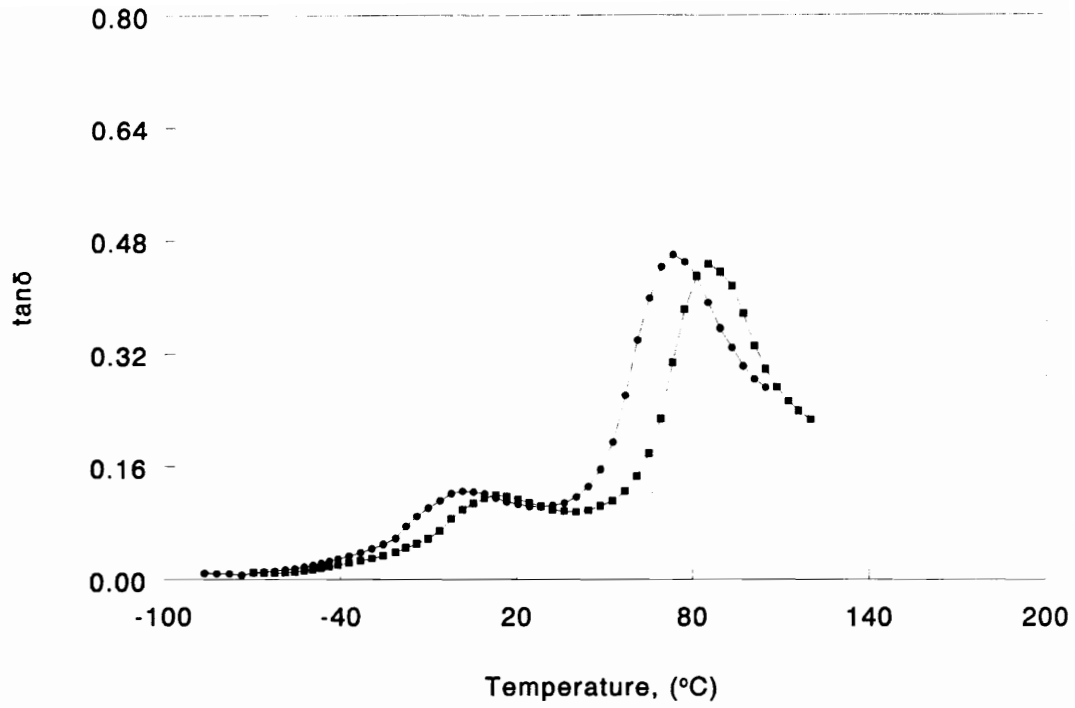

Figure 4-6. Temperature scan of chitosonium acetate/propionate. Two transitions are displayed at 10/-5°C and 82/77 °C. The low temperature transition is described as β-relaxation, and the other corresponds to the glass transition temperature of the uncured acetate/propionate, designated as $T_{g,o}$ in the TTT-cure diagram. ■ (acetate), ●(propionate).

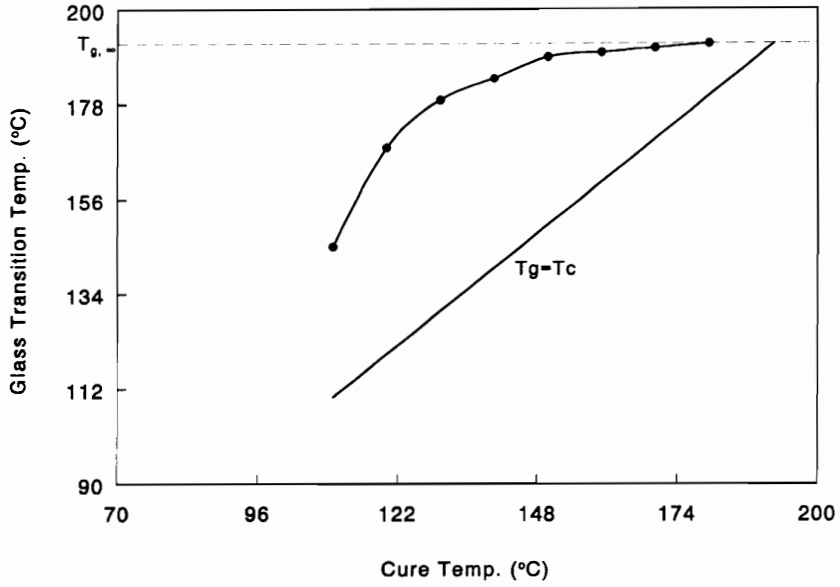

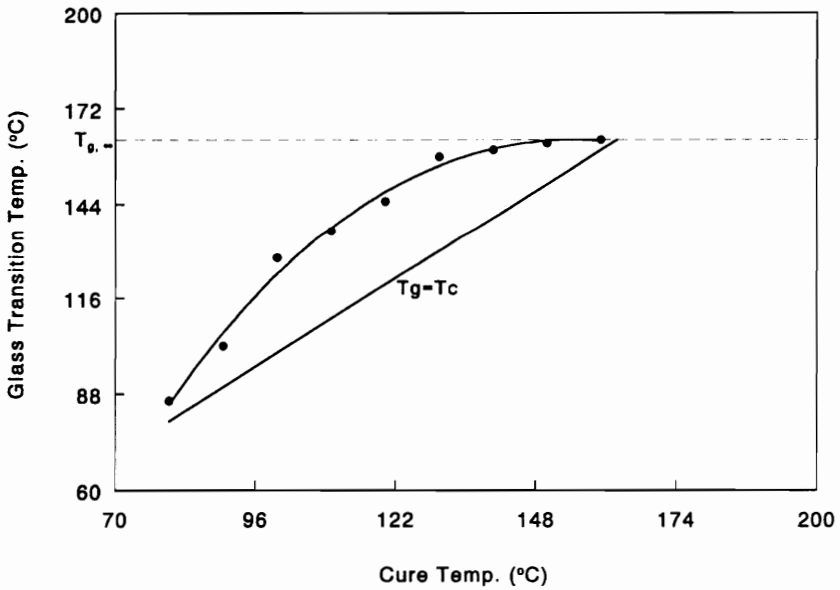

Figure 4-7. Glass transition temperature (T_g) vs cure temperature (T_c) of isothermally cured chitosonium acetate (top) and propionate (bottom). T_gs are higher than T_cs. This implies that amidization occurs even when the material is vitrified or further amidization is promoted during T_g measurement.

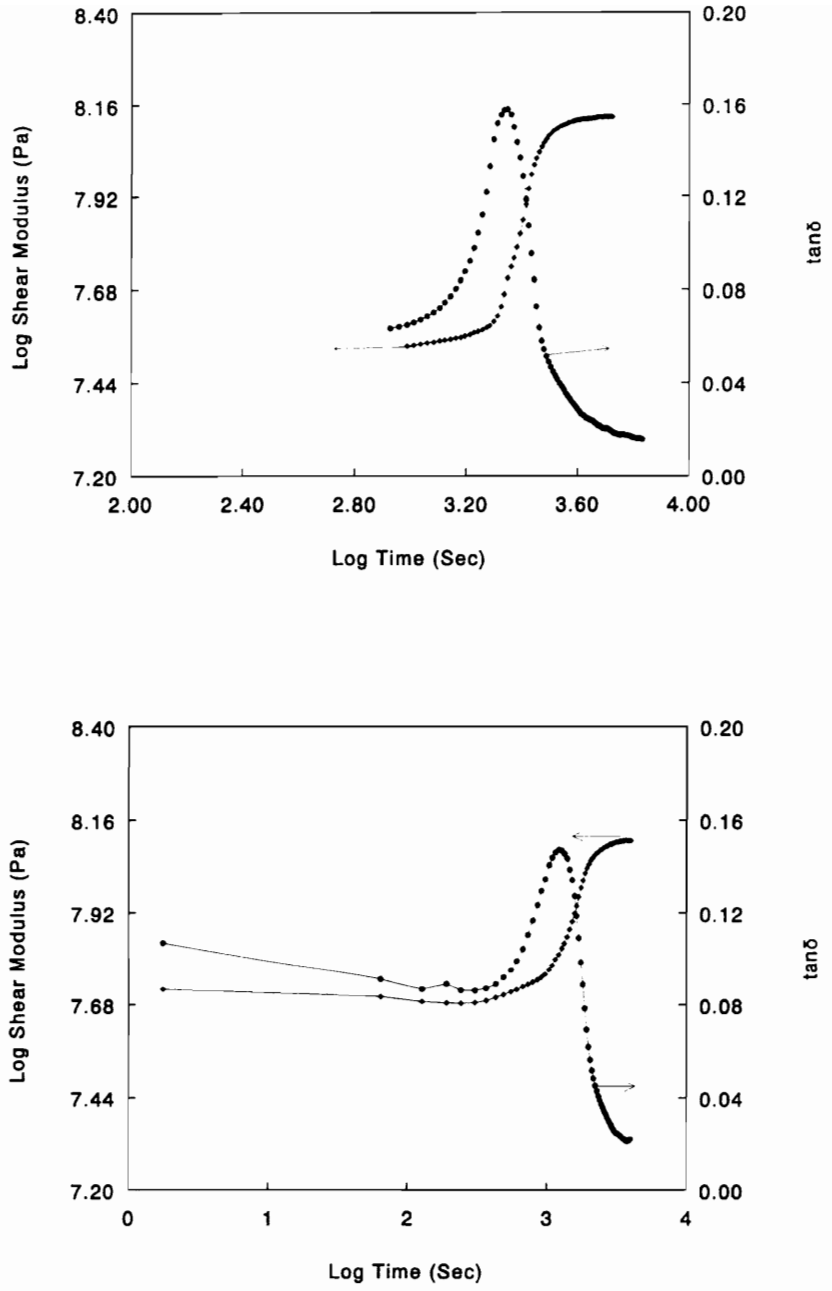

Figure 4-8. Isothermal cure of chitosonium acetate (top) and propionate (bottom) at 140°C. There is an increase in modulus with time and a corresponding peak in tan δ. The time at which the peak occurs is defined as the time to vitrification.

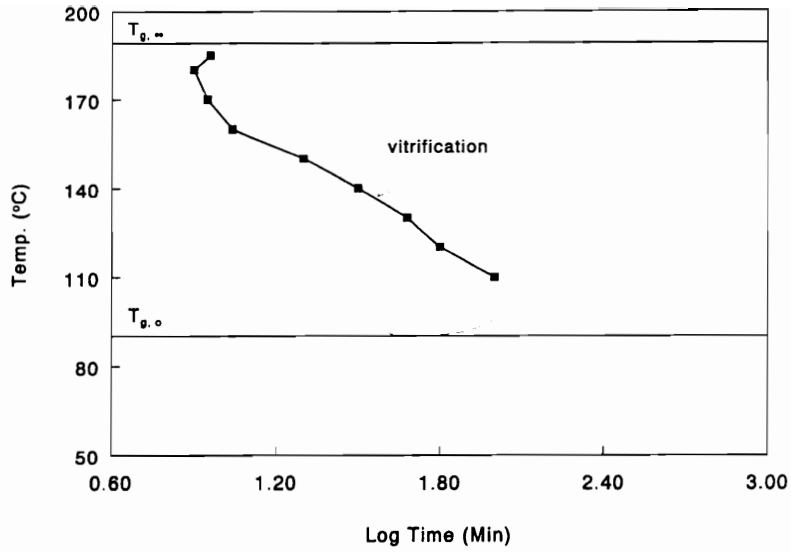

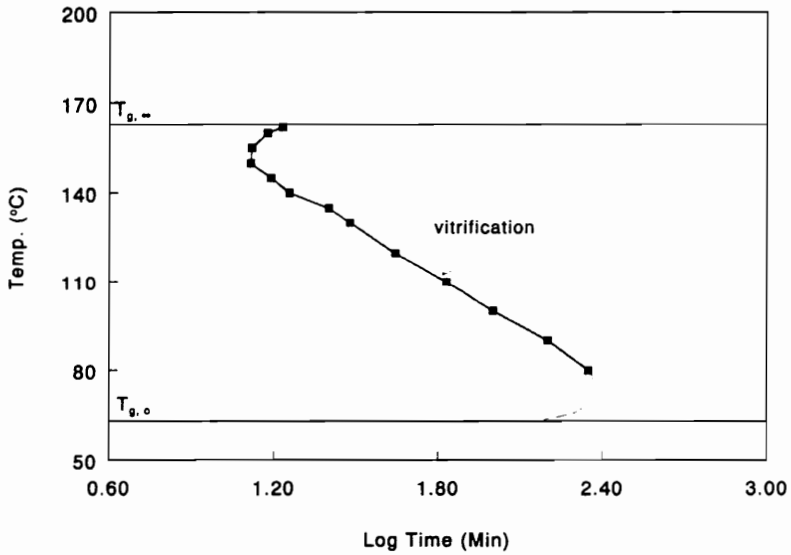

Figure 4-9. Time-temperature-transformation (TTT) cure diagrams for N-acetyl (top) and N-propyl (bottom) homologs of chitosan. The vitrification curve has an S-shaped upper shoulder, typical of thermosetting resins. Also included in the TTT cure diagram is the ultimate glass transition temperature, $T_{g,\infty}$ and initial glass transition temperature, $T_{g,o}$ of N-acetyl or N-propyl analog of chitosan. The dash line is hand drawn to illustrate the lower shoulder of the S-shape of the vitrification curve.

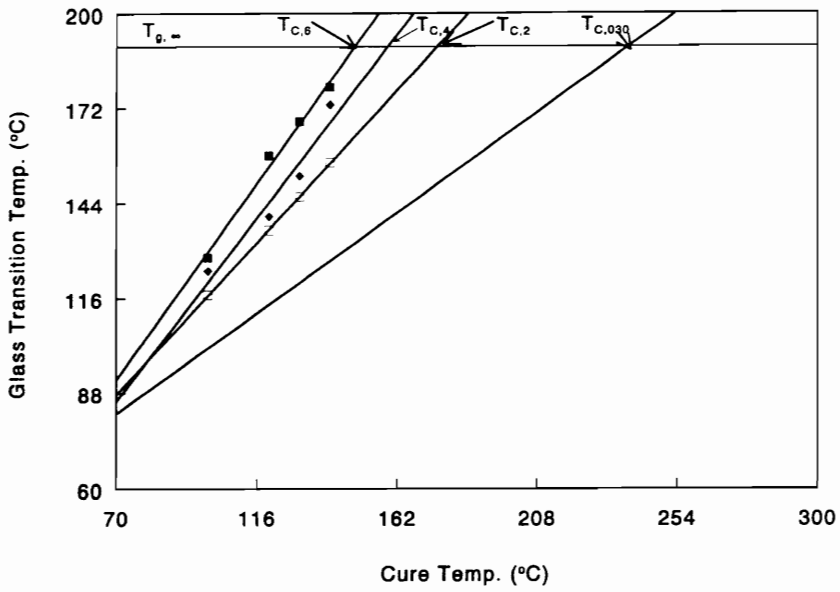

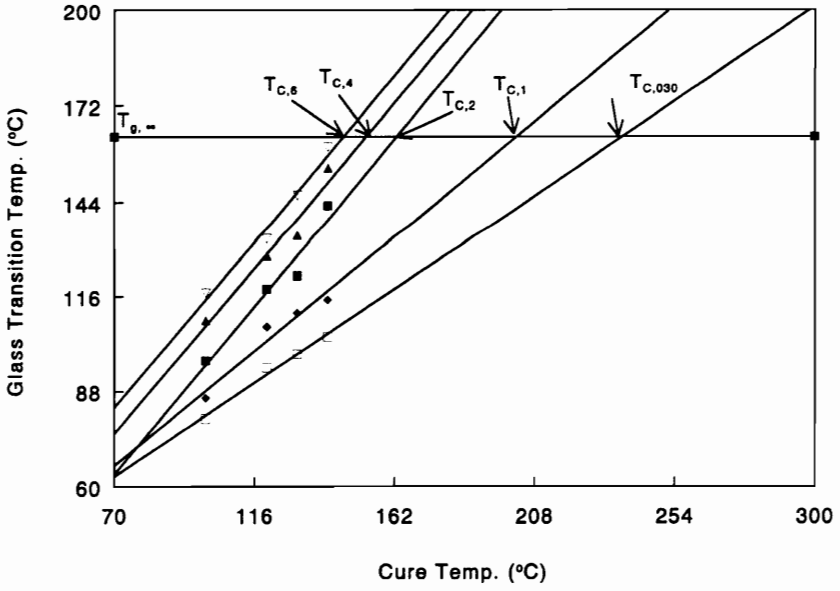

Figure 4-10. Glass transition temperature T_g vs cure temperature T_c. The data points represent the T_g vs T_c relationship for various cure times in hrs indicated as subscripts within the figure. The time to full cure can be determined by extrapolation of the curve fit line to $T_{g,\infty}$ or by the method of Peng and Gillham.

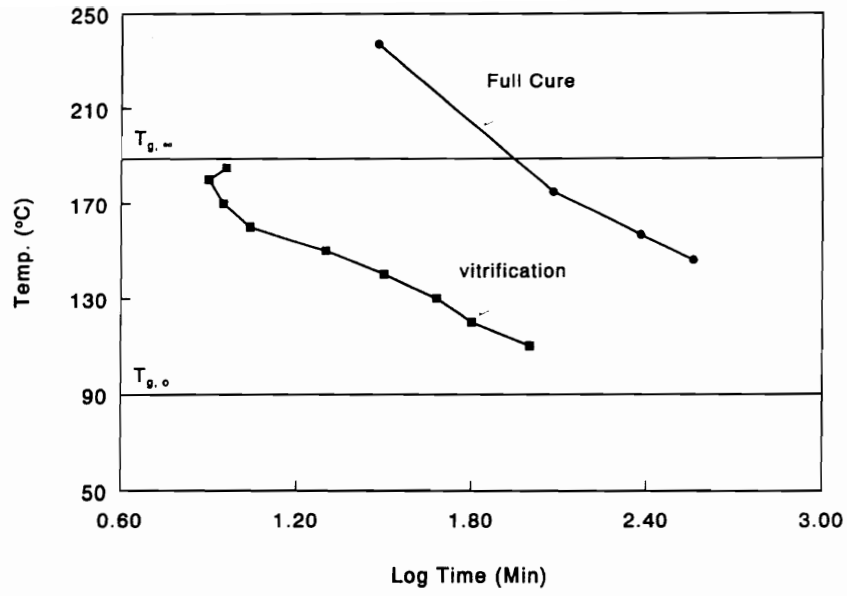

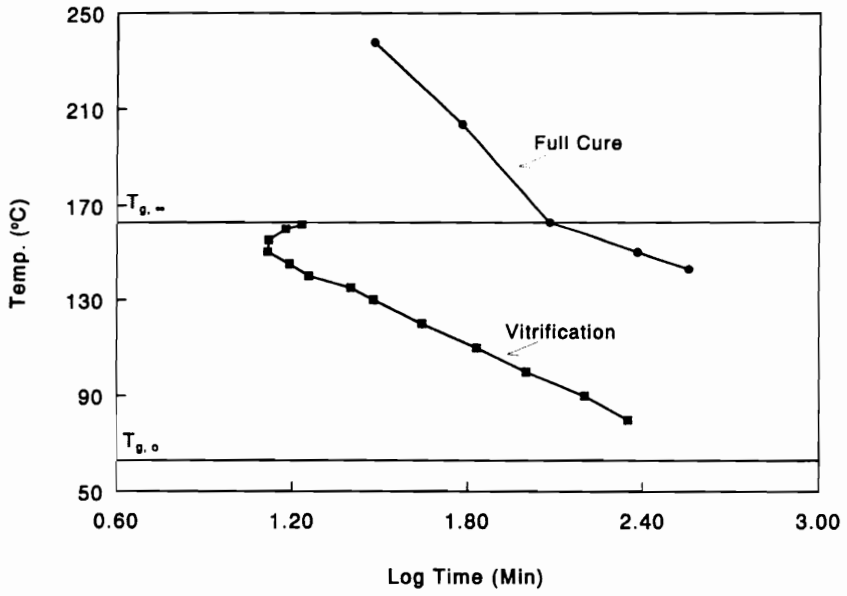

Figure 4-11. TTT cure diagram showing the times to vitrification and full cure of chitosonium- acetate (top) and propionate (bottom). The times to full cure are determined by an extrapolation method (solid line) and theoretical method after Peng and Gillham (data points).

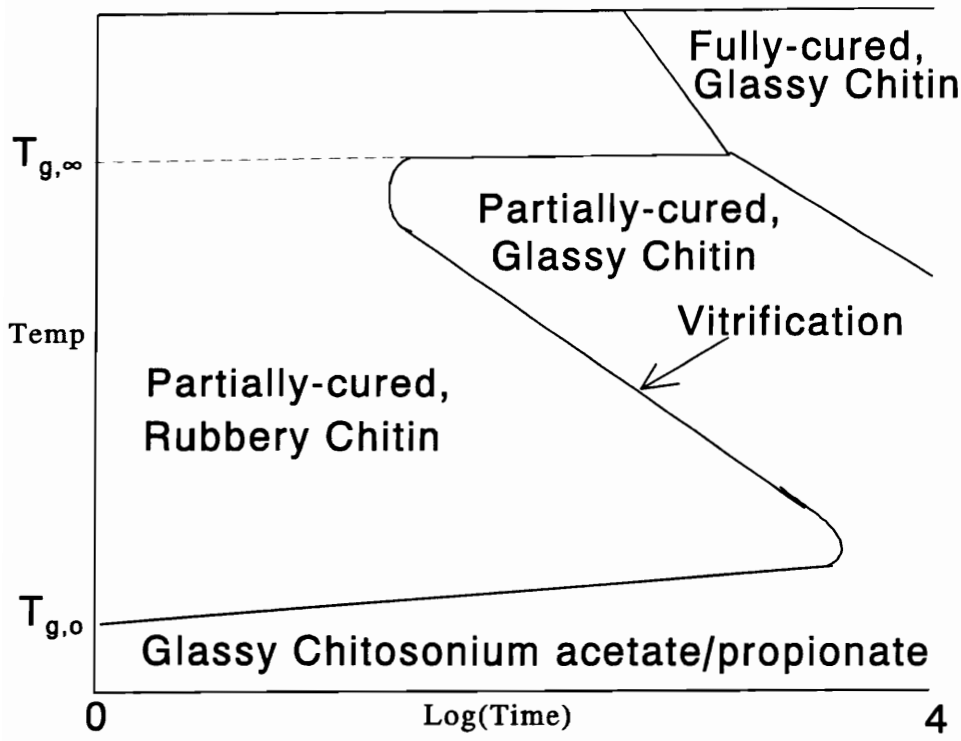

Figure 4-12. A schematic TTT cure diagram describing the regeneration of amidized chitosan from the ionic complexes of chitosan with acetic and propionic acids. The diagram depicts the various physical states during the regeneration. Also included are the times to vitrification and full cure.

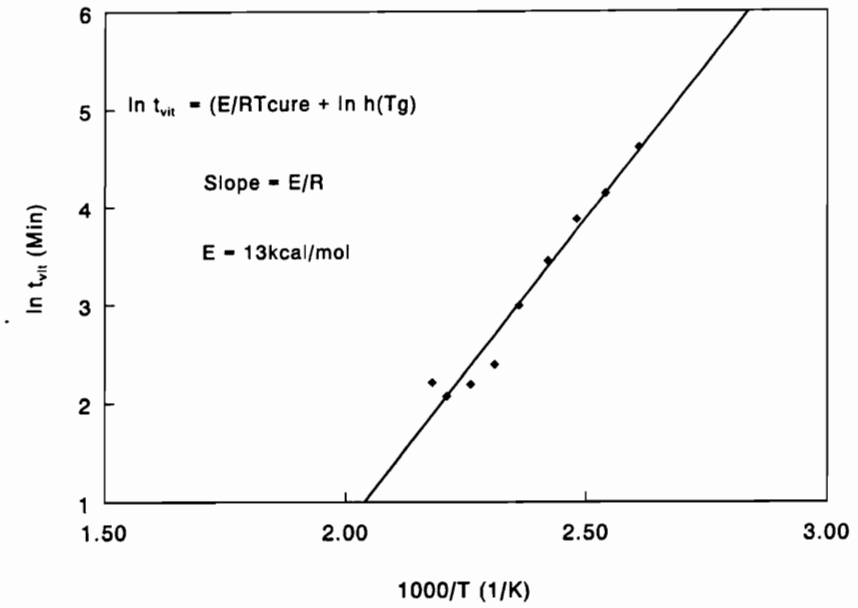

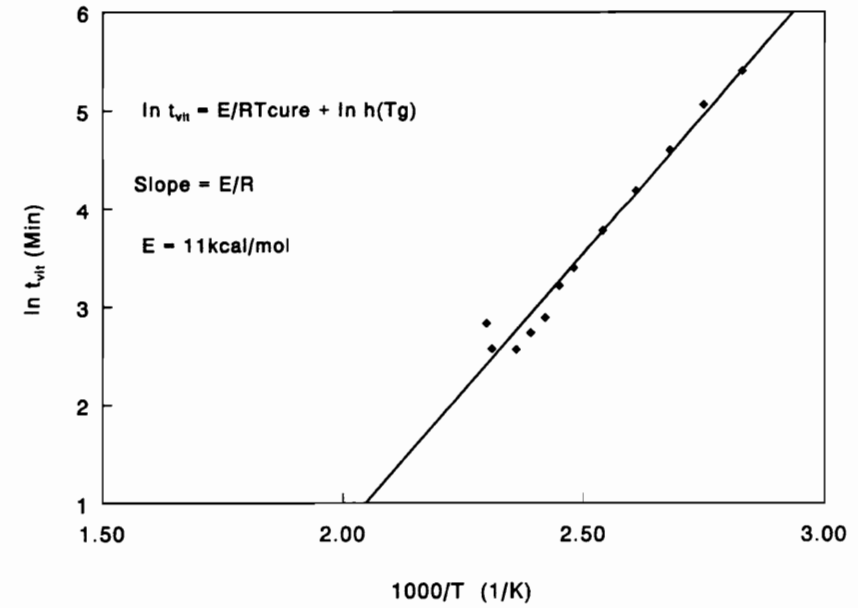

Figure 4-13. Arrhenius plot of time to vitrification (t_{vit}) vs cure temperature. The slope of the curve is used to determine the activation energy for vitrification. N-acetyl (top) and N-propyl (bottom).

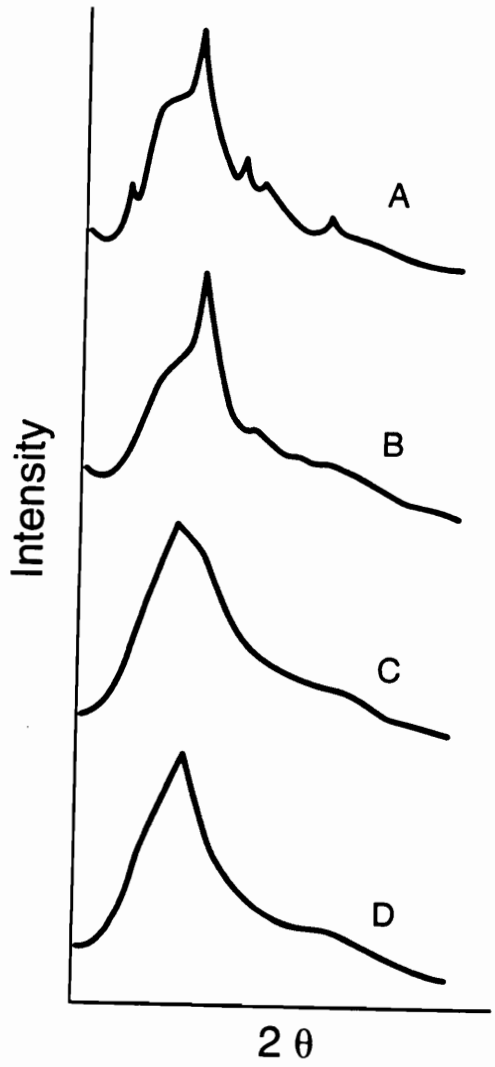

Figure 4-14. X-ray diffractograms of native chitin (A), chitosan (B), chitosonium acetate (C), and amidized chitosan (D). Both A and B display peaks typical of a crystalline morphology. There are no such peaks in C and D.

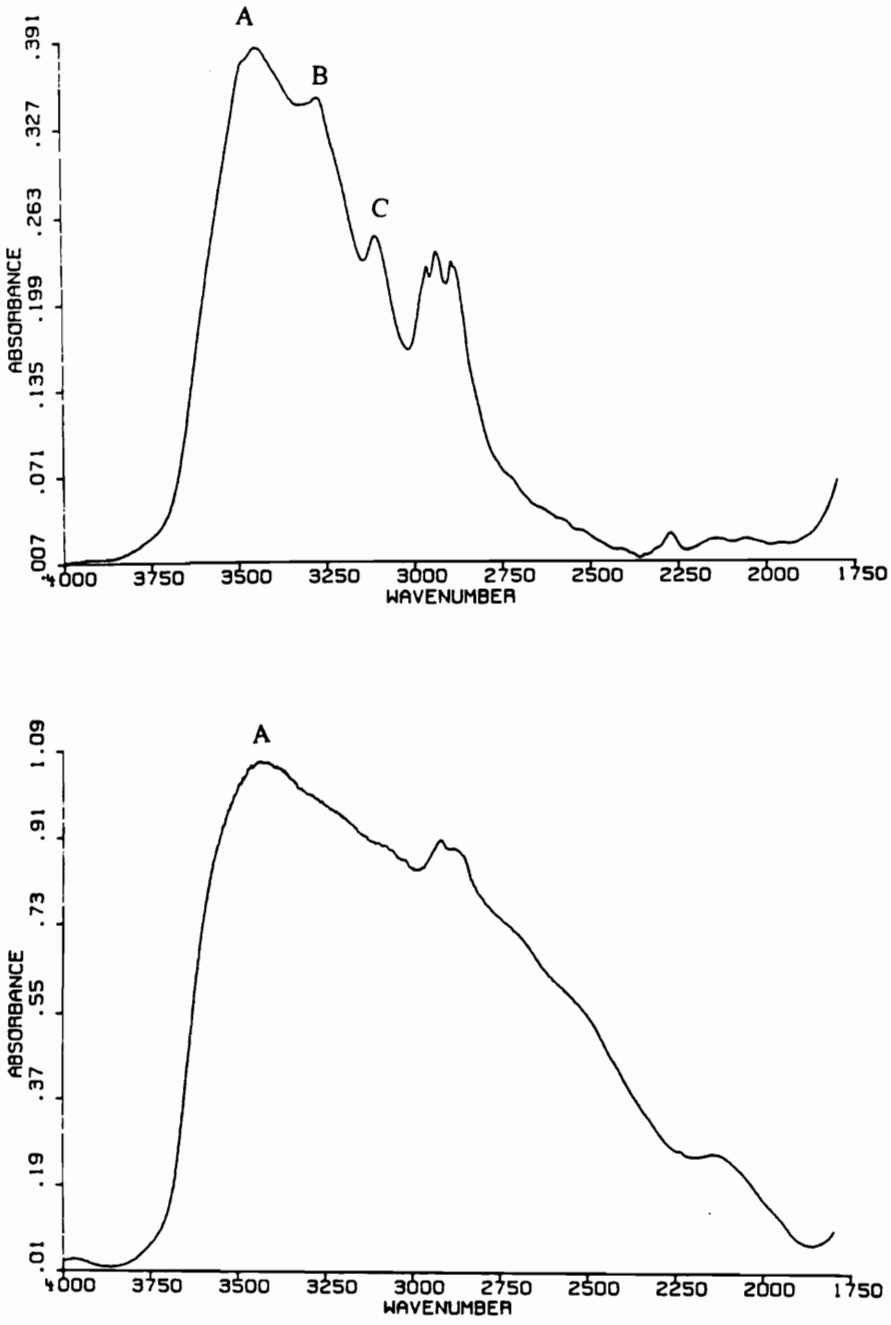

Figure 4-15. FTIR spectra of native chitin (top) and amidized chitosan (bottom). The former shows bands typical of polyamides, including non-hydrogen bonded N-H at 3439 (A), hydrogen bonded N-H at 3263(B) as well as hydrogen bonded amides which are neighbors at 3103cm^{-1}(C). Amidized chitosan displays only a band at 3439cm^{-1}(A).

CHAPTER 5

CHITIN DERIVATIVES. III. FORMATION OF AMIDIZED HOMOLOGS OF CHITOSAN

5.1 ABSTRACT

The kinetics of the formation of amidized homologs of chitosan from the ionic complexes of chitosan with four alkanoic acids, formic, acetic, propionic and butyric acid, have been studied. In addition, their degree of substitution (DS), thermal transitions and enzymatic hydrolysis have been investigated. The results suggest that heating of N-acylates of chitosan produces amidized chitosan homologs with DS, as determined by solid state NMR, between 0.1 and 0.6.

Thermal analysis by DMTA revealed that the ionic complexes of chitosan with formic, acetic, propionic, and butyric acids, as well as the respective amidized chitosan homologs, display two transitions designated as α- and β-relaxation. There was no indication of melting. The β-relaxations of the ionic complexes were more pronounced than those of their respective amidized chitosan derivatives. The ultimate T_g of the amidized chitosan homologs declined stepwise with acyl substituent length. The T_g-behavior was attributed to both substituent length and DS.

Kinetic analysis using T_g-changes with heating time can be used to describe the kinetics of amidization. The formation of amidized chitosan homologs followed first order rate kinetics in a two-stage process, as was observed previously. The activation energy for amidization was constant irrespective of the acid used in the chitosan

complex as well as the DS at ultimate T_g. It is 14±1 kcal/mol initially and 21±2 kcal/mol in a second stage. Since the transition from first to second stage occurs after the change from rubbery to glassy state (vitrification), vitrification is suspected to be responsible for the two-stage kinetics.

Enzymatic hydrolysis indicated that, despite variability of DS, there is no distinction among N-formyl-, N-acetyl-, N-propyl-, and N-butyryl homologs of chitosan and native chitin in terms of their recognition and degradation pattern by chitinolytic enzymes. Chitinolytic enzymes can recognize and degrade chitin irrespective of the type of acyl substituent at the C-2 position as well as DS. The action of the mixture of chitinase, chitosanase and β-N-acetylglucosaminidase on all types of amidized chitosan derivatives produced more glucosamine than any other degradation product.

5.2 INTRODUCTION

Chitin represents a class of polysaccharides which is second in abundance behind cellulose [1]. It is a linear polymer of β-1-4 linked anhydroglucose units. It is present in the exoskeleton of crustaceans and insects[1]. Chitin is well recognized for its excellent barrier polymer characteristics. However, chitin is even more difficult to deal with, "manage" and "reshape," in a chemical sense than cellulose. This disqualifies it as prospective (solvent or melt-) deformable film material. As a result of its inherent intractability in most common solvents, chitin is often deacetylated by alkaline hydrolysis to produce chitosan. Contrary to chitin, chitosan is well-soluble in water at

pH 5-6, especially in dilute (1%) organic acids. Chitosan is typically regenerated from organic acid solution by neutralization with alkali to produce chitosan in film[2-5] or even fiber form[6,7]. Our previous research has produced evidence that the ionic complex of chitosan with acetic acid, chitosonium acetate, undergoes a transformation to chitin at elevated temperatures in solid state[8]. Therefore, the N-acetyl group of chitin is produced (or regenerated) from the N-acetate group of chitosonium acetate. This conversion, which is tantamount to amidization, produces chitin films that are insoluble in all common solvents, and these film materials resemble crosslinked network polymers in most respects, especially regarding viscoelastic character, behavior at elevated temperature, swelling, etc.

Like chitosan, cellulose may also be derivatized with alkanoic acids. Novel homogeneous acylation of cellulose has produced a class of cellulose derivatives with varying properties[9-11]. For instance, whereas cellulose triesters with acyl substituents ranging in size from C-3 to C-14 have T_gs in close proximity to their T_ms, mixed cellulose esters, such as acetate hexanoates, showed greater $\Delta(T_m\text{-}T_g)$-values[10]. The increased $\Delta(T_m\text{-}T_g)$-values make the mixed esters melt-processable. It has been reported that both T_m and T_g of cellulose esters decrease with increasing degree of substitution (DS) [10]. This observation was limited to DS-levels above 1, except for fluorine-containing derivatives. All derivatives had their T_g-transitions obscured by moisture if DS was below 1. Additionally, thermal analysis of cellulose esters having a DS of about 3 suggests that T_g as well as T_m declines linearly as acyl substituent size

increases from C-2 to C-6. It remains nearly constant for C-6 to C-12 ester derivatives (**Figure 5-1**) [11]. This is followed by a linear increase of T_g and and sidegroup-T_m from C-12 to C-20 (**Figure 5-2**)[11]. These observations indicate that cellulose derivatives with desired, engineered properties can be produced by varying the size of the acyl substituent and DS. Besides T_m and T_g, the size of acyl substituent and DS cooperatively influence the hydrolytic action of cellulolytic enzymes. Glasser and coworkers have established that the smaller the size of the acyl substituent the higher may be the DS before enzymatic degradation ceases due to lack of substrate recognition[12].

We expect that the heat treatment of the ionic complex of chitosan films produced from other monocarboxylic acids such as formic, propionic, and butyric will, like chitosonium acetate, produce N-acyl homologs of chitosan. This heat-induced formation of various N-acyl homologs of chitosan can be likened to the homogeneous acylation of cellulose. However, they differ in terms of reaction phases as well as pattern of substitution. Whereas the formation of N-acyl homologs of chitosan occurs in the solid state, acylation of cellulose on the other hand takes place in solution. Furthermore, the N-acyl groups are introduced to only the C-2 position of chitosan producing a derivative with a maximum DS of 1. On the other hand acyl derivatives of cellulose can be trisubstituted. Notwithstanding these differences, amidization may represent a route to a class of chitosan derivatives that has not yet been explored.

An understanding of the dependence of thermal transitions on the size of

N-acyl substituents of amidized chitosan homologs is necessary for establishing structure-property relationships which form the basis for producing derivatives with engineered, predictable properties. Additionally, the DS of amidized chitosan homologs, like of cellulose esters, must be expected to have influence on their T_gs and susceptibility to enzymatic degradation. Consequently, the DS must be determined. The various analytical methods that have been used to determine DS of chitin include FTIR[13], enzymatic[14] and acidic hydrolysis[15], and solid state NMR[16-18]. DS-determination using FTIR is based on utilizing the amide I band as a measure of the N-acetyl group content and the hydroxyl band at 3450 cm^{-1} as an internal standard to account for variation in film thickness or chitin concentration[13]. It has been suggested that FTIR-data, which depend on deconvoluting the amide I band, have inherent resolution difficulties, particularly at low acetyl contents[19]. Acidic and enzymatic hydrolysis are based on the degradation of chitin / chitosan by appropriate enzymes/acids, subsequent separation and quantification of N-acetylglucosamine, glucosamine and acetic acid. The accuracy of these methods depends on whether or not complete hydrolysis of chitosan or chitin is achieved. Many recent reports have indicated that modern solid state NMR is an appropriate method for the determination of DS[16-18]. The quantitative principle underlying this method of DS determination involves the comparison (ratio) of the integral of the acetamido-methyl resonance (this is proportional to the acetyl content) to the resonance of the glucose carbons.

In previous studies we have investigated the kinetics of the transformation of chitosonium acetate to chitin. We found that the transformation follows a first-order reaction in two-stages[8]. That is, amidization as monitored by T_g-changes proceeds fast initially, with a characteristic activation energy (E_A) of 15 kcal/mol, followed by a slower rate with E_A of 21 kcal/mol. The slower rate of amidization was found to mark a decline in the rate at which T_g changes with time. The analysis of amidization kinetics, as is the case for thermosets, is useful in so far as it provides quantitative information on the extent of conversion (degree of cure) which forms the basis for defining appropriate heat processing conditions in relation to desired end product characteristics. For instance, once kinetic parameters, such as activation energy and pre-Arrhenius factor, are determined, it is possible to predict the degree of cure for any combination of time and temperature, and its relationship to performance[13]. Therefore, the need to systematically investigate the kinetics of formation of amidized homologs of chitosan is a necessary first step in the development of a class of chitosan derivatives.

In our previous report we tentatively assigned the observed two-stage reaction during amidization to the influence of vitrification by drawing parallels between amidization, imidization and network formation[8]. In the case of imidization, when T_g-changes decline towards the advanced reaction stages, a sudden increase in the cure temperature above the ultimate T_g of a fully-imidized material (polyimide) produces further significant changes in T_g. This observation was interpretated as evidence of

further imidization, and it was accounted for by a temporal relief of the polyimide chains from a frozen state, i.e. devitrification[21]. The structural transformations associated with both amidization and imidization are similar. Therefore, our hypothesis is that, if the dramatic decrease in T_g-changes in the later stage of amidization is related to the influence of vitrification, an increase of cure temperature above the ultimate T_g of regenerated chitin would lead to additional increases of T_g. This would also be true of the modulus since both increase during cure reactions.

The combined action of two classes of enzymes results in the complete hydrolysis of chitin to monomeric N-acetylglucosamine (GlcNAc)[15,22]. Chitin is first hydrolyzed by chitinase to oligosaccharides and N,N-diacetylchitobiose. Further hydrolysis of oligosaccharides and N,N-diacetylchitobiose to N-acetylglucosamine residues depends on the depolymerization action of β-N-acetyl-hexosaminidase as well as on chitosanase which is reponsible for the hydrolysis of unacetylated glucosamine units in chitin.

Nanjo et al. have studied the action of an enzyme mixture of chitinase, chitosanase and β-N-acetyl-hexosaminidase on N-acetylated chitosan having a degree of N-acetylation of 47 %. They reported 70-98% hydrolysis in 4 h[15]. Using high performance liquid chromatography, only glucosamine and N-acetylglucosamine monomers were identified as a result of the action of the enzyme mixture. Aiba[23] also studied the action of chitinase on homogeneously produced N-acetylated chitosan. He reported that this enzyme does not recognize differences in the sequence of N-acetyl

groups along the chitosan chain; random vs. block-type distribution. This conclusion was reached on the basis of heterogeneously deacetylated chitin (characterized by a blockwise acetyl sequence[24]) , and of homogeneously N-acetylated chitosan (having a random acetyl sequence[24]) with the same extent of N-acetylation. Although the homogeneously-produced N-acetylated chitosan of Aiba may differ from N-acyl homologs of chitosan with variable acyl size produced by thermal dehydration of the N-acylate, parallels may indeed exist. Therefore, it remains to be determined whether chitinase or the enzyme mixture of chitinase, chitosanase and β-N-acetyl-hexosaminidase studied by Nanjo et al. would be able to recognize differences between native chitin and regenerated N-acyl homologs of chitosan.

The cooperative influence of acyl substituent size and DS on enzymes' activity as observed for cellulose esters[12] provides an additional point of reference besides our previous hypothesis for studying N-acyl homologs of chitosan in terms of their recognition and subsequent degradation by chitinolytic enzymes. We recognize that the incubation of N-acyl homologs of chitosan with enzymes represents conditions different from natural environments. Nevertheless, the recognition and degradation of these materials by chitinolytic enzymes will provide some insights as to their biodegradability. Information on their biodegradability is critical to their potential use as biodegradable plastics.

The objectives of this study were

(1) to investigate the kinetics of the formation of N-acyl homologs of chitosan from the ionic complexes of chitosan with four alkanoic acids, formic, acetic, propionic and butyric acid, and to test the hypothesis that vitrification is responsible for the two-stage kinetics reported earlier;

(2) to examine the influence of N-acyl substituent size and DS on the thermal transitions of N-acyl homologs of chitosan; and

(3) to compare the N-acyl homologs of chitosan with native chitin in terms of the recognition and subsequent degradation by chitinolytic enzymes, and to examine the influence of DS on enzymatic degradation of N-acyl homologs of chitosan.

5.3 MATERIALS AND METHODS

5.3.1 Materials

This study employed chitosan obtained from Sigma, St. Loius, MO. The degree of deacetylation of chitosan was 89.3% (manufacturer's specification). Reagent grade formic, acetic, propionic and butyric acids were obtained from Aldrich Chemicals, Milwaukee, WI. Both chitosan and solvents were used as received.

5.3.2 Methods

5.3.2.1 Film Preparation

The preparation of films for the kinetic analysis involved the dissolution of 57 g of chitosan in 3 L of 10% solution of each of the four acids (formic, acetic, propionic, and butyric acid) with vigorous stirring to obtain clear solutions. Each

solution was centrifuged to remove suspended matter. About 150-250 mL of each solution was poured into evaporation dishes for solvent evaporation at room temperature for two days. Afterwards the evaporation dishes were covered with perforated aluminium foil. The dishes were left for a period of one week for additional solvent removal. This was followed by vacuum drying at room temperature for 24 h. The films thus obtained had a thickness of 0.2-1.4 mm.

5.3.2.2 Dynamic Mechanical Thermal Analysis (DMTA)

Dynamic mechanical thermal analysis of heat-treated chitosonium acetate films was performed with a Polymer Laboratory DMTA. Samples were tested by bending in a single cantilever mode, at a heating rate of 2.5°C/min, an oscillation amplitude of 0.4 mm and a frequency of 1 Hz. All samples had dimensions of 8 × 5 × 1.1 mm. A nitrogen purge at a rate of 25 cm^3/min was used during data collection. The glass transition temperature was determined from the peak in the tan δ curve.

5.3.2.3 Solid State NMR

Samples for solid state NMR experiments were produced by grinding into powder films of the various N-acylate of chitosan (as prepared in section 5.3.2.1). The powderous N-acylates were heated at 130°C for 24 h. Solid state NMR experiments were carried out on a Bruker MSL-300 at a resonance frequency of 75.47 MHz for ^{13}C nuclei. The proton spin-lock field strength was approximately 56 KHz. Powderous form of the various heat treated N-acylate of chitosan were loaded into a zirconium oxide rotor. The magic angle was set using the KBr method, and the rotor was spun at

5 KHz. Cross-polarization contact time was varied between 2 to 9 ms. The area of the acetamido alkyl resonance, as well as the total area of the resonances of the glucose carbons, derived by integration of peaks, for each contact time were both plotted against contact time. Absolute areas of the alkyl resonance and glucose carbons resonances were determined by extrapolation of the area vs. contact time plot to zero contact time. The DS of the various heat treated N-acylates of chitosan were determined according to the method of Fukamizo et al.[18] which relies on the ratio of absolute area of the acetamido alkyl resonance to the total absolute area of the resonances of the glucose carbons.

5.3.2.4 Preparation of Colloidal Chitin

The substrate used for enzyme assay was colloidal chitin. This was prepared by dispersing 5 g of either native or amidized chitosan in 30 mL of concentrated HCl at 5°C. After achieving a homogeneous dispersion, the temperature was quickly raised to 37°C and the mixture stirred for several minutes. The dispersed material was then added to 500 mL of distilled water and centrifuged. The water was then decanted and the gel-like material, with a dry weight of 1.7 g (from TGA measurement) was washed with distilled water to neutral pH. It was resuspended in 25 mL of distilled water with vigorous stiring. The product thus obtained and referred to as colloidal chitin was stored in a refrigerator until used.

5.3.2.5 Enzyme Assay

The digestibility of native chitin was examined using chitinase only. Native and amidized chitosan were also digested using an enzyme mixture of chitinase, chitosanase and β-N-acetylglucosaminidase. Chitinase was produced from *Streptomyces griseus*; β-N-acetylglucosaminidase came from *Aspergillus niger*; and chitosanase was derived from *Streptomyces griseus* (manufacturer's specification).

A reaction mixture consisting of 2 mL of colloidal chitin (regenerated or native); 0.5 mL of chitinase solution in phosphate buffer, pH 5; 0.5 mL of chitosanase in phosphate buffer, pH 5; and 0.2 mL of β-N-acetylglucosaminidase in ammonium sulphate and sodium citrate buffer, pH 5, contained in a glass tube was incubated at 30°C in a shaking water bath. After 4 h (the time to leveling-off obseved by Nanjo et al.)[15] the glass tube was placed in a boiling water bath for 5 min, and cooled to room temperature by placing it in a cold water bath.

5.3.2.6 High Performance Liquid Chromatography (HPLC)

The identification of the fractions of hydrolyzed colloidal chitin was carried out using HPLC. The set-up of the HPLC system involved an HPX 87H organic acid column from Bio-Rad, USA, and a refractive index detector. The mobile phase, flow rate, temperature and injection volume were 0.1N H_2SO_4, 0.6 mL/min, 65°C and 10 μL, respectively. Retention times were established for the various fractions by comparison with N,N,N-triacetylglucosamine (chitotriose), N,N-diacetylglucosamine (chitobiose), N-acetylglucosamine, and glucosamine as standards. These standards

were obtained from Aldrich Chemicals, USA, and were used as received except for glucosamine. This was purchased in the form of glucosamine hydrochloride, and was converted into glucosamine using cation exchange resin.

5.3.3 Data Interpretation

5.3.3.1 Kinetic Considerations

The progress of the thermal amidization process was described kinetically according to a modified version of the method of Provder et al. Their method relates the changes in modulus that take place during the process of network formation to the fractional extent of cure according to the following equation,[25]

$$F_{(t,T)} = G_{(t,\,T)} - G_{(0)} / G_{(\infty)} - G_{(0)} \qquad (1)$$

where $G_{(0)}$, $G_{(t,\,T)}$, $G_{(\infty)}$ are the modulus at the onset of cure, at a given time and temperature during the cure process, and after the cure process has stopped, respectively. In our case, a previous study has demonstrated that variation in T_g is more sensitive than modulus to small changes in cure time or temperature[8]. A modified form of equation (1) was therefore formulated as

$$F_{(t,\,T)} = T_{g\,(t,\,T)} - T_{g\,(0)} / T_{g\,(\infty)} - T_{g\,(0)} \qquad (2)$$

where $T_{g\,(0)}$, $T_{g\,(t,T)}$ and $T_{g\,(\infty)}$ are the T_g at the onset of cure, at a given time and temperature during the cure process, and after the cure process has stopped, respectively. The rate constant was calculated for several temperatures according to equation (3) , assuming a first order reaction;

$$\ln(1 - F) = k(T)t \qquad (3)$$

where k is the temperature-dependent rate constant and t is cure time.

An Arrhenius plot was generated from the derived first order rate constants according to equation (4)

$$\ln k = \ln A - \frac{E}{RT} \qquad (4)$$

where A is the Arrhenius frequency factor, E is the activation energy, and R is the universal gas constant. The activation energy for thermal amidization was calculated from the slope of the Arrhenius plot.

$T_{g\,(0)}$ in equation (2) was taken as the T_g of the unheated chitosan complex. $T_{g\,(0)}$ was determined as 60, 77, 82, and 93°C for chitosonium- butyrate, propionate, acetate, and formate, respectively. After the chitosan complex had been heated at a particular temperature for a specified time, an initial temperature scan to a post-heating temperature say $T_{c\,(\infty)}$ yielded $T_{g\,(t,\,T)}$. In each case $T_{c\,(\infty)}$ is selected such that beyond it no additional increase of modulus occurs. Therefore, the material is considered to be fully-cured at $T_{c(\infty)}$. A second scan of the material yielded $T_{g\,(\infty)}$ for each heating temperature. The average of $T_{g\,(\infty)}$s of all heating temperatures was taken as $T_{g\,(\infty)}$ in equation (2). $T_{g\,(\infty)}$ was determined as 160, 163, 189, and 190°C for N-butyryl, N-propyl, N-acetyl, and N-formyl homologs of chitin, respectively.

The major limitation of Provder's model is related to the value of $T_{g\,(\infty)}$. An assumption is made that at $T_{g\,(\infty)}$ the material is fully-cured because beyond it no modulus increase is observed. It is possible that beyond $T_{g\,(\infty)}$ thermal degradation sets in

such that any modulus increase that could otherwise occur is masked by degradation. Therefore, $T_{g(\infty)}$ may not be a true representation of a fully-cured material. Nonetheless, this model provides a reasonable description of cure kinetics.

5.3.3.2 HPLC Analysis

In order to identify the various fractions of hydrolyzed chitin we established retention times of suspected fractions using standards. The concentration of fractions were calculated using an external calibration procedure. This involved the variation of concentration of standards and the determination of peak areas by HPLC. The slope of a plot of the peak area vs. concentration was used to determine response factors of standards (**Appendix A**). Consequently, concentrations (x) of fractions were calculated by an equation of the form $y = mx + c$, where m is the response factor, y is the HPLC peak area and c is an intercept. The peak areas of the various fractions used in the above calculation are presented in **Appendix A**. The concentration of the various fractions as derived above were converted to amount in milliequivalents and subsequently used to calculate the yield of the various fractions on the basis of the amount of starting material. A sample calculation is presented in **Appendix B**.

5.4 RESULTS AND DISCUSSION

5.4.1 Degree of Substitution (DS) of Amidized Homologs of Chitosan

The DSs of the various amidized homologs of chitosan as well as that of native chitin, determined from the integrated area of glucose carbons and acetamido alkyl resonance peaks **(Figure 5-3)**, are presented in **Table 5-1**. Native chitin has a DS of

nearly 1.0; this is higher than all thermally-produced N-acyl homologs of chitosan. The thermally-produced derivatives have DS-levels that varied between 0.1 and 0.6 **(Table 5-1)**. A plausible explanation for the lower than expected DS, and for the differences in DS among the various derivatives **(Table 5-1)**, may be sought in the following arguments. In producing the various N-acylates, an equilibrium exists between the ionic complexes (N-acylates) and the free amine and acid (**Figure 5-4**). This equilibrium produces different volatile acid species in the various N-acylates; and it is influenced by equilibrium constants as well as by conditions of handling, especially of evaporation. The latter is a result of uncontrolled factors such as time, room temperature, vapor pressure, air velocity, etc. Presumably, these factors differ in their influence on the preservation of chitosonium alkanoate complexes (i.e., left side of the equilibrium of Figure 5-4), and free amine and acid (right side). This results in differences in the proportion of N-acylate groups available for conversion to N-acyl groups. Consequently, differences in DS would result despite similar heating conditions and general operational parameters.

5.4.2 Thermal Transitions of Amidized Homologs of Chitosan

Thermal analysis by DMTA of the various ionic complexes of chitosan reveals two distinct transitions; a subambient transition, designated as β-relaxation centered at-10±10°C as well as a high temperature transition, designated as α-relaxation varying between 60 and 93°C **(Figure 5-5)**. The amidized chitosan derivatives also display two transitions. The β-relaxation migrates to 25±5°C and the α-relaxation occurs at 160 to

190°C **(Figure 5-5)**. Both the ionic complexes and their amidization products exhibit no additional transitions that may be designated as their melting temperatures (this was also confirmed by differential scanning calorimetry). The extent of damping, measured as the height of the tan δ- peak, did not vary with the type of acyl substituent **(Figure 5-5)**. Damping associated with the β-relaxation in the ionic complexes is enhanced over that of the N-acyl homologs of chitosan. The α-relaxation of the N-acylate homologs and those of their respective N-acyl homologs of chitosan are pronounced, and they coincide with significant declines of modulus. When the α-relaxation of the N-acyl homologs of chitosan is related to their acyl substituent length, a stepwise decline is revealed **(Figure 5-6)**. This relation produced a linear decline in the case of cellulose triesters amounting to 16°C per carbon atom for substituents increasing in size from C-2 to C-6[11]. That amidized chitosan derivatives fail to reveal a similarly linear relationship must be attributed to the variability of DS. In the case of cellulose triesters, similarly high DS-levels (i.e., ≅2.84) are recorded as the acyl substituent length increases from C-2 to C-6. Since it must be expected that T_g is a function of both acyl substituent size and DS, and since DS of the N-acyl chitosan homologs is highly variable (0.1 to 0.6), due to a complex set of factors as described in section 5.4.1, the non-linearity of the behavior is not surprising.

The subambient temperature was identified as a β-relaxation because it had a characteristically modest change in modulus typical of such transitions. This may be related to side group (acyl substituent) motions. The enhanced damping associated

with the β-relaxation in the ionic complexes compared to the N-acyl homologs may be due to the influence of residual, free acid derived from the equilibrium shown in **Figure 5-4**, acting as a plasticizer. A similarly enhanced β-relaxation has been observed in wet as compared to dry chitosan films[26].

The appreciable modulus-drop that accompanied the high temperature transition was the basis for the assignment of an α-relaxation, and this can be described as the T_g. Scandola and coworkers have also observed a double transition (at -100 and 130°C) in dry chitosan films using DMTA[26]. A third transition designated as β-relaxation at -50±20°C was observed in wet films. The transition at -100°C was described as γ-relaxation. Surprisingly, these investigators suggest that the transition at 130°C does not warrant an assignment as T_g of chitosan. They claim that DSC does not reveal a transition at this temperature and that the modulus-drop marking the transition is too modest to correspond to a glass-to-rubber transition. They are of the opinion that if the transition at 130°C is in fact a T_g, the modulus-drop would have been substantial because x-ray diffraction proves that the material is fully amorphous. An alternate explanation of the modest modulus-drop is that chitosan has a rigid polysaccharide backbone; and that as such, it will not show several decades of modulus-drop in the glass-to-rubber transition region as is the case of a typical flexible, amorphous polymer. The absence of a transition in DSC merely indicates that calorimetry is not sensitive enough. We believe that the transition at 130°C observed by Scandola and coworkers, just like the α-relaxation of N-acyl homologs of chitin, is

in fact the T_g of chitosan. This is because the reported log E" and tan δ-curves show well-resolved peaks.

5.4.3 Kinetics of the Formation of N-acyl Homologs of Chitosan

When the ionic complex of chitosan with formic, acetic, propionic, and butyric acid was subjected to isothermal heating at temperatures ranging from 80-140°C, DMTA revealed that the heat-treated materials had variable T_gs with time (**Figure 5-7**). During the initial stages of heating, T_g-changes with time were more pronounced and tended to level off after prolonged heating. Likewise, the extent of reaction calculated according to equation (2) showed a dramatic increase initially before leveling off after prolonged periods of heat treatment **(Figure 5-8)**. On a log scale, the extent of reaction , expressed as (1-F) showed a linear relationship with time (t) until about 7 h. Beyond 7 h, a new (1-F) vs. t linear relationship emerged **(Figure 5-9)**. The rate constant calculated for each (1-F) vs. t linear plot according to equation (3) varied linearly with the inverse of heating temperature **(Figure 5-10)**. The activation energies derived for the reaction below and beyond 7 h were 14±1 kcal/mol and 21±2 kcal/mol, respectively. These activation energies are nearly constant irrespective of the monocarboxylic acid used for the formation of the chitosan complex **(Table 5-2)**.

As reported in our previous studies[8], the T_g-changes observed upon heating the various chitosan complexes provide evidence of thermal dehydration to form the respective homolog of chitosan. The derivation of two activation energies indicates the existence of a two-stage kinetic process for all four chitosan complexes, consistent with

our previous report. The similarity of activation energies for the formation of the four amidized chitosan homologs suggests that the process is insensitive to acyl substituent size and that the same mechanism is responsible for the process in each case.

The DS of the various amidized chitosan derivatives varied from 0.1 to 0.6. It would be expected that the low DS-derivatives, particularly the N-formyl, N-propyl, and N-butyryl homologs of chitosan, all with DS of 0.1-0.2, would not produce dramatic changes in T_g. Surprisingly, this was not the case. For example, the T_g of the N-formyl derivative of chitosan increased from an initial value of 93°C to a final value of 193°C. This enhanced T_g increase within a narrow DS range of 0.1 to 0.2 suggests that another phenomenon, most likely related to molecular reorganization occurs during amidization. Additionally, despite the variability of DS, the activation energies are the same for the formation of the four amidized chitosan derivatives. It needs to be emphasized that the kinetics of amidization, as described in this paper, are based on changes in a physical parameter, T_g. As such the kinetic parameters are apparent values describing a chemorheological process that accompanies amidization. Therefore, it is not appropriate to relate DS to the kinetic parameters of amidization.

Using 4 types of α-ethyl-α-methyl butanoic esters and 3-dimethylaminopropylamine in a solvent (toluene and methylnaphthalene), Worku et al. formed polyamides[27]. Contrary to the two-stage kinetics we are reporting in this study, their kinetic investigation produced the conclusion that amidization is a second order, single-stage reaction with an activation energy varying from 6.9 to 9.7 kcal/mol.

Summers[28] studied the conversion of polyamic acid to polyimide in solution. He concluded that the kinetics of solution imidization involves a first-order, single-phase reaction as opposed to the two-stage reaction kinetics which was found to be associated with solid state imidization[29,30]. Summers observed that the former produced about 100% conversion at several temperatures compared to the maximum of 70% reported for the latter. Additionally, Dine-Hart[31] and Kardash[32] have reported that the progress of solid-state imidization is accelerated by the presence of residual solvent. Based on these studies we suspect that the kinetics of amidization depend on whether the process occurs in the solid or the liquid state, with the latter proceeding with relative ease. Therefore, the difference in activation energy derived in our study and that of Worku et al. is not surprising. The discrepancies in reaction order cannot, however, be related to the physical state in which amidization occurs because Summers[28] also reported a first order reaction for solution imidization. An explanation may be sought in the mechanism underlying solid state amidization and amidization in solution. Whereas the former forms the amide group by thermal dehydration of an N-acylate group, the latter involves a chemical reaction between an ester or carboxylic group and an amine (NH_2) group.

When chitosonium acetate is heated at 100°C, a progressive increase in modulus is observed which tends to level off before 6 h. An immediate increase of the temperature to 200°C (above $T_{g(\infty)}$ (189°C) of regenerated chitin) results in an additional increase in modulus (**Figure 5-11**). This is consistent with our hypothesis that the two-stage kinetics of amidization is due to the influence of vitrification.

5.4.4 Enzymatic Hydrolysis

Chitinase hydrolysis of native chitin produced a series of monomers and dimers. These include N,N-diacetylglucosamine (chitobiose), N-acetylglucosamine, and a mixed dimer of glucosamine and N-acetylglucosamine **(Figure 5-12)**. When chitinase's action on native chitin is combined with chitosanase and β-N-acetylglucosaminidase the fractions produced were N,N,N-triacetylglucosamine (chitotriose), N-acetylglucosamine, a mixed dimer of glucosamine and N-acetylglucosamine, and glucosamine. Chitobiose was absent in this case (**Figure 5-12**). The structures of the degradation products with their respective retention times are illustrated in **Figure 5-13**. All fractions were identified by using standards except C. The basis for identifying C as a mixed dimer of glucosamine and N-acetylglucosamine is as follows; the deacetylated product of N-acetylglucosamine (E), glucosamine (A), has a retention of 5.8 min, about 5 min shorter than the corresponding N-acetyl derivative. A mixed dimer of glucosamine and N-acetyl glucosamine can therefore be expected to also have a shorter retention time than chitobiose (D). A mixed dimer is therefore, most likely positioned between chitotriose (B) and chitobiose(D).

Incubation of the four N-acyl homologs of chitosan with an enzyme mixture of chitinase, chitosanase and β-N-acetylglucosaminidase revealed the presence of N,N,N-triacylglucosamine, N,N-diacylglucosamine, N-acylglucosamine and the mixed dimer in the hydrolyzate (**Figure 5-14**). The HPLC chromatograms were similar regardless

of chitosan derivative type. The yields of the fractions from both native and amidized chitosan derivatives are summarized in **Table 5-3**. Regardless of their preparation method, the yield of glucosamine was always higher than any other fraction.

Previous work by other scientists has established that chitinase predominantly degrades native chitin to oligomers of N-acetylglucosamine[15,22]. These oligomers can have degrees of polymerization of between 2 and 5. The subsequent hydrolysis of these oligomers to the monomer requires the action of β-N-acetylglucosaminidase. When chitin was hydrolyzed by chitinase, the yield of N-acetylglucosamine was only 0.002%. It increased to 3% in the presence of β-N-acetylglucosaminidase. Since there was no chitobiose in the fractions produced by the enzyme mixture, our observation conforms to the expectation that β-N-acetylglucosaminidase is responsible for the degradation of chitobiose. In our case, chitinase produced predominantly a dimer of N-acetylglucosamine (chitobiose) as well as a mixed dimer of N-acetylglucosamine and glucosamine. Surprisingly, in the presence of β-N-acetylglucosaminidase, a trimer of N-acetylglucosamine (chitotriose) was produced as well. We can infer from this observation that besides degrading oligomers of N-acetylglucosamine, β-N-acetylglucosaminidase is capable of cleaving chitin chains at every three glucose units in sequence to produce chitotriose. Additionally, we can suggest that the rate at which chitobiose is degraded by β-N-acetylglucosaminidase to the monomer exceeds the rate at which it is produced by chitinase resulting in no accumulation of chitobiose in the case of the enzyme mixture.

The hydrolytic action of chitinase alone on native chitin did not indicate the presence of glucosamine. However, glucosamine was produced when all three enzymes were used. The yield of glucosamine was higher than N-acetylglucosamine (65% vs ≅3%) in all derivatives, regardless of DS. The higher yield of glucosamine as compared to N-acetylglucosamine seems to suggest that native chitin has a higher proportion of unacetylated glucosamine units than acetylated ones. This observation contradicts the experimental DS results by solid state NMR. A plausible explanation for this contradiction may be that the enzyme mixture of chitinase, chitosanase and β-N-acetylglucosaminidase contains a deacylating-enzyme (such as a lipase) as a contaminant. This enzyme may have effected the deacetylation of N-acetylglucosamine during the course of hydrolysis leading to a higher accumulation of glucosamine.

As noted previously N-formyl-, N-acetyl-, N-propyl-, N-butyryl homologs of chitosan and native chitin have the same HPLC pattern. This observation indicates that the enzyme mixture of chitinase, chitosanase and β-N-acetylglucosaminidase cannot distinguish between the N-acyl substituents of the various types of chitin studied. Therefore, it is likely that if amidized chitosan derivatives were incubated with chitinase alone, similar hydrolysis patterns that produced only dimers of N-acetylglucosamine (chitobiose) as well as the mixed dimer, but no glucosamine, would have been observed. Following hydrolysis of all four types of amidized chitosan derivatives, more glucosamine is detected than N-acetylglucosamine (68, 43, 47, 45%

for N-formyl, N-acetyl, N-propyl and N-butyryl, respectively vs. ≅1% for all). The higher accumulation of glucosamine may be related to enzymatic deacylation as indicated previously. Additionally, incomplete acylation of these chitosan derivatives would contribute to the preponderance of glucosamine following hydrolysis.

The order of increasing DS of the materials subjected to enzymatic hydrolysis is as follows; native chitin > N-acetyl > N-propyl ≅ N-butyryl ≅ N-propyl. Despite these marked differences in DS, there is only an insignificant difference in the yield of N-acylglucosamine, contrary to the expectation that the higher DS material must produce a higher yield of N-acylglucosamine. This deviation from expectation is suspected to be related to the suspected deacylation of N-acylglucosamine to glucosamine. Consequently, we are unable to derive a relationship between DS and yield of N-acylglucosamine. However, it suffices to say that despite DS variability, amidized chitosan derivatives, just like native chitin, are recognized and degraded by chitinolytic enzymes into monomeric and oligomeric mixtures of similar composition.

In summary, we can say that there is no distinction among N-formyl, N-acetyl, N-propyl, N-butyryl homologs of chitosan and native chitin in terms of their recognition by chitinolytic enzymes. Chitinolytic enzymes can recognize and degrade chitin irrespective of the type of acyl substituent at the C-2 position as well as DS. The action of the enzyme mixture of chitinase, chitosanase and β-N-acetylglucosaminidase on all types of chitin indicates a higher accumulation of glucosamine than any degradation product. This may be related to deacylation of N-acylglucosamine by a

contaminant in the enzyme mixture. In the case of N-acyl homologs of chitosan, unacylated glucosamine would be a contributing factor to the higher accumulation of glucosamine in the degradation products.

5.5 CONCLUSIONS

(1) The degree of amidization of heat-treated chitosonium alkanoate complexes varied between 0.1 and 0.6, and this is attributed to equilibrium factors influencing the ionic association of alkanoic acids with the amine.

(2) The ionic complexes of chitosan with formic, acetic, propionic, and butyric acid as well as their respective N-acyl homologs of chitin display two transitions designated as α- and β-relaxation. They do not have melting points. The β- relaxations of the ionic complexes are more pronounced than those of their corresponding N-acyl homologs of chitin. This may be related to the plasticizing effect of residual acid in the former. The T_g of these chitin homologs displayed a stepwise relationship with the length of N-acyl substituent. This is accounted for by variability of DS and acyl substituent length.

(3) T_g-changes with amidization time can be used to describe the kinetics of formation of N-acyl chitosan homologs produced from the ionic complexes of chitosan with formic, acetic, propionic and butyric acid.

(4) The kinetics of formation of these homologs suggests a two-stage process. The activation energy for amidization curing is constant irrespective of the acid

used for the formation of the chitosan complex, or of the DS. The activation energies are 14 ± 1 kcal/mol and 21 ± 2kcal/mol for the first and second stage, respectively.

(5) Vitrification is responsible for the two-stage kinetics of amidization.

(6) There is no distinction among N-formyl-, N-acetyl-, N-propyl-,N-butyryl homologs of chitosan and native chitin in terms of their recognition by chitinolytic enzymes. Chitinolytic enzymes can recognize and degrade amidized chitosan and native chitin irrespective of the type of acyl substituent at the C-2 position at any DS. The action of the enzyme mixture of chitinase, chitosanase and β-N-acetylglucosaminidase on all types of chitin produces more glucosamine than any other degradation product.

5.6 ACKNOWLEDGEMENT

This is to thank Ms. Jody Jervis of the Department of Wood Science and Forest Products, Virginia Tech, for assistance with HPLC analysis. We also express thanks to Dr. Charles E. Frazier of the Department of Wood Science and Forest Products, Virginia Tech, for various discussions in the course of this study. The assistance of Tom Glass of the Chemistry Department, Virginia Tech, with solid state NMR experiments is acknowledged with gratitude.

5.7 REFERENCES

1. Muzzarelli, R.A.A, Encyclopedia of Polymer Science and Engineering, vol 3,. Wiley, NY, pp430-40.

2. Rutherford, F.A., and Austin, P.R., In: Proceedings of the first International Conference on Chitin and Chitosan, Muzzarelli, R.A.A. and Pariser, Eds., MIT, Cambridge, MA, 1978.

3. Averbach, B.L., in: Proceedings of the first International Conference on Chitin and Chitosan, Muzzarelli, R.A.A. and Pariser, Eds., MIT, Cambridge, MA, 1978.

4. Hepturn, H.R., and Chandler, H.D., in: Proceedings of the first International Conference on Chitin and Chitosan, Muzzarelli, R.A.A. and Pariser, Eds., MIT, Cambridge, MA, 1978.

5. Mima, S., Miya, M., Iwamoto, R., and Yoshikawa, S., J. Appl. Poly. Sci., Vol. 28, 1909-1917, 1983.

6.East, G.E., and Qin, Y., J. Appl. Poly. Sci., Vol. 50.1773-1779, 1993.

7. Wei, Y.C., Hudson, S.M., Mayer, J.M., and Kaplan, D.L., J. Polym. Sci., Part A, 30, 2187-2193, 1992.

8. Toffey, A., Samaranayake, G., Frazier, C.E., and Glasser, W.G., J. Appl. Polym. Sci., 60, 75-85, 1996.

9. Samaranayake, G., and Glasser, W.G., Carbohydr. Polym. 22, 1-7, 1993; 22, 79-86, 1993

10. Glasser, W.G., Samaranayake, G., Dumay, Michelle, and Dave, V., J. Polym. Sci., Part B: Polym. Phys., 33, 2045-2054, 1995.

11. Sealey J.E., Samaranayake, G., Todd, J.G., and Glasser, W.G., J. Polym. Sci., Part B: Polym. Phys., 34, 1613-1620, 1996; and references therein

12. Glasser, W.G., McCartney, B.K., and Samaranayake, G., Biotechnol. Prog., 10, 214-219, 1994

13. Domszy, J.G., and Roberts, G.A.F., Makromol. Chem., 186, 1671-1677, 1985

14. Frederic, N., Basora, N., Chornet, E., and Vidal, P.F., Carbohy. Res., 238, 1-9, 1993

15. Nanjo, F.K., Katsumi, R., and Sakai, K., Analytical Biochem., 193, 164-167, 1991

16. Pelletier, A., Lemire, I., Sygusch, J., Chornet, E., and Overend, R.P., Biotech. and Bioeng., Vol. 36, 310-315, 1990

17. Raymond, L., Marin, F.G., and Marchessault, R.H., Carbohy. Res., 246, 331-336, 1993

18. Fukamizo, F., Kramer, K.J., Mueller, D.D., Schaefer, J., Garbow, J., and Jacob, G.S., Archieves of Biochem. and Biophys., Vol. 249, No. 1, 15-26, 1986

19. Alasdair, B., Michael, B., Taylor, A., and Roberts, G.A.F., Int. Biol. Macromol., 14, 166-169, 1992

20. Turi, E.A., Thermal Characterization of Polymeric Materials, Academic Press, Inc., New York, 1981

21. Shun-Ichi, N., Fujisaki, K., and Kinjo, N., In Polyimides: Synthesis, Characterization and Applications, Vol. 2, Mittal, K.L., ed., Plenum Press, NY, p259, 1984.

22. Bartnicki-Garcia, S. In Advances in Chitin and Chitosan, Skjaki, Braek, G., Anthonsem, T. and Sandford, P., eds., Elsevier, Essex, UK, pp23-35

23. Aiba, S., Int. J. Biol. Macromol., 15, 421-425, 1993

24. Aiba, S., Int. J. Biol. Macromol., 14, 225-288, 1989

25. Provder, T., Holsworty, R.M., and Grentzer, T.H., In Adv. Chem. Ser. 203, America Chemical Society, Washington, D.C., 1981

26. Pizzoli, M., Ceccorulli, G., and Scandola, M., Carbo. Polym., 222, 205-213, 1991

27. Worku, A., Srisiri, W., Padias, A.B., and Hall, H.K., ACS Polym. Preprint., 678-679, 1996

28. Summers, J.D., Ph.D. Dissertation, Virginia Tech., pp298, 1988

29. Johnson, C., Mao, J., and Wunder, S.L., In Polyimides: Materials, Chemistry and Characterization., Proceedings 3rd International Conference on Polyimides, Feger,C., Khojasteh, M.M., and McGrath, J.E., eds., Elsevier Press, NY, p348, 1989.

30. Kruez, J.A., Endrey, A.L., Gay, F.P., and Sroog, C.E. ., J. Polym. Sci., Part A-1: Polym. Phys., 34, 1613-1620, 1996.

31. Dine-Hart, R.A., and Wright, W.W., J. Appl. Polym. Sci., 11, 609, 1967

32. Kardash, I.Y., Ardashnikov, A. Y., Yakushin, F.S., and Pravednikov, A.N., Polym. Sci., U.S.S.R., 17, 689, 1975

Table 5-1. Degree of Substitution (DS) of native chitin and of N-acyl derivatives of chitosan.

Material Type	DS
Native chitin	0.96
N-formyl chitosan derivative	0.10
N-acetyl chitosan derivative	0.60
N-propyl chitosan derivative	0.18
N-butyryl chitosan derivative	0.13

Table 5-2. Activation energies for amidization curing of various complexes of chitosan.

Material Type	$E^{1)}$ (kcal/mol)	$E^{2)}$(kcal/mol)
Formate	15.30	19.10
Acetate	15.11	21.00
Propionate	14.00	23.00
Butyrate	12.80	2.50

[1)] First phase of amidization
[2)] Second phase of amidization

Table 5-3. Composition of hydrolyzates of native chitin and of N-acyl chitosan derivatives using an enzyme assay of chitinase, chitosanase, and β-N-acetylglucosaminidase

Material Type	Degradation Product[1] Yield (meq of degradation per meq of anhydroglucosamine repeat unit (%)				
	A	B	C	D	E
Native chitin	63	≈0.1	1	0.5[2]	2.6
N-formyl chitosan derivative	68	≈0.1	1	N/P	≈0.3
N-acetyl chitosan derivative	43	≈0.1	1	N/P	≈1
N-propyl chitosan derivative	47	≈0.1	1	N/P	≈1
N-butyryl chitosan derivative	45	≈0.1	1	N/P	≈1
Response Factor [3](10^6)	6.62	14.68	4.30[4]	2.8	2.04

[1]Glucosamine (A); Chitotriose (B); Mixed dimer of glucosamine and N-acylglucosamine mixture (C);Chitobiose (D); and N-acylglucosamine (E)

N/P; Not present

[2] Hydrolysis was performed with chitinase only

[3] Calculated as the slope of a plot of integrator response area of standards vs. concentration

[4] Assumed as an average of response factors of A and E

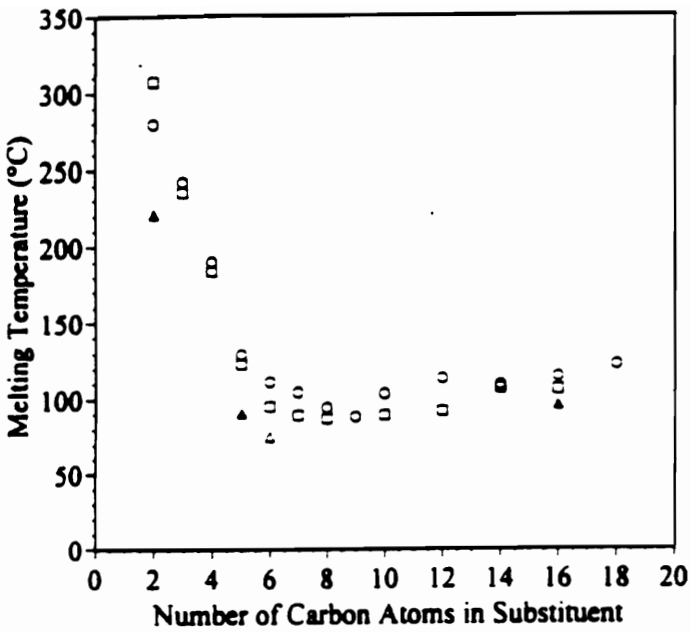

Figure 5-1. Melting points and glass transitions of cellulose triesters as a function of acyl substituent size (□). Apparent T_m (visual observation) (O) and T_g (▲). Adapted from reference 11 and references therein.

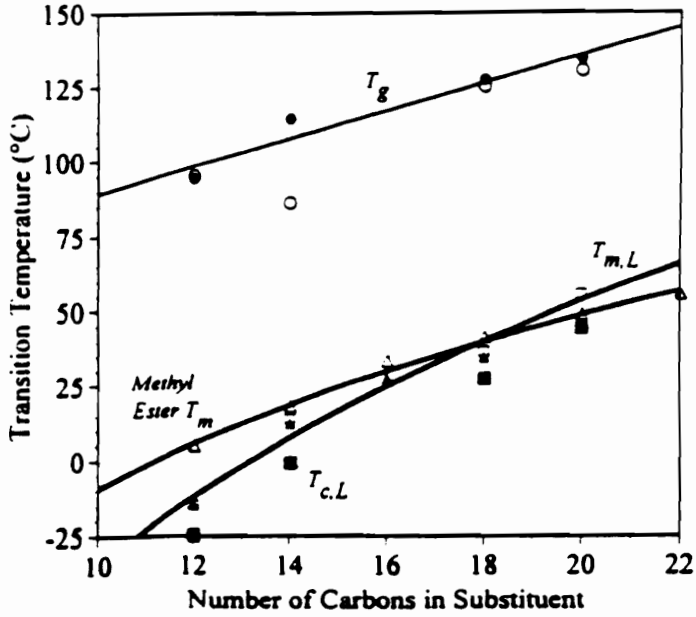

Figure 5-2. Thermal transitions of waxy cellulose esters. (●) T_g (DSC); (O)T_g (DMTA); (□) side-chain melting point, $T_{m,L}$ (DSC); (■) side chain crystallization. Adapted from reference 11 and references therein.

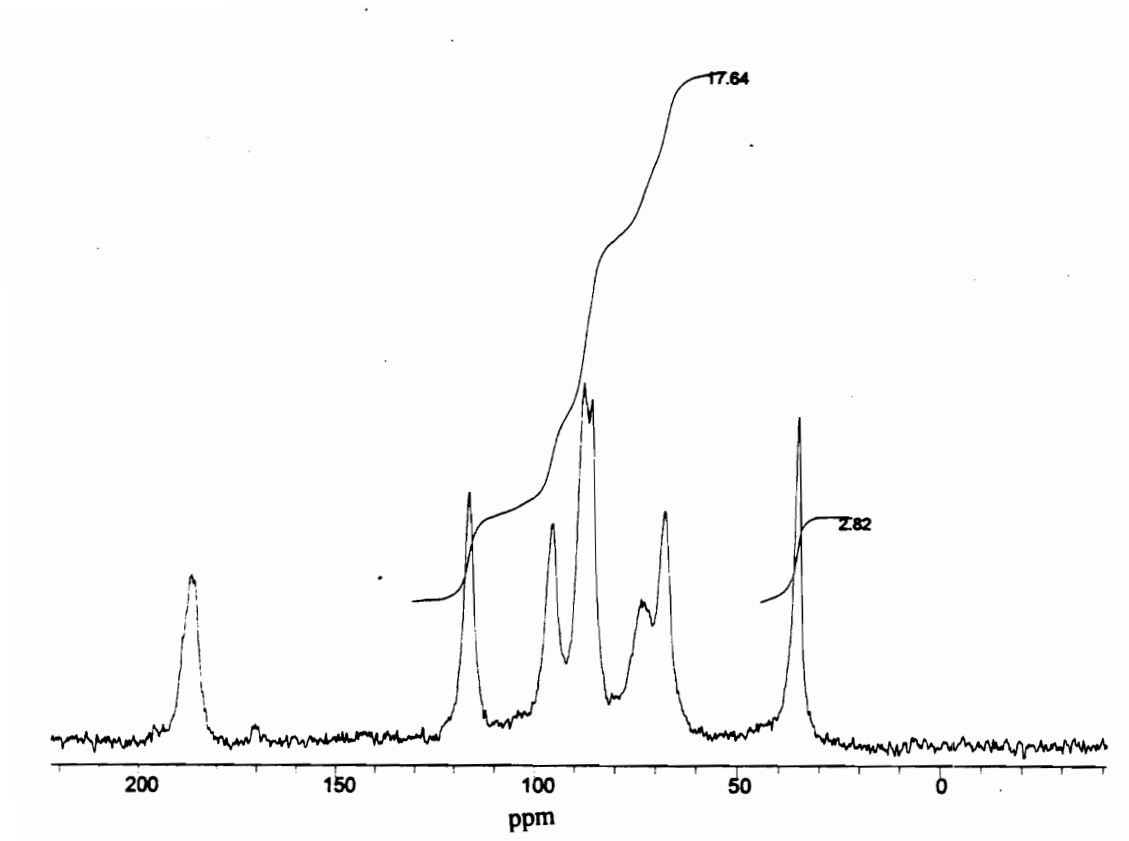

Figure 5-3a. CP-MAS ^{13}C-NMR spectrum of native chitin. The peaks at 23 and 173 ppm are identifiable as methyl carbon (CH_3) and N-acetyl carbonyl carbon, respectively. The area of the methyl carbon (2.82), and the total area of the glucose carbons (17.64) are used to determine the DS of chitin.

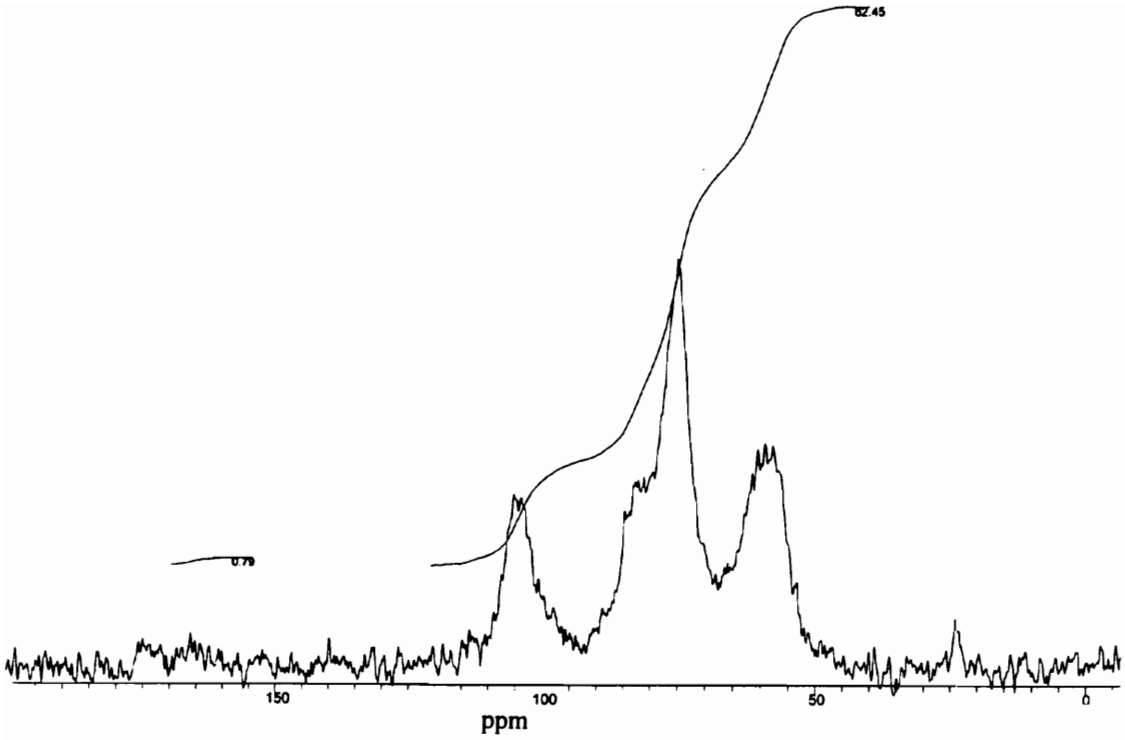

Figure 5-3b. CP-MAS ^{13}C-NMR spectrum of N-formyl homolog of chitosan.
The peak at 173 ppm is identifiable as N-formyl carbonyl carbon. N-formyl homolog of chitosan is not expected to have an alkyl carbon peak as in native chitin. Its DS is estimated by comparing the N-formyl carbonyl carbon peak to those of other amidized chitosan derivatives.

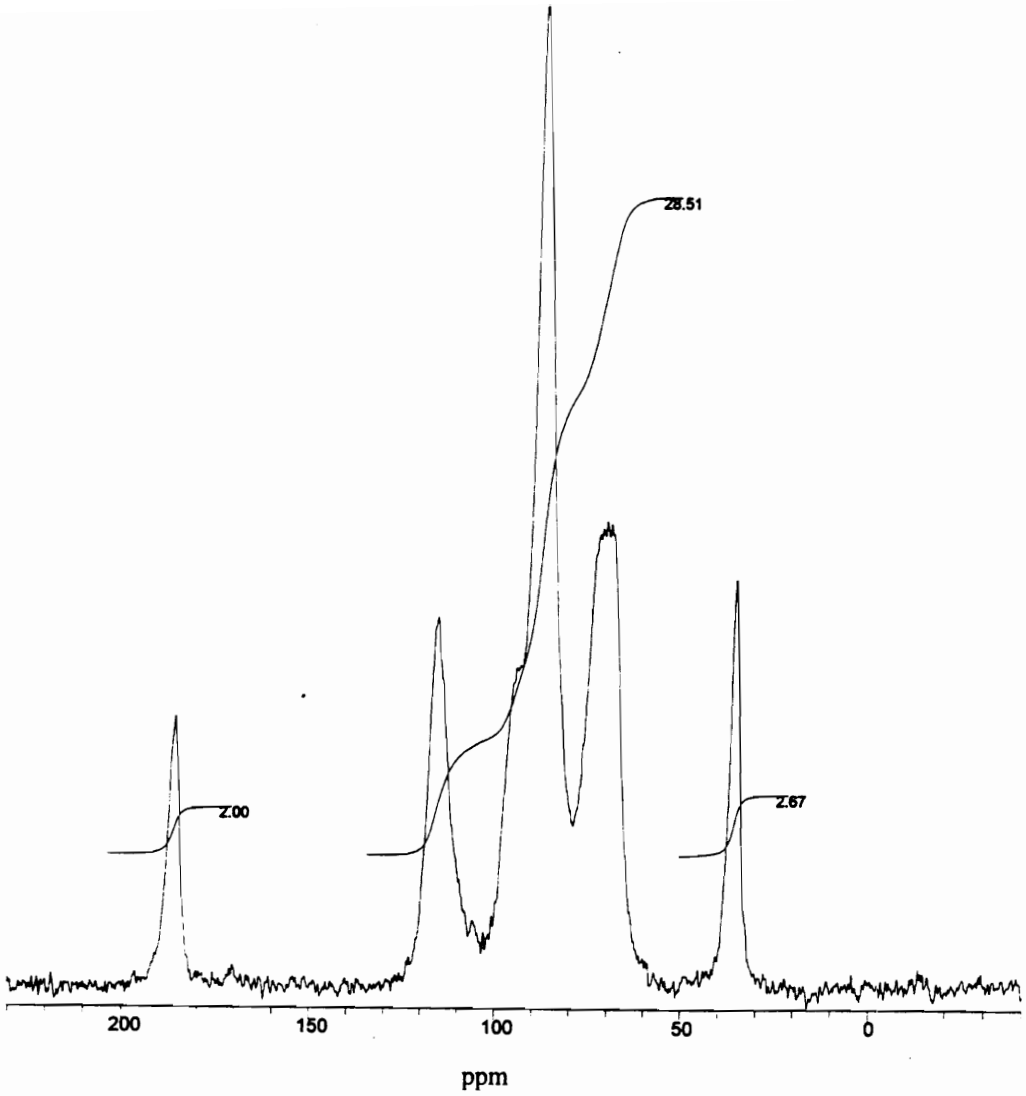

Figure 5-3c. CP-MAS ^{13}C-NMR spectrum of N-acetyl homolog of chitosan. The peaks at 23 and 173 ppm are identifiable as methyl carbon (CH_3) and N-acetyl carbonyl carbon, respectively.

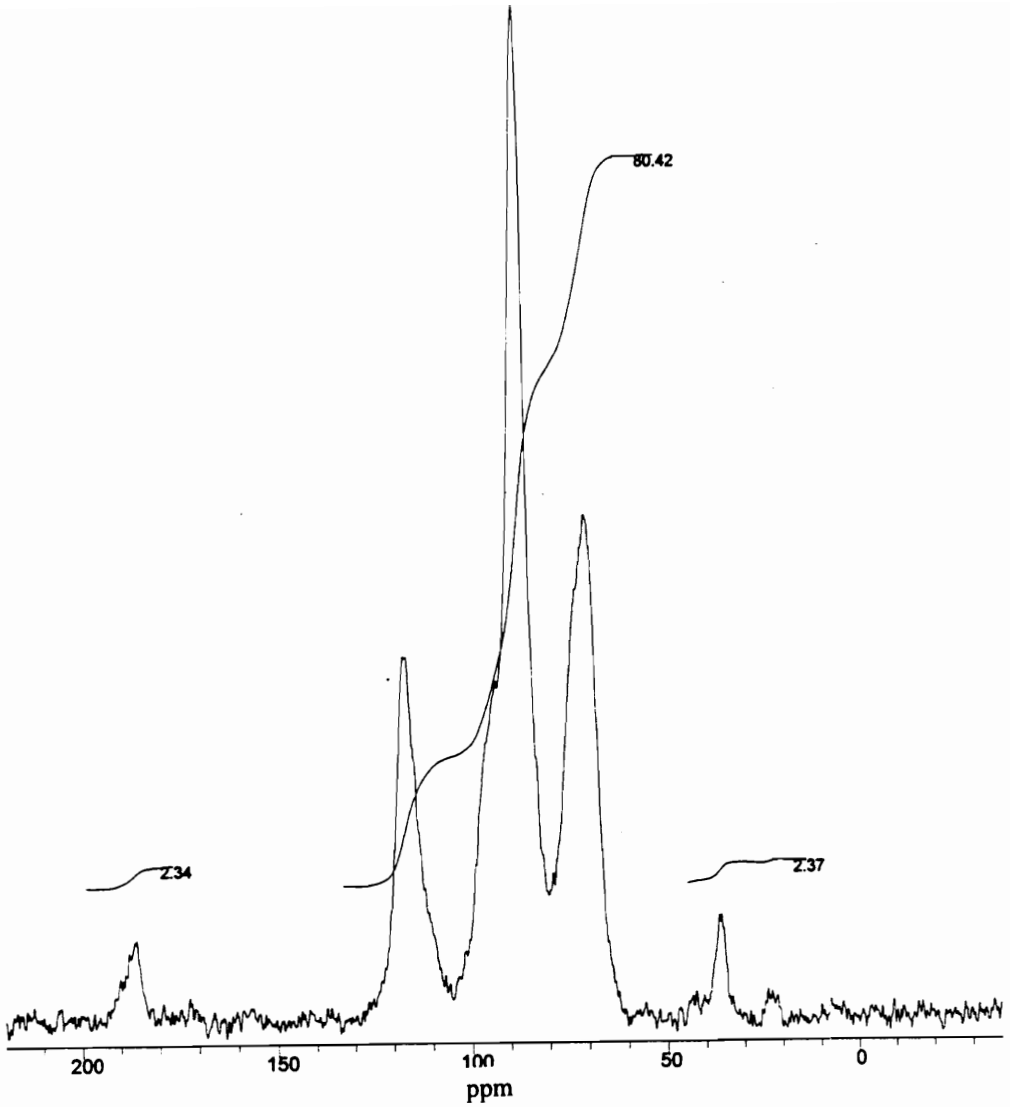

Figure 5-3d. CP-MAS ^{13}C-NMR spectrum of N-propyl homolog of chitosan. The peaks at 23 and 173 ppm are identifiable as propyl carbon and N-propyl carbonyl carbon, respectively.

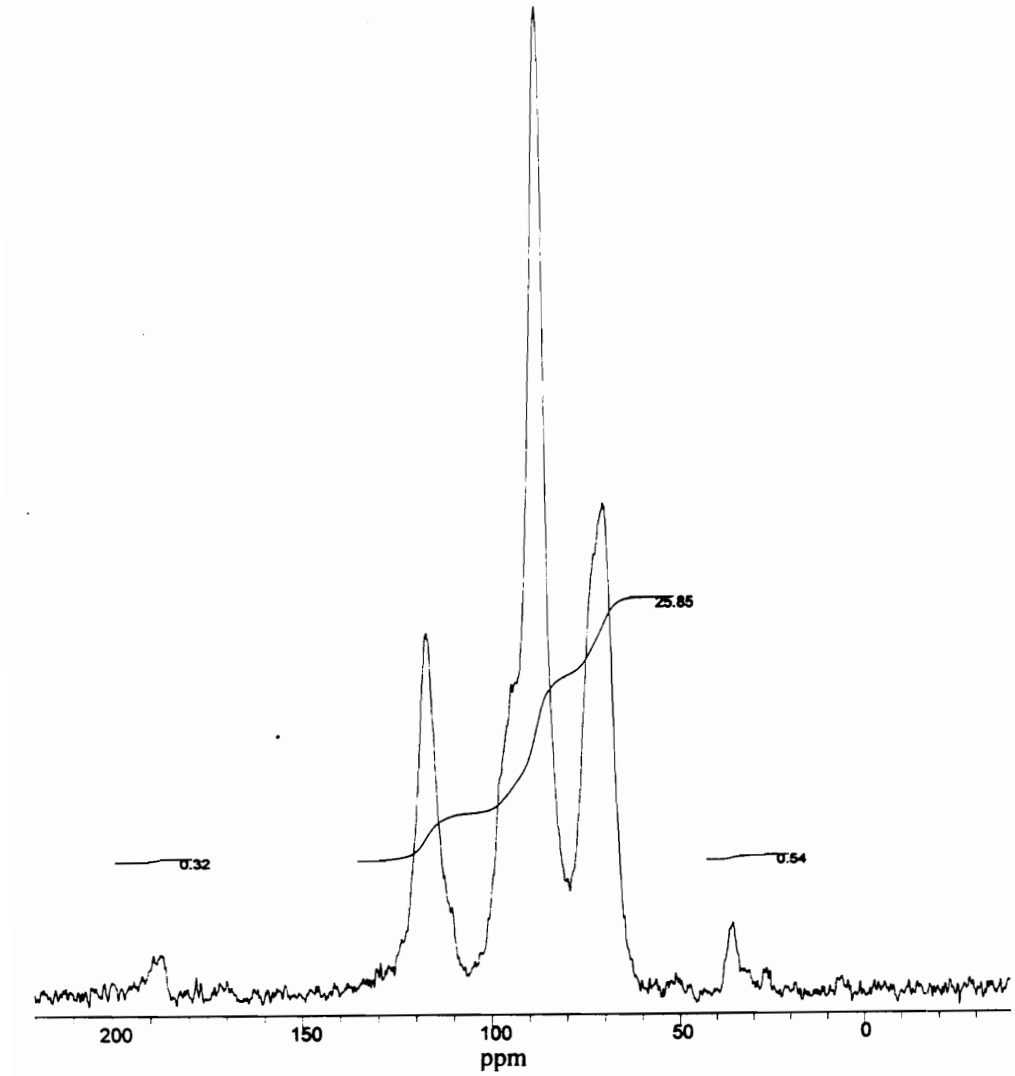

Figure 5-3e. CP-MAS ^{13}C-NMR spectrum of N-butyryl homolog of chitosan. The peaks at 23 and 173 ppm are identifiable as butyryl carbon and N-butyryl carbonyl carbon, respectively.

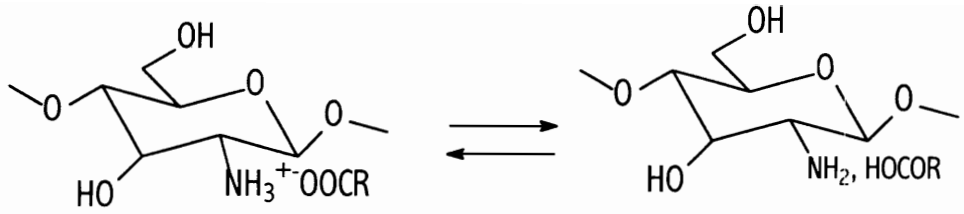

Figure 5-4. Chemical equilibrium between chitosonium alkanoate complexes and the free amine and acid. R corresponds to either H or an alkyl group.

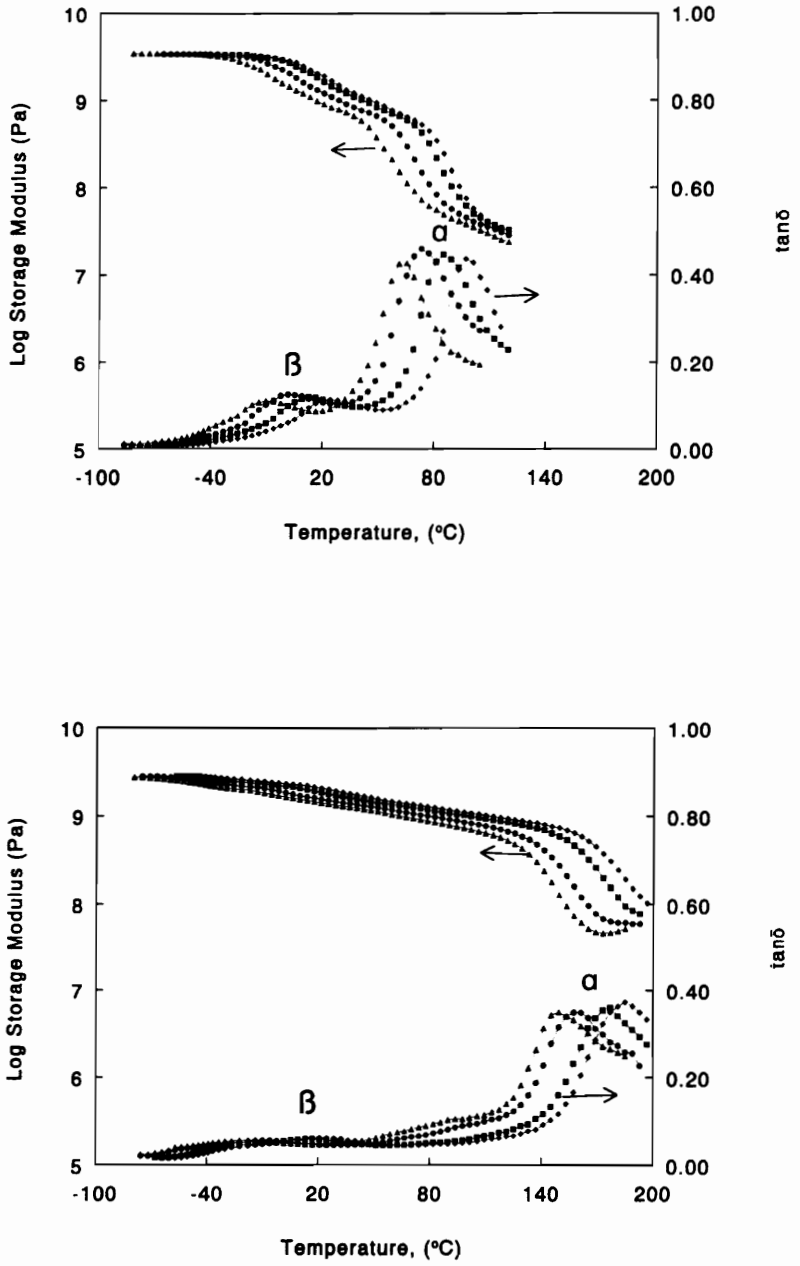

Figure 5- 5. DMTA thermograms of ionic complexes of chitosan (top) and their respective N-acyl homologs of chitin (bottom). Two transitions designated as α- and β-relaxation are discernible. The β-relaxation is enhanced in the ionic complexes. ▲ (butyrate/N-butyryl); ●(propionate/N-propyl); ■(acetate/N-acetyl); and ◆(formate/N-formyl).

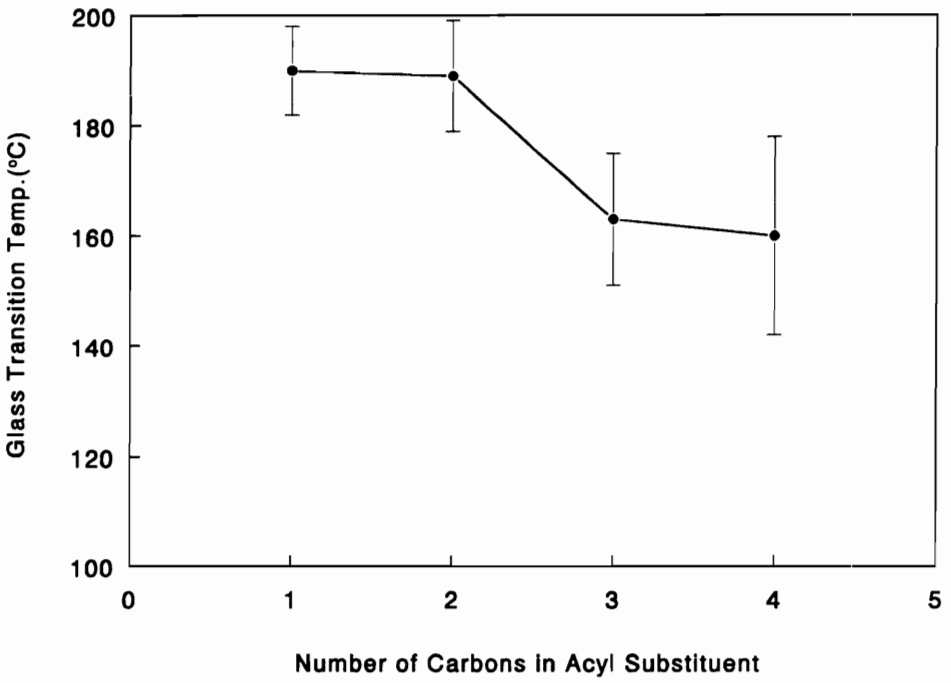

Figure 5-6. Variation of T_g of N-acyl homologs of chitosan ($T_{g,\infty}$) with length of acyl substituent. The T_g shows a stepwise decline with the number of carbon atoms in the N-acyl substituent. The vertical lines are error bars obtained by plotting the extremes of 5 T_g-values for each data point.

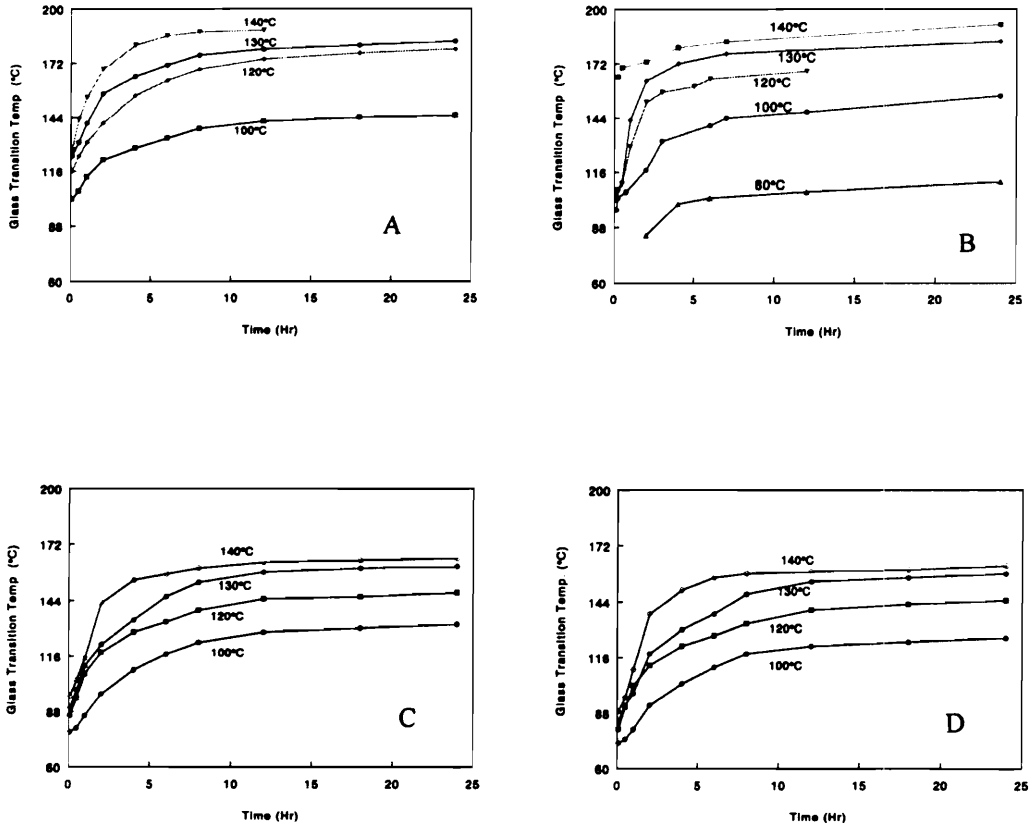

Figure 5-7. Glass transition temperature variation with time at various isothermal cure temperatures. This figure can be transformed to conversion variation with time, according to equation (4). A, B, C, and D correspond to isothermal curing of chitosonium formate, acetate, propionate and butyrate, respectively. T_gs were determined using DMTA except B where T_gs were determined using TMA. B was adapted from reference 8.

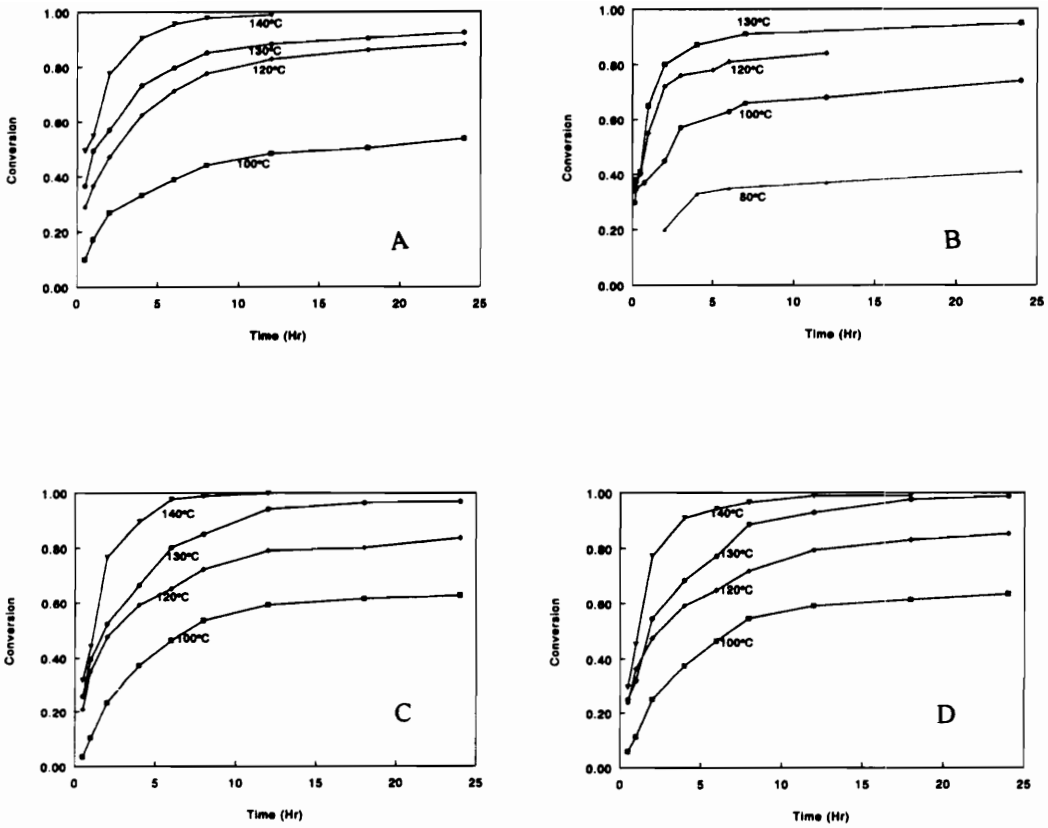

Figure 5-8. Conversion with time at various isothermal cure temperatures calculated using equation (2). A, B, C, and D correspond to conversion with time for isothermal curing of chitosonium formate, acetate, propionate and butyrate, respectively. B was adapted from reference 8.

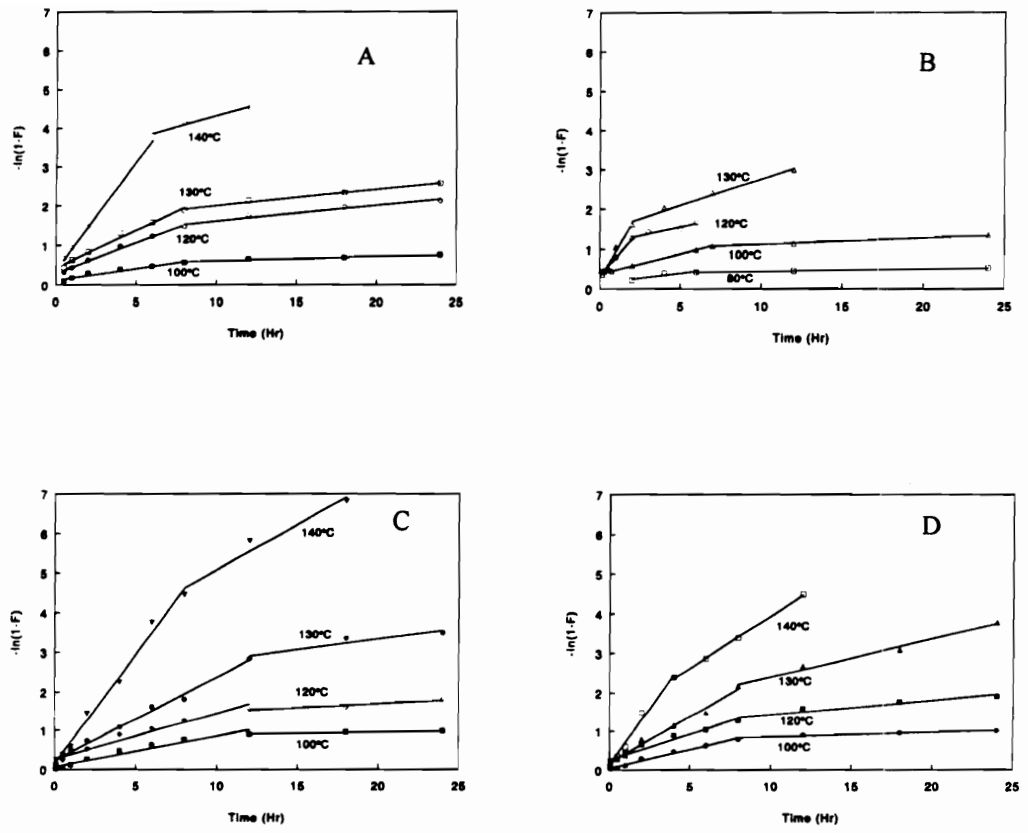

Figure 5-9. First-order plot of chitosonium formate (A), acetate (B), propionate (C) and butyrate (D) to amidized chitosan transformation according to equation (2). There is a change in slope of each line following prolonged heat treatment. This suggests that two steps are involved in the transformation of ionic complexes of chitosan to amidized chitosan. B was adapted from reference 8.

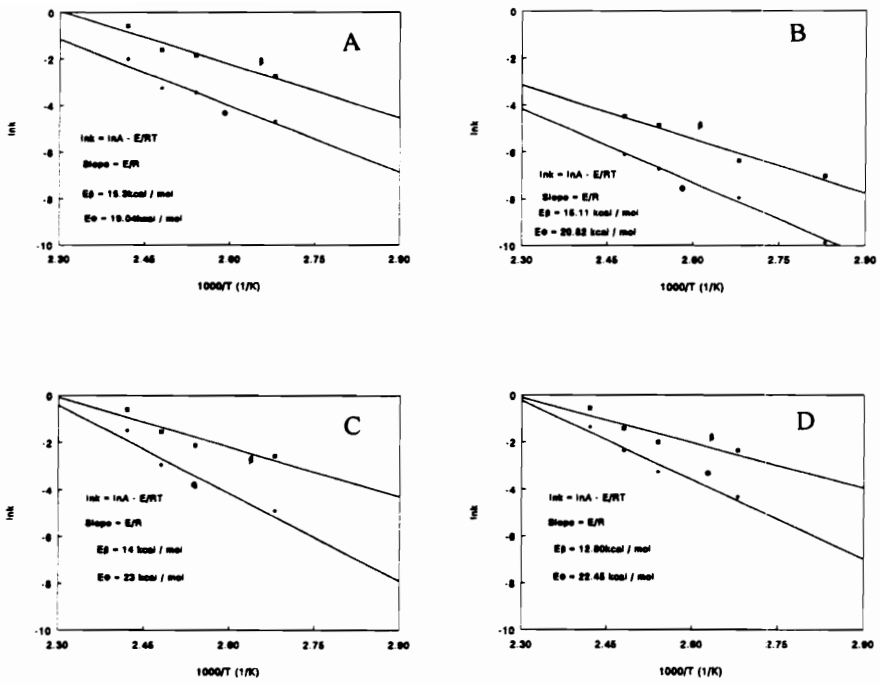

Figure 5-10. Arrhenius plot of rate constants vs. temperature for activation energy determination of amidization curing of various ionic complexes of chitosan.β: First step reaction, Φ: second step reaction. Eβ and EΦ are the corresponding activation energies. A, B, C, and D correspond to conversion with time for isothermal curing of chitosonium formate, acetate, propionate and butyrate, respectively. B was adapted from reference 8.

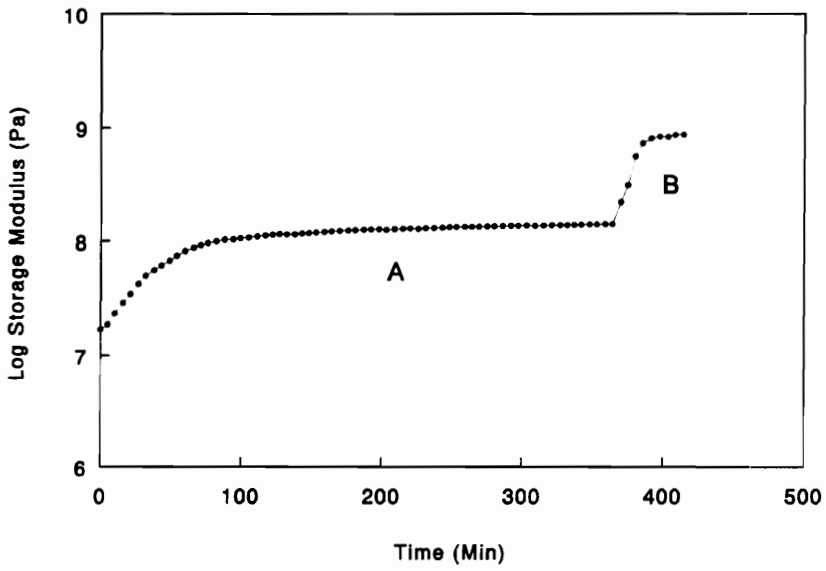

Figure 5-11. Isothermal cure monitoring of chitosonium acetate at 100°C. The increase of modulus levels off after ca 2 h. A sudden increase of temperature to 200°C results in a further increase of modulus. A and B represent where cure temperature is 100°C and 200°C, respectively. The additional increase of modulus is related to a release of the polymer chains from a frozen state.

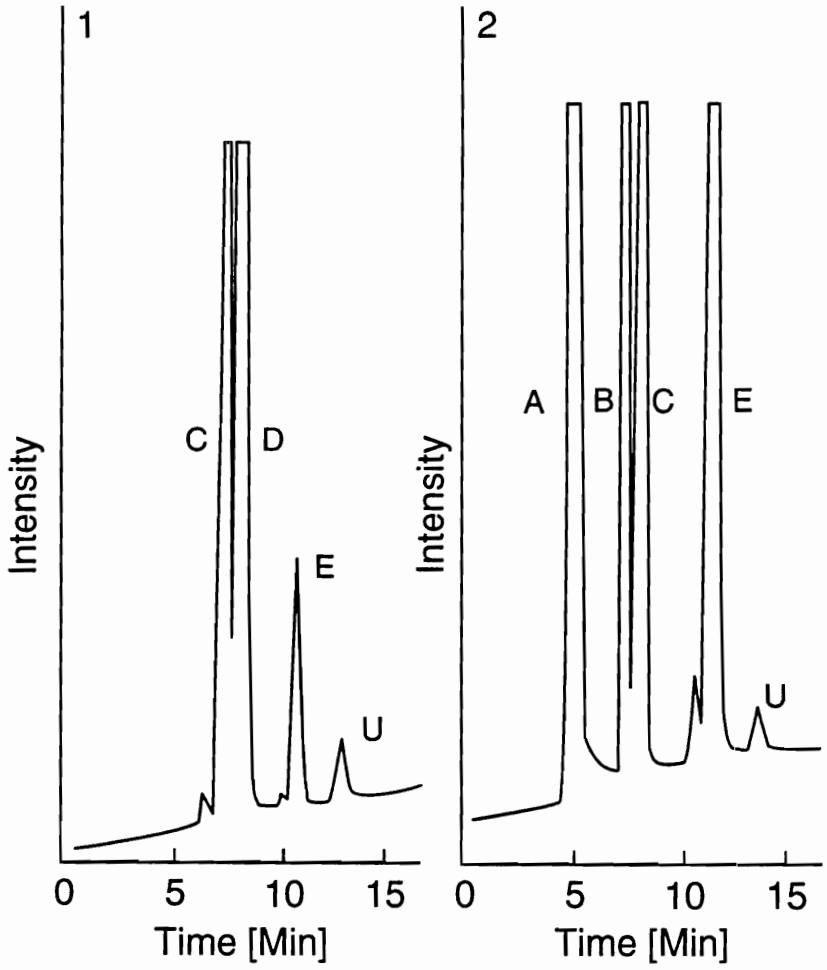

Figure 5-12. HPLC chromatograms of hydrolyzed chitin. The identified fractions include glucosamine (A), chitotriose (B); mixed dimer of glucosamine and N-acetylglucosamine (C), chitobiose (D), and N-acetylglucosamine (E). U is unknown. 1: Hydrolysis of chitin was done using chitinase only; 2: Hydrolysis of chitin was done using chitinase, chitosanase and β-N-glucosaminidase. All fractions were identified using standards except C. The basis for identifying the peak at 8.6 min (ie, peak C) in the chromatogram is as follows; the deacetylated product of (E), glucosamine (A), has a retention of 5.8 min, about 5 min shorter than the corresponding N-acetyl derivative. A mixed dimer of glucosamine and N-acetyl glucosamine can therefore be expected to also have a shorter retention time than chitobiose (D). It is most likely positioned between (B) and (D).

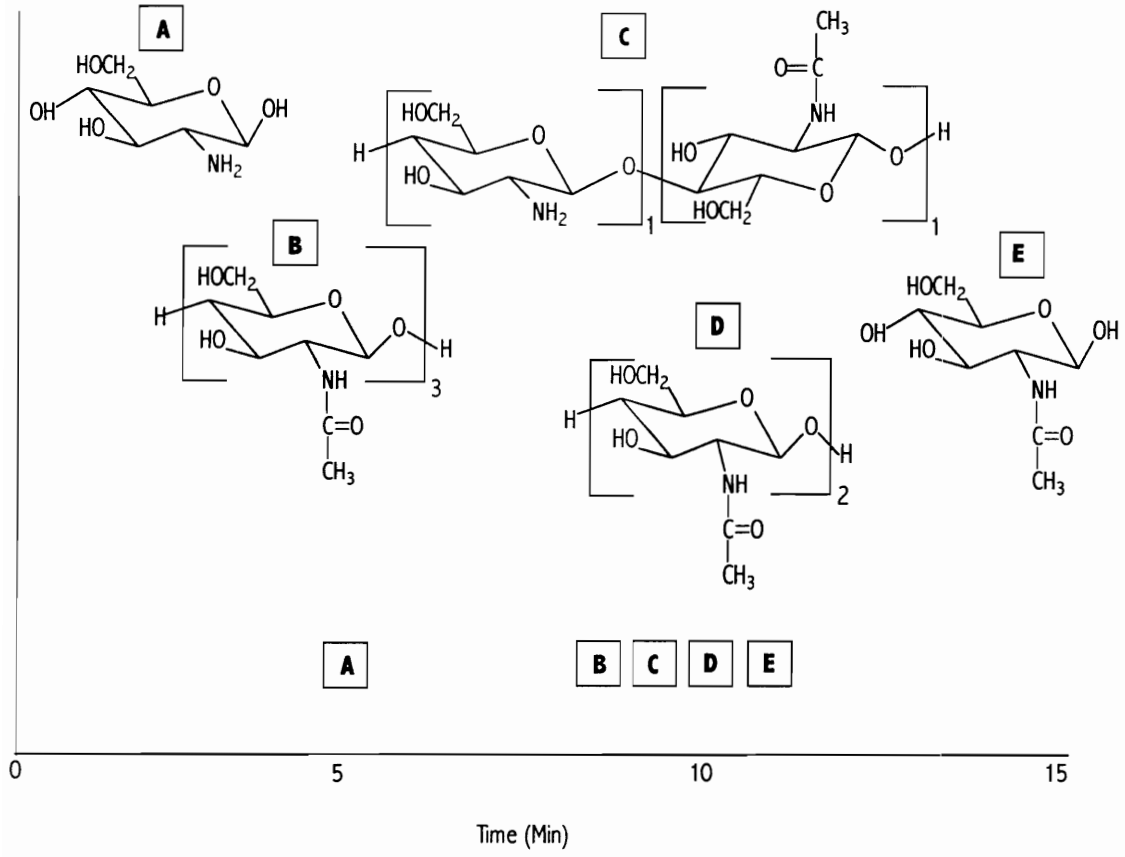

Figure 5-13. Structures and retention times for various hydrolysis products of enzymatic hydrolysis of native chitin and N-acyl homologs of chitosan. These include glucosamine (A); chitotriose (B); mixed dimer (glucosamine and N-acetylglucosamine) (C); chitobiose (D); and N-acetylglucosamine, where the location of the N-acetyl group may be in the reducing or non-reducing glucosamine unit (E). All fractions were identified using standards except C. C was identified as a mixed dimer of glucosamine and N-acetylglucosamine on the basis of arguments presented in the legend of Figure 5-13.

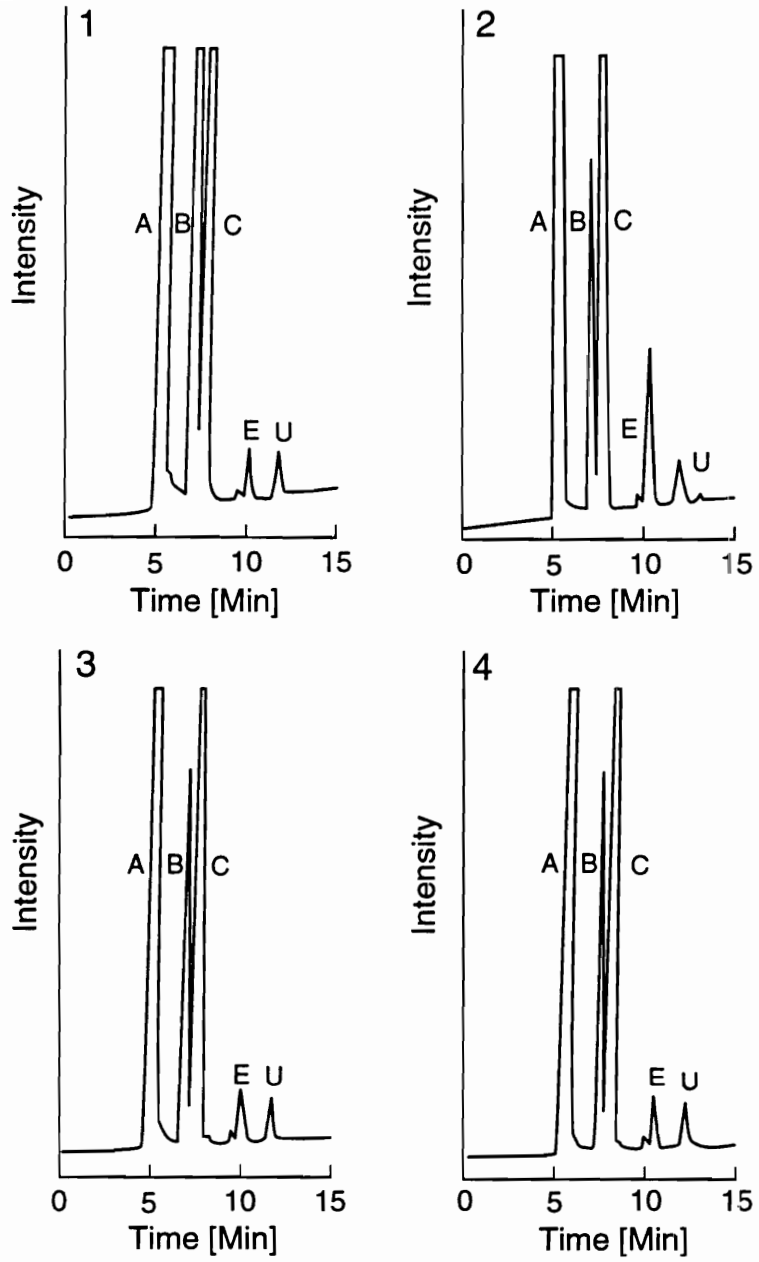

Figure 5-14. HPLC chromatograms of hydrolyzates of N-acyl homologs of chitosan. The products identified include glucosamine (A), chitotriose (B); mixed dimer (glucosamine and N-acetylglucosamine) (C), chitobiose (D). N-acetylglucosamine (E).U is unknown. Hydrolysis of N-acyl homologs of chitin was done using chitinase, chitosanase and β-N-glucosaminidase. 1, 2, 3, and 4 correspond to regenerated chitin from chitosonium- formate, acetate, propionate and butyrate, respectively. All fractions were identified using standards except C. The basis for identifying the peak at 8.6 min in the chromatogram is as described in the legend of Figure 5-13.

Appendix A[1]. Hydrolysis products of native chitin and N-acyl chitosan homologs using an enzyme assay of chitinase, chitosanase, and β-N-acetylglucosaminidase and their respective peak areas as determined by HPLC.

Source	Hydrolysis Product[2] Peak Area				
	[3]A	B	C	D	E
Native chitin	17.5	67.7	157.1	192.1[4]	262.5
N-formyl chitosan homolog	21.2	100.0	156.2	N/P	5.8
N-acetyl chitosan homolog	11.9	30.9	154.3	N/P	19.62
N-propyl chitosan homolog	12.7	33.0	153.3	N/P	6.5
N-butyryl chitosan homolog	12.6	33.0	152.3	N/P	6.4
Response Factor[5] (10^6)	6.62	14.68	4.30^6	2.8	2.04

[1] Peak areas of fractions are converted into their respective concentrations on the basis of their response factors
[2] Glucosamine (A); Chitotriose (B); Mixed dimer of glucosamine and N-acylglucosamine (C); Chitobiose (D); N-acylglucosamine (E)
N/P; Not present
[3] values are multiples of 10^7
[4] Hydrolysis was done using chitinase only
[5] Calculated as the slope of a plot of integrator response area of standards vs concentration
[6] Assumed as an average of response factors of A and E
Except where indicated the values presented in appendix A are multiples of 10^5

Appendix B. Sample calculation of amount of various fractions of hydrolysis of native chitin and N-acyl chitosan homologs using an enzyme assay of chitinase, chitosanase, and β-N-acetylglucosaminidase and their respective yields. The calculation presented here represents native chitin. Concentration of each fraction was calculated from an equation of the form y=mx+c, where y is HPLC peak area, m is response factor, and x is a constant representing the intercept of a linear fit of peak area vs. concentration of standards.

Hydrolysis Experiment

Amount of chitin = 1.7g

Considering 100% N-acetylation molecular weight of chitin repeat unit is 222 g/eq

Therefore amount of chitin expressed in meq of N-acetyl anhydroglucosamine is

$$\frac{1.7g}{222g/eq} = 7.7meq$$

Total Volume of enzyme assay = 3.2mL

HPLC Experiment

Concentration of Glucosamine = 10^{-2}g/mL{$(17.5\times10^{7}) + (13.1\times10^{6})$}/$6.62\times10^{6}$ = 28.42×10^{-2}g/mL

Amount of glucosamine = 28.42×10^{-2}g/mL × 3.2mL = 0.909g

Amount of glucosamine expressed in meq = $\frac{0.909}{179g/eq} = 5meq$

Yield of Glucosamine (%) = $\frac{5}{7.7}\times100 = 65\%$

Concentration of N-acetylglucosamine = 10^{-3}g/mL{$(262\times10^{5}) + (2.6\times10^{6})$}/$2.04\times10^{6}$ =14.18×10^{-3}g/mL

Amount of N-acetylglucosamine = 14.18×10^{-3}g/mL×3.2mL= 0.045g

Amount of N-acetylglucosamine expressed in meq = $\frac{0.045g}{221g/eq} = 0.2$meq

Appendix B. (continued)

Yield of N-acetylglucosamine (%) $= \frac{0.2}{7.9} \times 100 = 2.6\%$

Concentration of chitotriose $= 10^{-3}$g/mL{(67.7×10^{5}) - (0.001)}/$14\times10^{6} = 0.46\times10^{3}$g/mL

Amount of chitotriose = 0.46×10^{-3}g/mL×3.2mL = 0.0014g

Amount of chitotriose expressed in meq = $\frac{0.0014g}{627g/eq} = 0.0023meq$

Yield of Chitotriose (%) = $\frac{0.0023(3)}{7.7} \times 100 = 0.089\%$

Concentration of mixed dimer of glucosamine and N-acetylglucosamine =

10^{-3}g/mL{(157×10^{5}) + (7.9×10^{6})}/4.3×10^{6} = 5.5×10^{-3}g/mL

Amount of mixed dimer of glucosamine and N-acetylglucosamine

5.5×10^{-3}g/mL×3.2mL = 0.018g

Amount of mixed dimer of glucosamine and N-acetylglucosamine in meq =

$\frac{0.018g}{400g/eq} = 0.044meq$

Yield of mixed dimer of glucosamine and N-acetylglucosamine (%) =

$\frac{0.044(2)}{7.7} \times 100 = 1\%$

CHAPTER 6

CONCLUSIONS AND RECOMMENDATIONS

6.1 CONCLUSIONS

In this study several characterization methods including DMTA, TMA, TGA, X-ray diffraction, FTIR, Solid state CP-MAS ^{13}C NMR and HPLC were used to study the transformation of various ionic complexes of chitosan (N-acylate) to their respective N-acyl homologs of chitosan, and some properties of these materials. DMTA and TMA provided information on changes in glass transition temperature as well as modulus-changes and glass formation underlying the transformation of the N-acylate to the N-acyl. X-ray diffraction and FTIR, shed some insights on the morphology of N-acetyl homolog of chitosan in relation to native chitin. Solid state CP-MAS ^{13}C NMR provided evidence of the conversion of N-acylate to N-acetyl. Enzymatic hydrolysis of native chitin and amidized chitosan homologs and subsequent identification of fractions by HPLC allowed a comparison of various amidized chitosan homologs in terms of their recognition and degradation by chitinolytic enzymes.

Solid state CP-MAS ^{13}C NMR showed that the heat treatment of the ionic complex of chitosan results in thermal dehydration leading to the formation of the N-acetyl group at the C-2 of chitin. The degree of amidization of heat-treated chitosonium alkanoate complexes varied from 0.1 to 0.6. T_g-changes with time and heating temperature was used as a variable to monitor this regeneration of N-acetyl.

Kinetic analysis indicated that the amidization of various ionic complexes of chitosan is a first order, two-phase process with activation energies of 14±1 kcal/mol and 21±2 kcal/mol for the first and second phase, respectively. These values did not vary with the type of acid used in the formation of the chitosan complex. This two-phase behavior is related to the influence of vitrification.

In-situ DMTA was found to be a suitable technique to monitor the phase transformation of chitosonium acetate and chitosonium propionate from a rubbery phase to a glassy phase (vitrification). Consequently, the concept of TTT cure diagram was used to describe such phase changes to map out vitrification and full cure curves. As in thermosets the vitrification curve describing glass formation in these materials is S-shaped. The time to full cure decreased with increasing heating temperature. Activation energy for vitrification is the same irrespective of the type of acid used in the preparation of the chitosan complex.

Thermal analysis revealed that T_g declines stepwise with the length of N-acyl substituent of N-acyl homologs of chitosan. These materials are characterized by two transitions designated as α- and β-relaxation. Additionally enzymatic hydrolysis of N-acyl homologs of chitosan using an enzyme mixture of chitinase, chitosanase, and β-N-acetylglucosaminidase and subsequent identification of fractions revealed that irrespective of the N-acyl substituent at the C-2 position of chitin, as well as DS these enzymes recognize and degrade chitin.

6.2 RECOMMENDATIONS

This study has described the formation of various N-acyl homologs of chitosan using chitosan-acetic acid complexes. In chapter 1 we advocated that these N-acyl homologs of chitosan have the potential to serve as protective wood and/or paper coatings. Therefore, the following suggestions have been made for testing the qualifications of a chitin-from-chitosan regeneration technique for application as a waterborne wood coatings material.

The mechanical strength and moisture sorption characteristics of various N-acyl homologs of chitosan in relation to the extent of regeneration of N-acyl group should be studied to evaluate the suitability of these materials as coatings.

Regenerated amidized chitosan should be utilized as a top coat on solid wood surfaces, and examinations made of such aspects of grain raising, adherence to wood surfaces, surface appearance (sheen and clarity), hardness, crack resistance, etc. in relation to application parameters (solids content, viscosity, additives, etc.) and heat treatment protocol.

Its barrier and surface wetting properties should be studied and compared to those of conventional wood coatings.

VITA

The author, Ackah Toffey, son of Mr. J.S.A Toffey and Ms. Ekye Menwube, was born in October 1965, in Kumasi, Ghana. He earned a bachelor's degree in Natural Resources Management in 1989 at the University of Science and Technology (UST), Kumasi, Ghana. After graduation, Ackah was employed by the Institute of Renewable Natural Resources at UST as a teaching/research assistant, where he worked for two years. In August 1991, he enrolled in the Wood Science and Forest Products program at Virginia Polytechnic Institute and State University. During his enrollment at this university he was awarded a research fellowship by the Center for Adhesives and Sealant Science (CASS), Virginia Tech. In December 1993, Ackah received his master's degree under the supervision of Dr. Wolfgang G. Glasser. After receiving his master's degree, he continued at the same university towards a Doctor of Philosophy in Wood Science and Forest Products under the same supervisor. In June of 1996, Ackah Toffey was awarded the second prize winner of the Forest Products Society 47th Annual Wood Award. Ackah will earn his Ph.D. in December 1996. In October 1996, he will begin work with Georgia Pacific Resins Inc. as a Development Chemist.